②

GL-TR-89-0114   SSS-TR-89-10395

REGIONAL DISCRIMINATION OF QUARRY BLASTS, EARTHQUAKES AND UNDERGROUND NUCLEAR EXPLOSIONS

AD-A223 148

T. J. Bennett
B. W. Barker
K. L. McLaughlin
J. R. Murphy

S-CUBED
A Division of Maxwell Laboratories, Inc.
P. O. Box 1620
La Jolla, California 92038-1620

7 April 1989

Final Report
23 March 1987–22 March 1989

Approved for Public Release,
Distribution Unlimited.

GEOPHYSICS LABORATORY
Air Force Systems Command
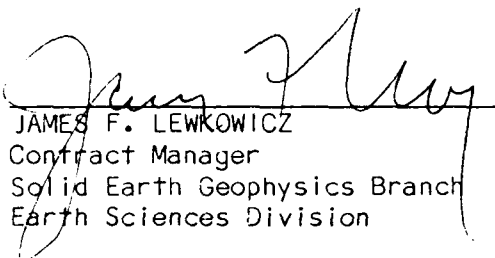Hanscom Air Force Base
Massachusetts 01731-5000

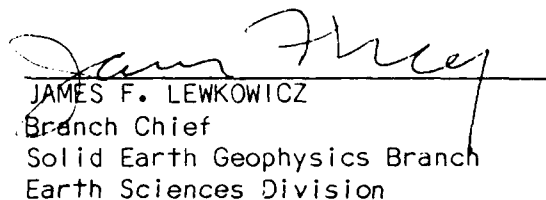This technical report has been reviewed and is approved for publication.

JAMES F. LEWKOWICZ
Contract Manager
Solid Earth Geophysics Branch
Earth Sciences Division

JAMES F. LEWKOWICZ
Branch Chief
Solid Earth Geophysics Branch
Earth Sciences Division

FOR THE COMMANDER

DONALD H. ECKHARDT, Director
Earth Sciences Division

This report has been reviewed by the ESD Public Affairs Office (PA) and is releasable to the National Technical Information Service (NTIS).

Qualified requestors may obtain additional copies from the Defense Technical Information Center. All others should apply to the National Technical Information Service.

If your address has changed, or if you wish to be removed from the mailing list, or if the addressee is no longer employed by your organization, please notify AFGL/DAA, Hanscom AFB, MA 01731-5000. This will assist us in maintaining a current mailing list.

Do not return copies of this report unless contractual obligations or notices on a specific document requires that it be returned.

REPORT DOCUMENTATION PAGE

1a. REPORT SECURITY CLASSIFICATION	1b. RESTRICTIVE MARKINGS
Unclassified	

2a. SECURITY CLASSIFICATION AUTHORITY	3. DISTRIBUTION/AVAILABILITY OF REPORT
	Approved for public release;
2b. DECLASSIFICATION/DOWNGRADING SCHEDULE	distribution unlimited.

4. PERFORMING ORGANIZATION REPORT NUMBER(S)	5. MONITORING ORGANIZATION REPORT NUMBER(S)
	GL-TR-89-0114

6a. NAME OF PERFORMING ORGANIZATION	6b. OFFICE SYMBOL (If applicable)	7a. NAME OF MONITORING ORGANIZATION
S-Cubed, Division of Maxwell Laboratories, Inc.		Geophysics Laboratory

6c. ADDRESS (City, State, and ZIP Code)	7b. ADDRESS (City, State, and ZIP Code)
P.O. Box 1620 La Jolla, CA 92038-1620	Hanscom Air Force Base Massachusetts 01731-5000

8a. NAME OF FUNDING/SPONSORING ORGANIZATION Defense Advanced Research Projects Agency	8b. OFFICE SYMBOL (If applicable)	9. PROCUREMENT INSTRUMENT IDENTIFICATION NUMBER
		F19628-87-C-0093

8c. ADDRESS (City, State, and ZIP Code)	10. SOURCE OF FUNDING NUMBERS			
1400 Wilson Boulevard Arlington, VA 22209-2308	PROGRAM ELEMENT NO. 62714E	PROJECT NO. 7A10	TASK NO. DA	WORK UNIT ACCESSION NO. DB

11. TITLE (Include Security Classification)
REGIONAL DISCRIMINATION OF QUARRY BLASTS, EARTHQUAKES AND UNDERGROUND NUCLEAR EXPLOSIONS (U)

12. PERSONAL AUTHOR(S)
Bennett, T. J., Barker, B. W., McLaughlin, K. L., Murphy, J. R.

13a. TYPE OF REPORT	13b. TIME COVERED	14. DATE OF REPORT (Year, Month, Day)	15. PAGE COUNT
Final	FROM 870323 TO 890322	890407	146

16. SUPPLEMENTARY NOTATION

17. COSATI CODES			18. SUBJECT TERMS (Continue on reverse if necessary and identify by block number)
FIELD	GROUP	SUB-GROUP	Seismic NTS Explosions Mine/Quarry Blasts
			Discrimination East Kazakh Explosions
			Regional Phases

19. ABSTRACT (Continue on reverse if necessary and identify by block number)

The investigations conducted under this contract focused on analyses of the higher-frequency phases observed at regional distances from underground nuclear explosions, earthquakes, and commercial blasts. These analyses systematically compared the time-domain amplitude and spectral characteristics of the observed regional seismic signals in order to identify diagnostic differences which would be indicative of source type. The sources were located in three tectonic environments: (1) eastern North America, (2) southern Soviet Union, and (3) western United States. Each source environment provides a unique contribution to the regional discrimination problem. For these source regions digital data from several different high-quality seismic networks were analyzed. The data sources were the Regional Seismic Test Network (RSTN), the Eastern Canada Telemetered Network (ECTN), the Chinese Digital Seismic Network (CDSN), the Soviet/Natural Resources Defense Council (NRDC) network, and the Lawrence Livermore National Laboratory (LLNL) network.

20. DISTRIBUTION/AVAILABILITY OF ABSTRACT	21. ABSTRACT SECURITY CLASSIFICATION
☒ UNCLASSIFIED/UNLIMITED ☐ SAME AS RPT. ☐ DTIC USERS	UNCLASSIFIED

22a. NAME OF RESPONSIBLE INDIVIDUAL	22b. TELEPHONE (Include Area Code)	22c. OFFICE SYMBOL
James Lewkowicz	617/377-3028	LWH

DD FORM 1473, 84 MAR   83 APR edition may be used until exhausted.   SECURITY CLASSIFICATION OF THIS PAGE
                              All other editions are obsolete.

9. ABSTRACT (Continued)

The eastern North America database included small commercial blasts and earthquakes ecorded at RSTN station RSCP and stations in the ECTN. At RSCP the blasts frequently roduced strong R_g signals not seen in the earthquakes. Lg and Pg spectra for the blasts ppeared to decay more rapidly at high frequencies than corresponding earthquake spectra. g/P amplitude ratios were observed to be larger for earthquakes, but these results were ntermingled. The study of ECTN data focused on cepstral analysis of regional P-waves to istinguish source multiplicity. The results showed evidence of deterministic modulation n the P-wave spectra for both quarry blasts and earthquakes, but this observation does ot appear to be caused by multiple sources.

For the southern Soviet Union we compared regional phases recorded at CDSN station MQ from East Kazakh nuclear explosions and regional earthquakes with similar magnitudes nd ranges. Broadband Lg/P amplitude ratios were observed to be larger for earthquakes non comparable explosions, and the differences were found to be concentrated at higher frequencies based on bandpass filter analyses. The Soviet/NRDC network around the East Kazakh test site was found to record a large number of presumed mine blasts. R_g was strong for many of these events, and in some cases there was evidence of spectral scalloping in the recorded Lg signals which could be related to time-delayed blasting.

For the western U.S. the primary analysis was performed on a sample of NTS explosions and nearby earthquakes recorded by the LLNL stations at ranges from 160 to 485 km. Spectral analyses of the Pg and Lg signals for these events indicated that the earthquake signals appeared relatively richer in high frequencies in agreement with prior observations. The differences may be enhanced at higher frequencies and appear to show some dependence on explosion depth. For NTS explosions and California earthquakes recorded at larger ranges at RSTN station RSSD, spectral analysis of the regional Lg signals also showed a tendency for the explosion spectra to be more sharply peaked; but path differences may again be affecting the observation.

DTIC
COPY
INSPECTED
6

Accession For

NTIS GRA&I	☒
DTIC TAB	☐
Unannounced	☐
Justification

By
Distribution/
Availability Codes
Avail and/or
Dist Special

A-1

Table of Contents

List of Illustrations

List of Tables

I. INTRODUCTION

Although the majority of large seismic events can be identified as earthquakes or explosions on the basis of teleseismic measurements, regional signal properties are expected to play an important part in identifying smaller events. Since the early days of interest in seismic discrimination, numerous methods have been proposed for using regional signal measurements to achieve identification (cf. Blandford, 1981; Pomeroy et al., 1982). However, the discovery of suitable regional discriminant measures has proven to be elusive. Determination of reliable regional discrimination techniques requires testing of signal measurements on well-controlled samples of explosions and nearby earthquakes so as to minimize differences which are not related to the source type. Ideally, the methods should be tested in the areas where they are intended to be used. If regional discriminants cannot be suitably tested in such areas, methods must be developed to extrapolate the experience from other areas. The latter requires development of understanding of why a regional discriminant works including knowledge of the signal behavior to permit separation of source and propagation effects. The research described here was designed to improve regional discrimination capability by analyzing the regional seismic signal characteristics from a variety of sources observed in different tectonic environments.

The investigations conducted under this contract have focused on analyses of the higher-frequency phases observed at regional distances from three different types of sources: (1) underground nuclear explosions, (2) earthquakes, and (3) mine or quarry blasts. In our analyses we systematically compared the time-domain amplitude and spectral characteristics of the observed regional seismic signals while seeking to identify diagnostic differences which would be indicative of the source. Tectonic environments which were investigated in this study included (1) eastern North America, (2) the southern Soviet Union and (3) the western United States. Each of these environments provides a unique contribution to the regional discrimination problem. Stable continental areas of central and eastern North America are thought to be analogous in many ways to platform regions of the Soviet Union with regard to regional seismic wave generation and transmission. Past studies of regional

1

phases from Soviet underground nuclear explosions were frequently forced to rely on measurements at far-regional stations where the signals were extremely weak (cf. Nuttli, 1981; 1986). Recent installation of new stations have made available regional data from the southern Soviet Union enabling relevant testing of regional discrimination methods for this area where the capability is most needed. Finally, the western U.S. sample of underground nuclear explosions and nearby earthquakes provides the controlled source sample which permits closer analyses of how regional signal generation is influenced by various source factors.

The analyses were performed on the high-quality digital seismic data which were available from each of these tectonic environments. For eastern North America we used data from the Regional Seismic Test Network (RSTN) and the Eastern Canada Telemetered Network (ECTN). For the southern Soviet Union the data sources were the Chinese Digital Seismic Network (CDSN) and the Soviet/Natural Resources Defense Council (NRDC) seismic network surrounding the East Kazakh test site. For the western U.S. we relied on data from the Lawrence Livermore National Laboratory Network (LLNL) and some RSTN stations. Although the useful frequency range of these different seismic systems varies, in general the data permit analysis of higher frequency signals than those used in most previous investigations of regional discrimination. Furthermore, because of the potential interest in extending discrimination capability to lower thresholds, added focus in these investigations was given to consideration of commercial blasts which appear to be frequent contributors to the regional event samples in areas of interest for nuclear monitoring.

For eastern North America we compared the characteristics of the regional signals from mine blasts and earthquakes recorded by the RSTN and ECTN systems. The RSTN analysis included data from 22 presumed mine blasts, 14 earthquakes and a mine collapse recorded at station RSCP. The records showed good P and L_g phases. The L_g/P_{max} amplitude ratios were generally larger for the earthquakes than the blasts, but observations showed considerable scatter and intermingling which made the distinction unreliable. Many blasts and the mine collapse produced strong, short-period Rayleigh waves, R_g, but this was not the case for all blasts. L_g and P_g spectra indicated more rapid spectral decay above the corner frequency for blasts than for earthquakes.

2

The North America database at ECTN consisted of 36 events with magnitudes between 1.0 and 5.1 including seven presumed quarry blasts. These were recorded at multiple stations in the network to a fairly high digitizing rate (viz 60 samples per second). Our analyses of these data focused on an attempt to identify potential evidence of multiplicity in the source which is expected from the delay shooting typical of commercial blasting practice. Using the multiple station data, cepstral analyses were performed on the P-wave spectra from selected events. These analyses revealed evidence of deterministic modulation in the spectra from both quarry blasts and earthquakes with fairly large quefrencies. It is suspected that this observation may correspond to a propagation effect rather than a source effect.

For the southern Soviet Union we analyzed observed regional phases from East Kazakh explosions and comparable earthquakes recorded at the CDSN station WMQ and from presumed mine blasts recorded at the Soviet/NRDC network stations. The WMQ database included 12 East Kazakh explosions and 20 earthquakes with magnitudes from 4.5 to 6.1 m_b. Because of the lack of natural seismicity near East Kazakh, the comparable earthquakes were selected from throughout the region surrounding WMQ. The records showed strong P and L_g phases from both earthquakes and explosions. Broadband L_g/P amplitude ratios tended to be larger for earthquakes than for explosions, and the differences were concentrated at high frequencies. This result suggests a promising discriminant, but it must be strongly noted that the effects of attenuation differences in the crustal paths for the explosions and earthquakes have not been completely taken into account.

The analysis of the Soviet/NRDC network data focused on the characteristics of the regional phases from a large number of presumed mine blasts in the East Kazakh region which were recorded during the operation of the network. These events produced strong P_g and L_g signals to ranges of at least 400 km. R_g was also strong for many but not all events, and some evidence was found of spectral scalloping which might have been associated with shot delays in the presumed blasts.

For the western U.S. we used the LLNL database to continue our analysis (cf. Bennett et al. , 1987a,b) of the L_g and P_g spectral characteristics of 10 NTS explosions and eight nearby earthquakes. The observations were

generally in agreement with previous findings (cf. Murphy and Bennett, 1982; Bennett and Murphy, 1986) that the earthquake L_g signals appear to be relatively richer in high frequencies than comparable explosions. We also found evidence that burial of the explosion below the water table at Yucca Flat may enhance high frequencies in the regional phase signals, but this effect may not be adequate to compromise the discriminant.

For the western U.S. we also compared amplitude and spectral characteristics of the regional signals recorded at RSTN station RSSD from several larger NTS explosions and comparable earthquakes in California. The observed L_g spectra seemed to be somewhat more sharply peaked for the explosions than the earthquakes. Bandpass filter analyses of the signals revealed some interesting dependencies of the L_g-to-P amplitude ratio on frequency; but significant source and path differences exist between the events compared, and the dependence on these factors needs further study.

This report is divided into five sections including this introduction. Section II describes the analysis of eastern North American quarry blasts and earthquakes using the RSTN and ECTN data. Section III presents the observations for the southern Soviet Union using the CDSN and Soviet/NRDC network data. Section IV describes the analysis of the LLNL and RSTN data from western U.S. nuclear explosions and earthquakes. Finally, in Section V we summarize the main conclusions from these studies and offer recommendations for further investigations of regional discrimination techniques.

II. EASTERN NORTH AMERICAN QUARRY BLASTS AND EARTHQUAKES

2.1 Eastern North America Data Sources

The stable continental areas of the central and eastern U.S. are thought to be analogous in many ways to the platform regions of the Soviet Union with regard to crustal properties and seismic wave transmission. Based on this analogy considerable research efforts (cf. Blandford, 1981; Pomeroy, 1977, 1979; Pomeroy et al. , 1982; Gupta et al. , 1984) over more than a decade have focused on understanding the propagation of regional phases in the eastern U.S. with the idea that this experience could be extended to the Soviet Union when regional seismic monitoring stations become available there. A particular problem in such monitoring environments is likely to be the identification of the frequent small explosions used in commercial development such as quarrying, mining and construction activities. The seismic discrimination problem could be greatly facilitated if simple procedures could be determined to distinguish these commercial blasts from small underground nuclear explosions. With this in mind a part of the current research effort was devoted to investigation of the regional phase seismic signals from small commercial blasts and nearby earthquakes in eastern North America. In these investigations we utilized data from two sources: the Regional Seismic Test Network (RSTN), in particular station RSCP, and the Eastern Canada Telemetered Network (ECTN). Each of these sources provided good quality digital seismic data with relatively high sampling rates permitting extraction and analysis of high frequency characteristics of the regional signals.

2.2 Analysis of RSTN Data

The Regional Seismic Test Network was established in the early 1980's as a prototype of a high quality network of digital seismic stations providing real-time regional monitoring capability for North America. The network consisted of five stations located in New York (RSNY), Tennessee (RSCP), South Dakota (RSSD), Ontario, Canada (RSON) and Northwest Territories, Canada (RSNT) with digital data transmitted by satellite link to a central processing

5

facility.

It is well known from historical seismic monitoring in the eastern U.S. that the region frequently experiences small mine and quarry blasts which are detected on seismographs out to large regional distances. So it was not unexpected that the RSTN network stations would record numerous commercial blasts as well as regional earthquake activity; and a review of the recorded data revealed this to be true. In assembling a database of commercial blasts and regional earthquakes recorded at RSTN stations, we initially reviewed published reports and earthquake catalogs and bulletins appropriate to the regions surrounding the RSTN stations. Goncz et al. (1987) analyzed regional L_g, P_n and S_n attenuation using recordings at the RSTN stations from earthquakes located throughout much of eastern North America during 1983 and 1984. The report provides a fairly extensive catalog of the larger eastern U.S. earthquakes during that time interval which were well recorded at the RSTN stations. To supplement that data set, we reviewed the NEIS catalogs, as well as regional catalogs published by St. Louis University, the Tennessee Earthquake Information Center (now Center for Earthquake Research Information), the Virginia Polytechnic Institute and State University and Boston College. Because of the extensive local seismic networks, the coverage is thought to be nearly complete for much of the eastern U.S. down to fairly low magnitudes (≈ 2 M_L). However, for most of these bulletins an attempt has been made to exclude known or suspected quarry and mine blasts from the reported events. As a result only a few such explosions have been identified in the regional bulletins. Gupta et al. , (1984) identified six quarry blasts recorded at RSTN stations (5 at RSCP and 1 at RSNY) from a list of 20 such events provided by local university or state network operators. Smith (1987) looked for evidence of ripple firing in several northern Minnesota quarry blasts, but his primary data source was a temporary station near RSON although signals from some of these blasts were also recorded at RSON and RSSD. Personal communications with several operators of local seismic networks in the eastern U.S. suggested that formal catalogs of quarry and mine blasts detected by the networks do not exist. Most of the operators indicated that suspect events with strong short-period Rayleigh waves or with signals and locations close to those of known quarries in the region were eliminated from the earthquake catalogs on an ad hoc basis.

6

In the current investigation it was decided to focus on regional seismic signals recorded at station RSCP because it is well known from historical monitoring that the station records frequent mine blasts from the surrounding region which could be compared to similarly recorded earthquakes. Starting with the five blasts identified by Gupta et al. (1984), we found two additional presumed blasts identified in the Southeastern U.S. Seismic Network Bulletins. A few other presumed quarry blasts identified in the catalogs were not recorded at RSCP. To supplement the quarry blast database for RSCP, the detections recorded during a single day (viz June 19, 1985) were analyzed. Of the total detections on that date, about 40 events appear to have waveforms which look like real seismic signals (i.e., not typical ground or cultural noise). Sixteen of those 40 events which had the strongest signals were selected for further analysis. Only one of the 16 events selected was reported in the regional earthquake catalogs, and that was an apparent mine collapse in southwestern Virginia. None of the other 15 events were reported as earthquakes, and we therefore assume that they were mine or quarry blasts. The identification of these events as blasts appears to be corroborated by the observations of strong, short-period R_g phases in most cases suggesting a shallow focus and by the repetitive character of the waveforms for several of the events. The relative times of the P and L_g phases were used to estimate the epicentral distances and three-component analyses were performed on clear P-wave first motions to determine event azimuths. This location procedure was tested on the signals from the mine collapse, for which the location was known, and was found to give a nearly comparable result. So, although the locations determined by this single station procedure for these events would not be expected to have the precision of network locations, we believe them to be reasonable.

Table 1 provides the event locations and magnitudes (estimated from the L_g amplitudes) for 22 presumed mine blasts recorded at RSCP including the 15 newly identified events described in the preceding paragraph. The blasts had magnitudes from 2.2 to 3.5 $m_b(L_g)$ and epicentral distances in the range from 210 km to 369 km. Table 2 provides the locations and magnitudes of the 15 earthquakes and the mine collapse included in the database. The magnitudes were in the range 2.2 to 4.1 $m_b(L_g)$; and the epicentral distances were between 147 km and 490 km, except for one more distant earthquake at 942 km. The locations of all the events in the database relative to RSCP are shown in Figure 1. The events cover a wide range of azimuths surrounding RSCP; and, as

7

Table 1

Presumed Mine Blasts Recorded at RSCP

Date	Origin Time	Lat.(°N)	Lon.(°W)	Δ(km)	$m_b(L_g)$[†]	h(km)
01-29-83	16:05:31.7	34.70	88.37	274	2.9	0
02-05-83	13:08:19.5	34.70	88.37	274	3.5	0
02-22-83	13:09:18.2	38.05	82.77	369	3.0	0
06-09-83	21:07:43.7	37.42	83.12	298	2.9	0
06-21-83	21:13:20.4	37.42	83.12	298	3.0	0
06-23-83	21:06:09.3	37.41	83.11	298	3.2	0
06-19-85	00:06:22*	37.0*	87.3*	220	3.1	0
06-19-85	01:37:58*	-	-	210	3.0	0
06-19-85	14:57:04*	37.3*	82.7*	310	2.5	0
06-19-85	15:59:58*	37.0*	87.3*	220	3.0	0
06-19-85	17:14:21*	33.2*	86.7*	280	3.3	0
06-19-85	18:20:29*	33.2*	86.7*	280	3.7	0
06-19-85	19:02:21*	37.3*	82.7*	310	2.9	0
06-19-85	19:22:26*	-	-	220	2.8	0
06-19-85	20:25:32*	33.2*	86.7*	280	3.2	0
06-19-85	20:55:34*	37.3*	82.7*	310	2.9	0
06-19-85	21:26:47*	-	-	210	3.1	0
06-19-85	22:10:26*	37.0*	87.3*	220	2.2	0
06-19-85	23:01:07*	37.0*	87.3*	220	2.4	0
06-19-85	23:11:22*	33.2*	86.7*	280	2.9	0
06-19-85	23:35:18*	-	-	200	2.6	0
11-07-85	08:17:13.0	33.77	84.07	245	2.3	1.1

* Approximate origin times and locations estimated from relative times of P and L_g phases and three-component analysis of clear P-wave first motion.

† Magnitudes estimated from L_g amplitudes observed at RSCP using the magnitude formula for the Central U.S. - $m_b(L_g) = 1.91 + 0.9 \log \Delta(km) + \log A (\mu m)$.

Table 2

Regional Earthquakes and Mine Collapse Recorded at RSCP

Earthquakes

Date	Origin Time	Lat.(°N)	Lon.(°W)	Δ (km)	$m_b(L_g)$	h (km)
01-26-83	14:07:44.7	32.85	83.56	356	3.5	0
01-27-83	22:09:35.1	36.06	83.63	182	2.6*	12.8
03-25-83	02:47:11.1	35.33	82.46	283	3.2*	11.5
08-28-83	22:45:07.4	36.68	83.82	198	3.1*	18.1
02-14-84	22:56:20.4	37.21	89.00	356	3.6	2.0
04-17-84	04:44:44.9	38.41	88.48	405	3.2	14.3
04-23-84	01:36:00.1	39.92	76.36	942	4.1*	5.0
06-26-84	15:15:19.9	36.10	89.39	349	3.2	11.8
06-29-84	07:58:29.3	37.70	88.47	348	3.8	1.6
06-10-85	12:22:38.3	37.25	80.49	491	$2.3^\dagger$	11.1
08-15-85	17:31:52.9	35.67	83.95	147	$2.6^\dagger$	13.8
12-22-85	00:56:05.0	35.70	83.72	170	$3.6^\dagger$	13.4
04-27-86	22:30:26.4	35.92	83.73	170	$2.2^\dagger$	19.7
06-24-86	19:22:42.0	35.99	83.93	154	$3.3^\dagger$	24.3

Mine Collapse

Date	Origin Time	Lat.(°N)	Lon.(°W)	Δ (km)	$m_b(L_g)$	h (km)
06-19-85	22:28:08.9	37.22	82.04	360	3.5	0

* Magnitudes reported by Goncz et al., 1987.

† Magnitudes estimated from L_g amplitudes observed at RSCP using the magnitude formula for the Central U.S. - $m_b(L_g) = 1.91 + 0.9 \log \Delta (km) + \log A (\mu m)$.

9
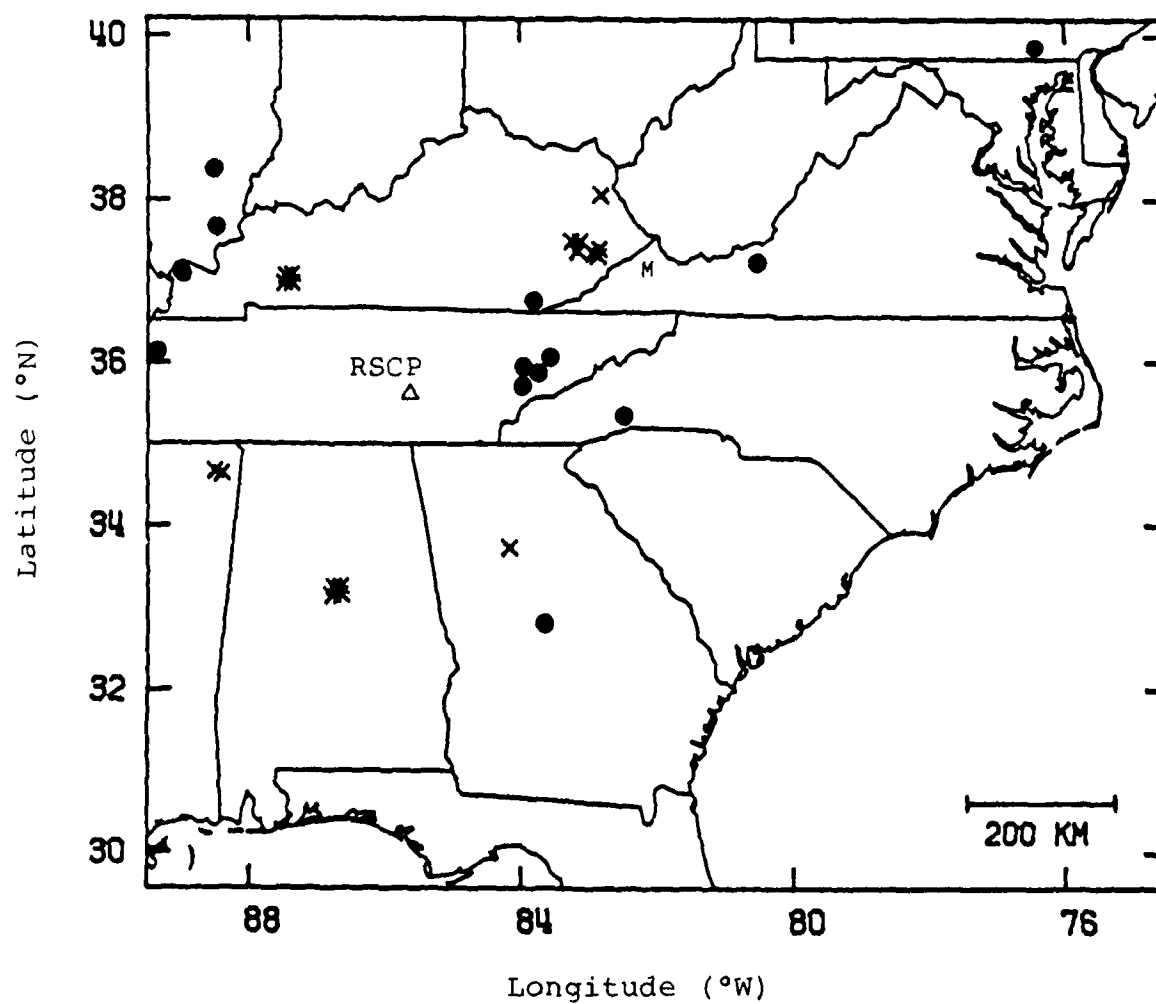
Figure 1.   Locations of regional events recorded at RSCP.
Earthquakes (●), presumed blasts (x), and mine
collapse (M).

a result, there are some variations in propagation path. In general, events to the north and east were located in the Appalachian mountain chain while those to the west and south were located in stable continental platform areas as is the station.

Figure 2 shows typical vertical-component recordings of the seismic signals at RSCP from several source types at different ranges and azimuths. In all cases the records include clear P and L_g phases. These phases are typically quite complex in character apparently because of structure in the crust and upper mantle which controls propagation of these phases. The top three records illustrate the strong short-period dispersed Rayleigh-wave (R_g) signals which are usually recorded from the mine and quarry blasts in the region. The observed R_g phase frequently has a predominant frequency near 1 Hz. Similar R_g signals have been reported for mine and quarry blasts throughout eastern North America (e.g., McEvilly, 1964; Herrmann, 1969; Kafka, 1988) and are believed to be associated with seismic excitation of shallow sedimentary layers in the crust by the near surface blast sources (cf. McEvilly, 1964; Kafka, 1987). The bottom four records in Figure 2 show the signals at RSCP from two additional mine blasts, an earthquake, and a mine collapse. In these records the R_g signals from the blasts are not nearly as obvious as for the top three examples. If the R_g signals are present, they are apparently buried in the coda of the L_g phase. There is little evidence of R_g in the earthquake, but the mine collapse produced a strong R_g.

First, considering the P and L_g phases, we compared the maximum P and L_g signal amplitudes for evidence of any source-dependent differences. The maximum amplitudes before and after the S_n arrival time (excluding the R_g signal), were measured from the broadband records for this purpose. In all cases the post-S_n maximum corresponded to L_g while the pre-S_n maximum sometimes corresponded to P_g but also was frequently the initial $P(P_n)$ particularly for more distant events. For all 37 events in the RSCP database, the maximum P amplitude was smaller than the maximum S (viz L_g) amplitude; this was true for the presumed blasts as well as the earthquakes and mine collapse. Figure 3 shows the amplitude ratio (L_g maximum/ P maximum) for all the events. The data overlap in magnitude (top) and epicentral distance range (bottom); and there appears to be little evidence of dependence of the amplitude ratio on either magnitude or distance. The results indicate that on

11

Blast   R = 220 km

Blast   R = 280 km

Blast   R = 310 km

|— 20 sec —|

Blast   R = 270 km

Blast   R = 370 km

Earthquake   R = 350 km

Mine Collapse   R = 360 km
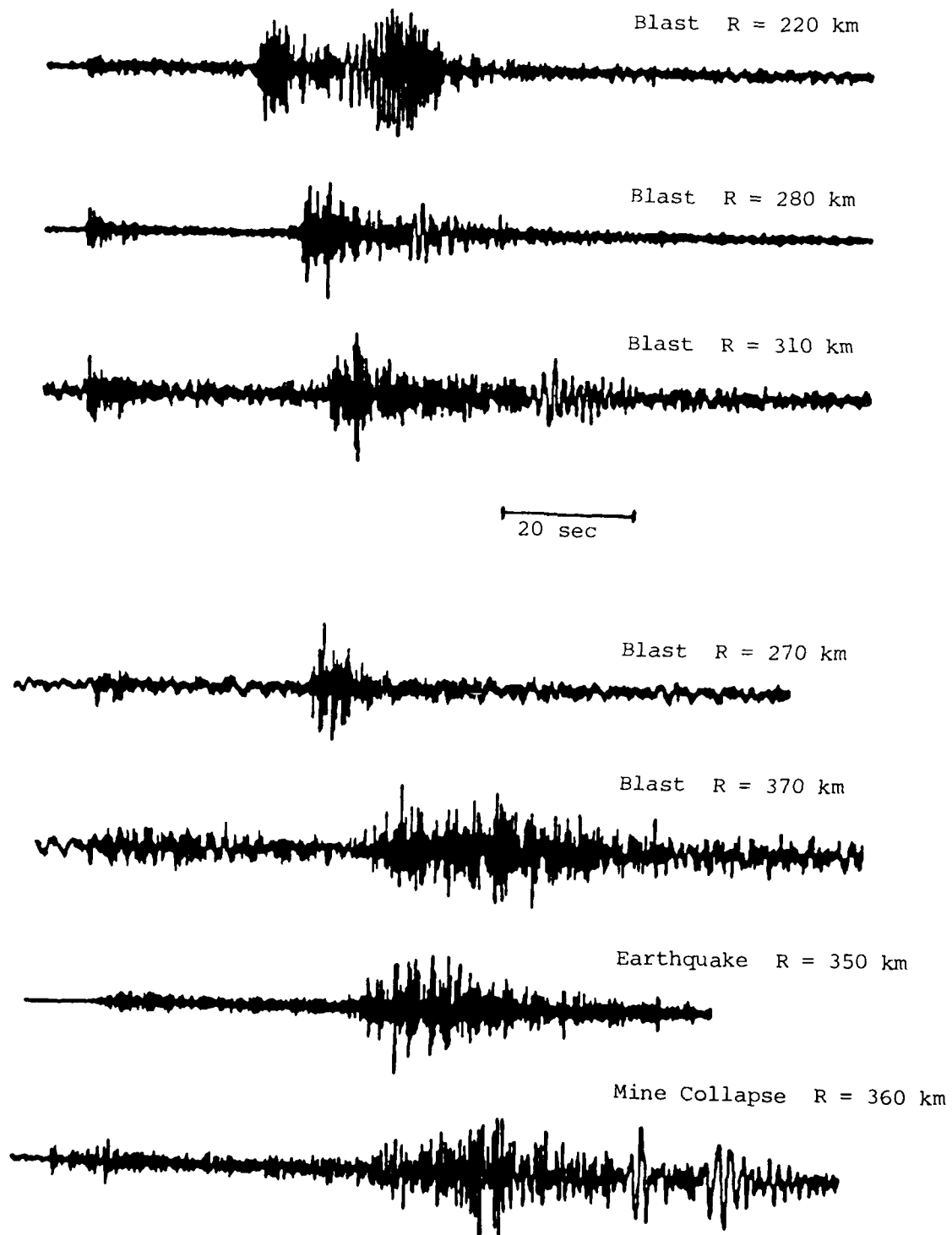
Figure 2.   Vertical-component records at RSCP from typical
regional events.

12
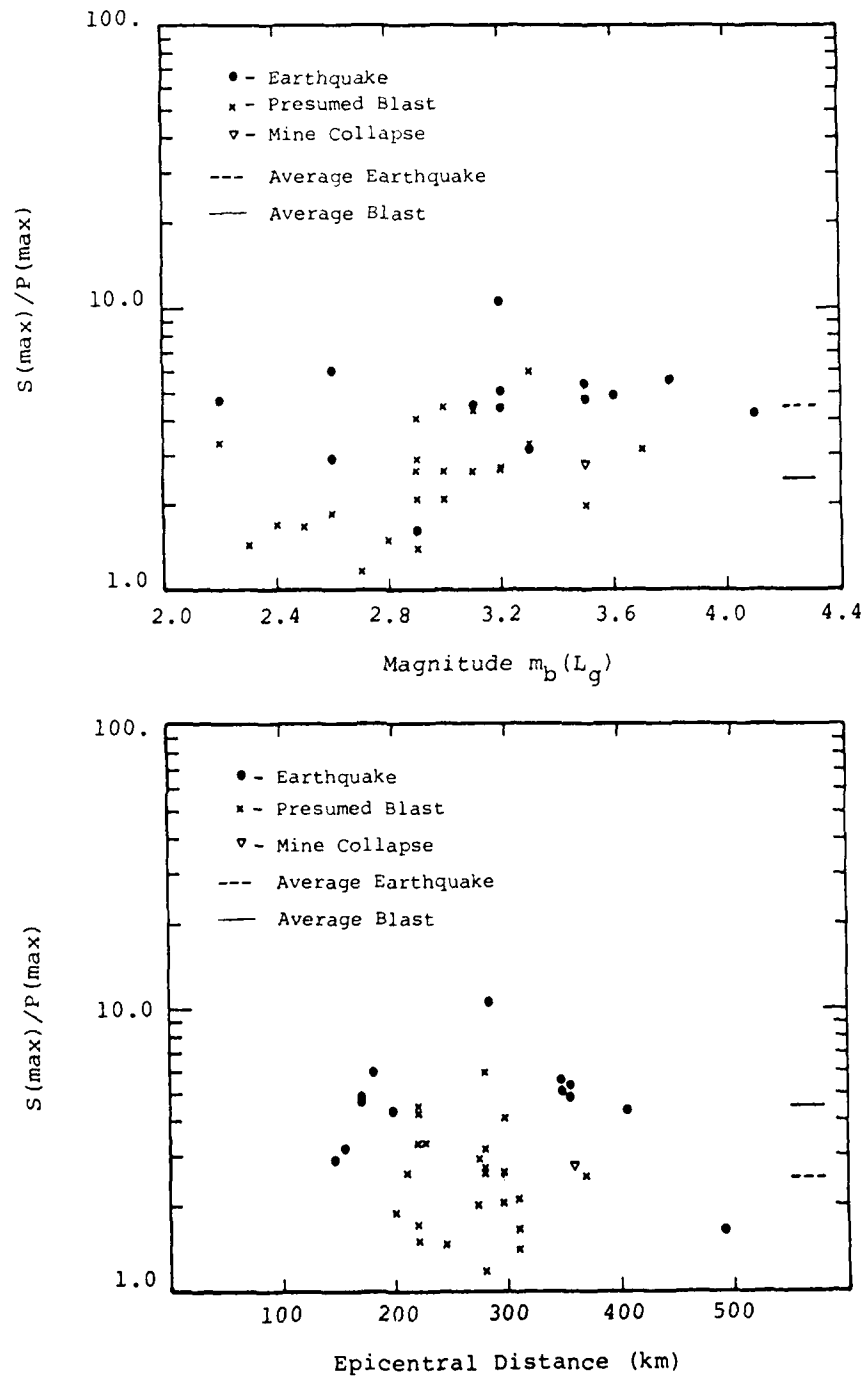
Figure 3. Peak amplitude ratio (S_{max}/P_{max}) observed at
RSCP as a function of magnitude (top) and
epicentral distance (bottom).

13

average the earthquakes tend to have larger S(max)/ P(max) ratios than the explosions in the sample, but there is considerable intermingling. So. simple peak-amplitude comparisons of the broadband P and L_g signals would not appear to provide reliable discrimination of the blast and earthquake sources.

In Figure 2 above we also found that the relative excitation of the R_g signal may not always provide a clear distinction between blasts and earthquakes. In an effort to enhance such differences, we band-pass filtered the records from several blasts, earthquakes and the mine collapse. These results are shown in Figure 4 where two alternate band-pass filters were applied to the vertical-component signals. The filter passbands were 0.5 to 1.5 Hz and 2.0 to 4.0 Hz; the unfiltered traces are also shown with each set for reference. For the first three blasts (cf. Figure 4, top), the 0.5 to 1.5 Hz filter sharply enhances the R_g signal relative to the P and L_g phases, which are concentrated in the higher frequency band. The 0.5 to 1.5 Hz filter in Figure 4, bottom, also enhances the R_g phase for the nearer blast and for the collapse, but the R_g phase does not stand-out in the filtered trace for the more distant blast. To some extent this is caused by relatively high ground noise in the filter passband for the latter event, but low excitation of the R_g phase may also be associated with some unusual blasting practice or depth for this event. We have no specific information on any of the blasts which have been analyzed, but normal shooting practice involves spatially-distributed and time-delayed charges which should enhance or nullify specific frequencies of the ground motion (cf. Willis, 1963; Frantti, 1963; Baumgardt and Ziegler, 1988). Finally, application of the filters to the earthquake record produces little evidence of any R_g signal. A slight trace of R_g appears in the second earthquake which was the shallowest of the three events with a focal depth of 2 km. In all cases the low-frequency R_g signal in the earthquakes is smaller relative to the higher-frequency P and L_g signals than in the explosions.

Spectral analyses were performed on the P and L_g signals from selected eastern U.S. earthquakes and quarry blasts to identify characteristics which could be distinctive. From the available data sample in Tables 1 and 2 above, we selected eight events which had relatively large signal-to-noise levels. An effort was made to pick events which correspond to different source types at somewhat comparable epicentral distance ranges. Figure 5 shows the vertical-component records for four events with ranges between about 170 km

14
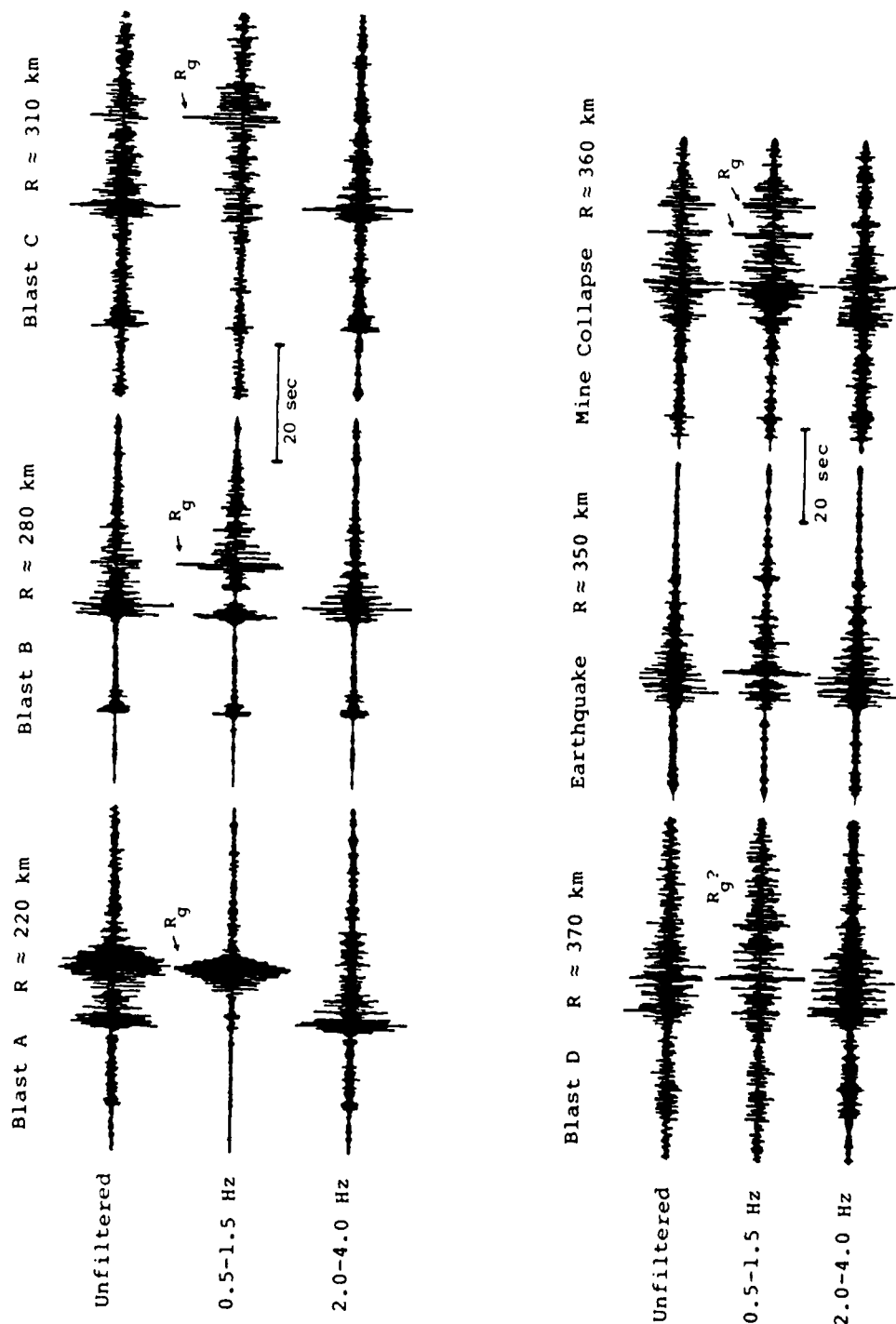
Figure 4. Application of band-pass filter at RSCP to enhance R_g signals.
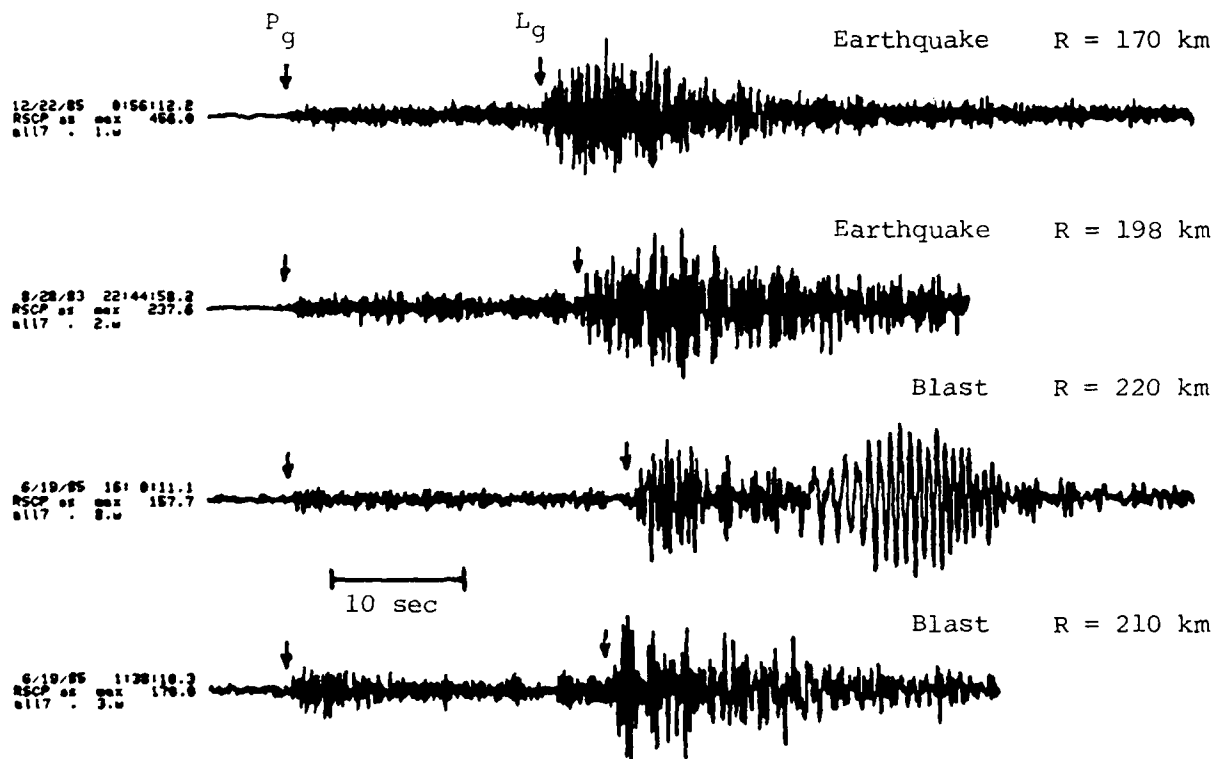
Figure 5. Vertical-component records for four events recorded at RSCP.

and 220 km from RSCP. The top two events are from the regional earthquake list (Table 2, above) and the bottom two are from the presumed regional blast list (Table 1, above). The events have roughly comparable magnitudes in the range 3.0 to 3.5 $m_b(L_g)$ with the earthquakes in the upper part and the blasts in the lower part of that range. We computed the spectra for windows surrounding the rather clear P_g and L_g signals whose starts are indicated by the arrows in Figure 5. The P_g windows were taken to be 256 points (6.4 seconds) in length and the L_g windows were taken to be 512 points (12.8 seconds). Noise windows including 128 points (3.2 seconds) were also analyzed at the start of each record. The spectra were all corrected for the RSCP instrument response.

Figures 6 and 7 show the corrected L_g and P_g spectra for the four events; the corresponding pre-P noise spectra are superimposed on the plots. In general, the ground noise is well below the signals for frequencies above about 1 Hz. Unfortunately, however, the dynamic range of the recording system at RSCP is low; so the signal spectra are not good above about 10 Hz even though the Nyquist frequency is at 20 Hz. This dynamic range problem is somewhat apparent in the lower left L_g spectrum of Figure 6 which starts to flatten at 7 Hz well above the ground noise level. In any case, the useful frequency band for spectral analysis at RSCP is extremely limited. Out to 10 Hz we see little evidence in the blast signals of spectral scalloping which has been found for time-delayed shots in some areas (cf. Smith and Grose, 1987; Baumgardt and Ziegler, 1988); it seems likely that the limited frequency band may impede such observations at RSCP. The spectra do appear to show other differences between earthquakes and explosions. The L_g spectra in Figure 6 have apparent corner frequencies near 3 Hz. Above the corner the spectra for the blast signals appear to fall-off much more rapidly than the earthquake signals. For the P_g signals the corner frequencies are somewhat more difficult to identify, but again the spectral fall-off above 3 Hz is greater for the blasts than for the earthquakes. The observed behavior in the L_g spectra are analogous to the behavior seen by Murphy and Bennett (1982) and Bennett and Murphy (1986) in L_g signals from NTS explosions and nearby earthquakes although the mechanism responsible for this observation could be considerably different.

17

Figure 6. L$_g$ spectra (solid line) and noise (dashed line) for the four events in Figure 5.

18
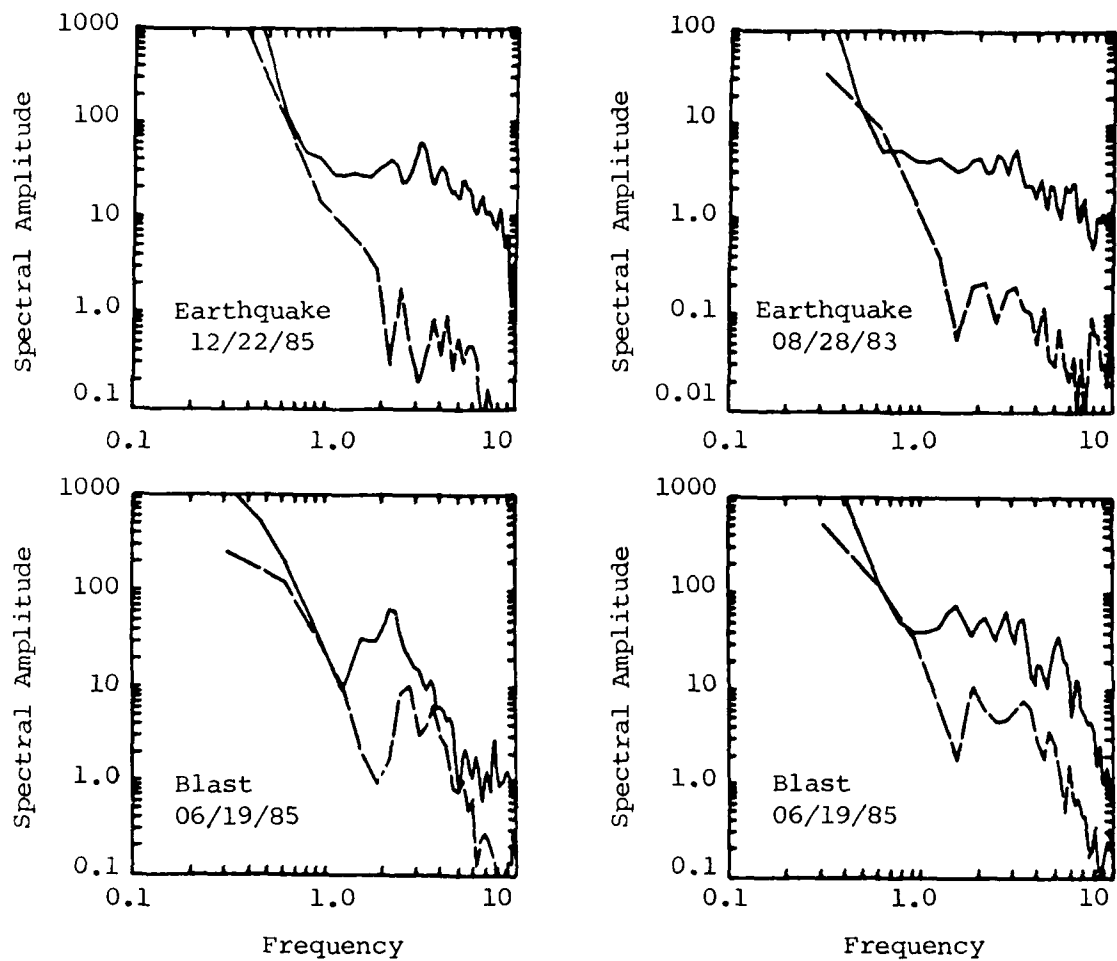
Figure 7. P$_g$ spectra (solid line) and noise (dashed line) for the four events from Figure 5.

Figure 8 shows the vertical-component time histories for four additional events with ranges between about 270 km and 300 km from RSCP; the magnitudes are between 3.2 and 3.7 $m_b(L_g)$. The top event is from the earthquake list, and the bottom three events are from the blast list. L_g, P_g and noise spectra were computed for window lengths of 12.8 seconds, 6.4 seconds and 3.2 seconds, respectively; and the results, after correcting for instrument response, are plotted in Figures 9 and 10. The L_g spectra again show an apparent corner frequency near 3 Hz. Above this corner the L_g spectra for the bottom two events plotted in Figure 9 are observed to fall-off with frequency much more rapidly than for the top two events. A similar behavior is observed for the P_g spectra in Figure 10 although the corner frequencies are not so easily identified. A confusing aspect of these figures is that the top right spectrum in each of these figures corresponds to an event (Date 02/05/83) which had originally been identified as a blast in our tables, but the spectral behavior seems to be more comparable to the earthquake signal than to the blast signals. Reinvestigation of this event reveals that its identification as a blast in Table 1 was based on its assignment to a "blast" database by the Southeastern U.S. Seismic Network Bulletin. However, further investigation has revealed that, in addition to presumed mine blasts, this database included other unknown events from outside the geographical domain for which the Southeastern Network claims coverage. In fact, this event is identified in the St. Louis University Central Mississippi Valley Earthquake Bulletin as an earthquake with a felt report from Mississippi; and field studies by the Tennessee Earthquake Information Center (TEIC Quarterly Seismological Bulletin, January-March, 1983) confirm the earthquake identification. Concluding that this event was an earthquake, the L_g and P_g spectra in Figures 9 and 10 are again consistent with the previous observation that the earthquake spectra are relatively richer in higher frequencies than the corresponding blast spectra.

The spectral differences in regional phase signals between earthquakes and blasts is interesting but needs additional corroboration. It should be noted that the observations presented here correspond to a small number of events and that the propagation paths between comparable events do not coincide. As a result, path differences like attenuation or structural boundaries, which could affect the regional phase spectra, have not been taken into account. Other factors like changes in shooting practice between quarries or mines could also affect the P_g and L_g spectra. Considering the large number of

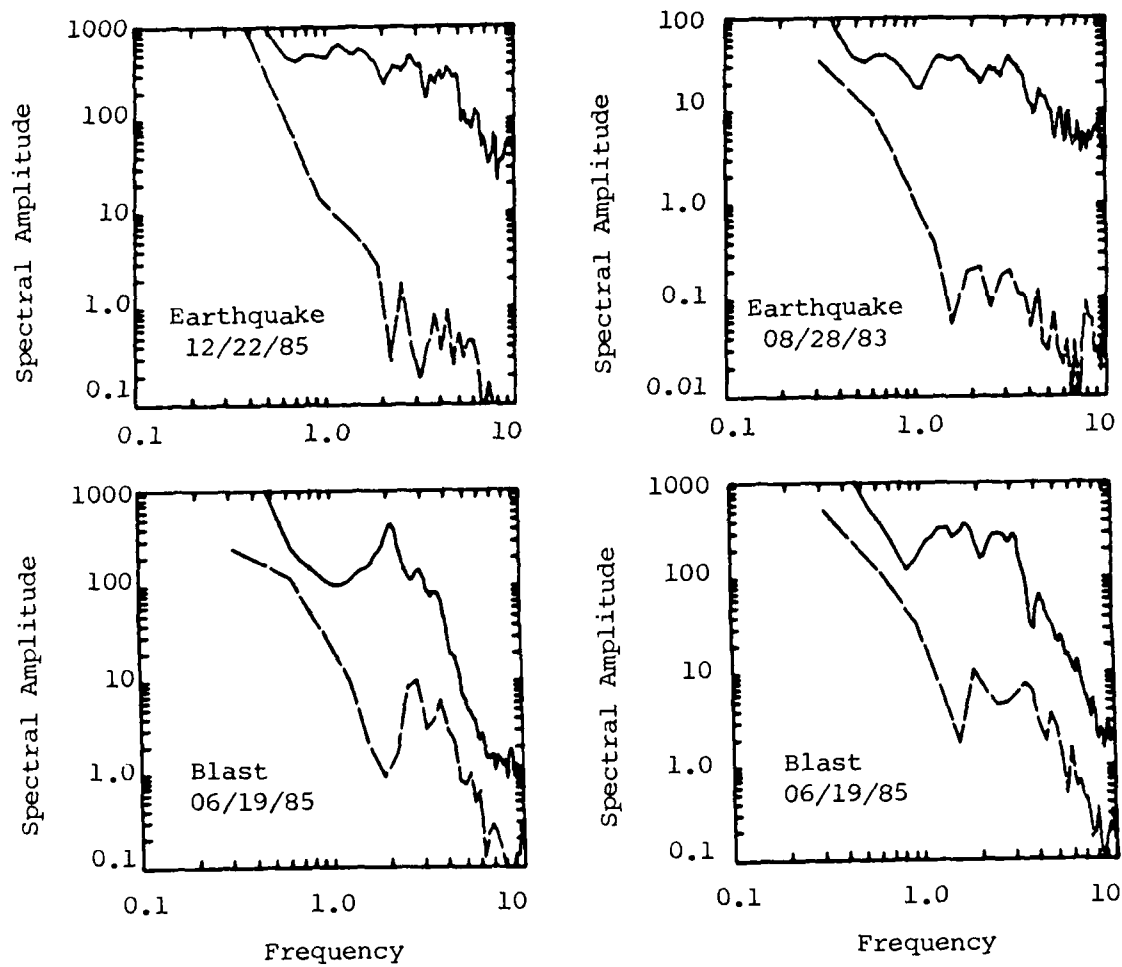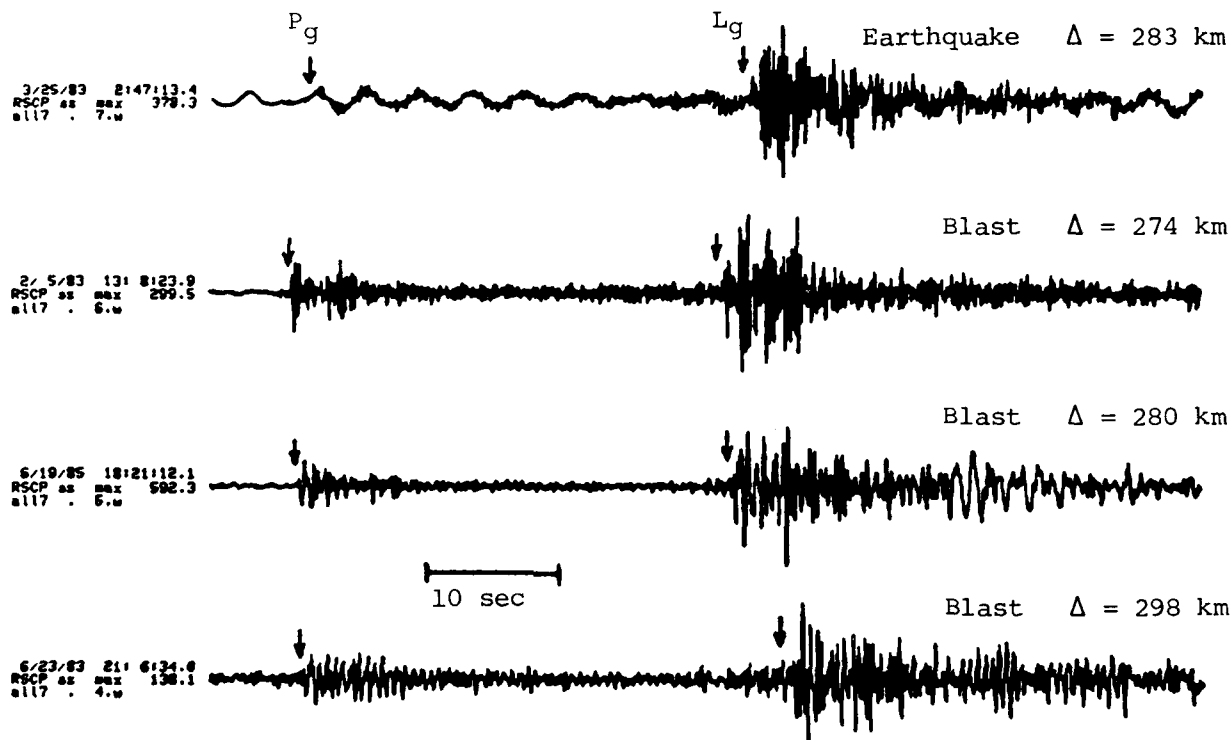Figure 8.   Vertical-component records for four other events
recorded at RSCP.
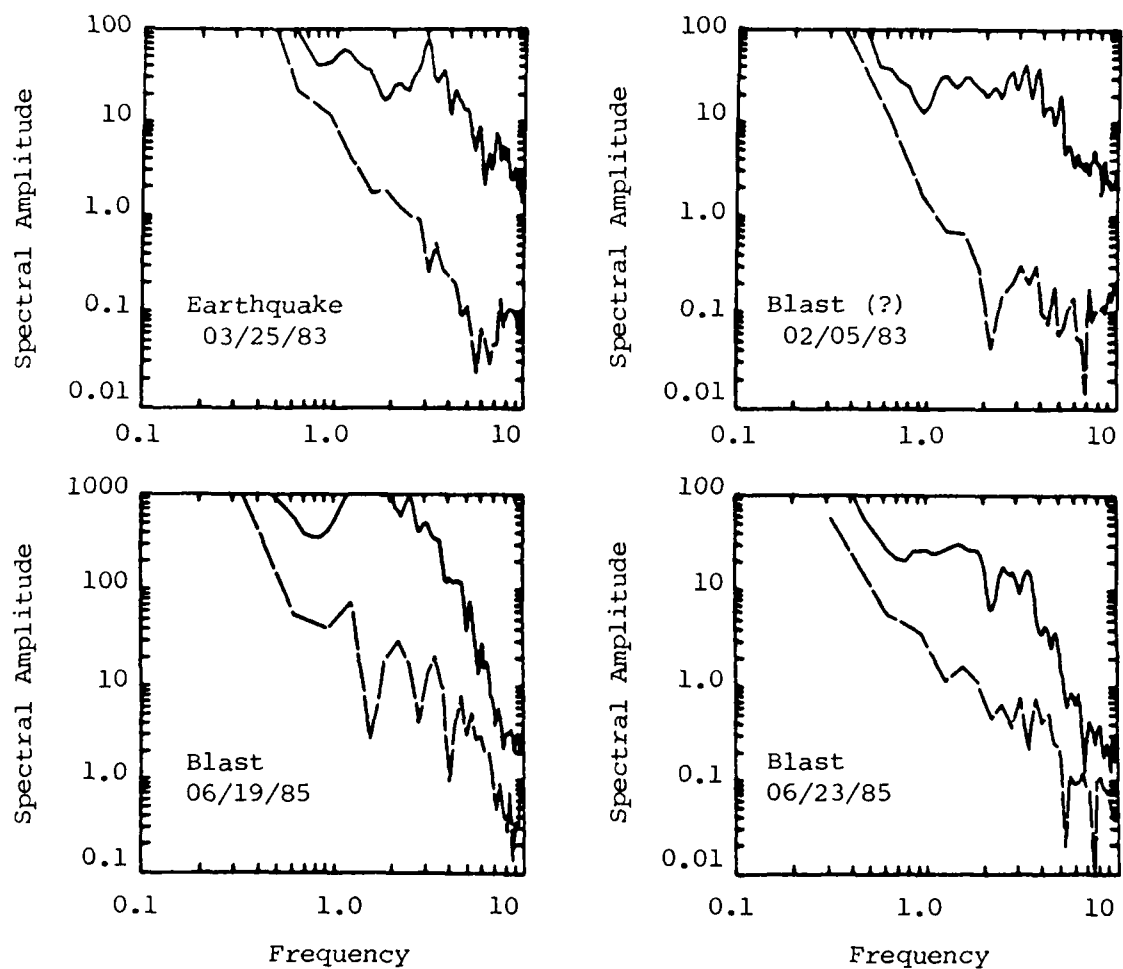
Figure 9. L$_g$ spectra (solid line) and noise (dashed line) for the four events from Figure 8.
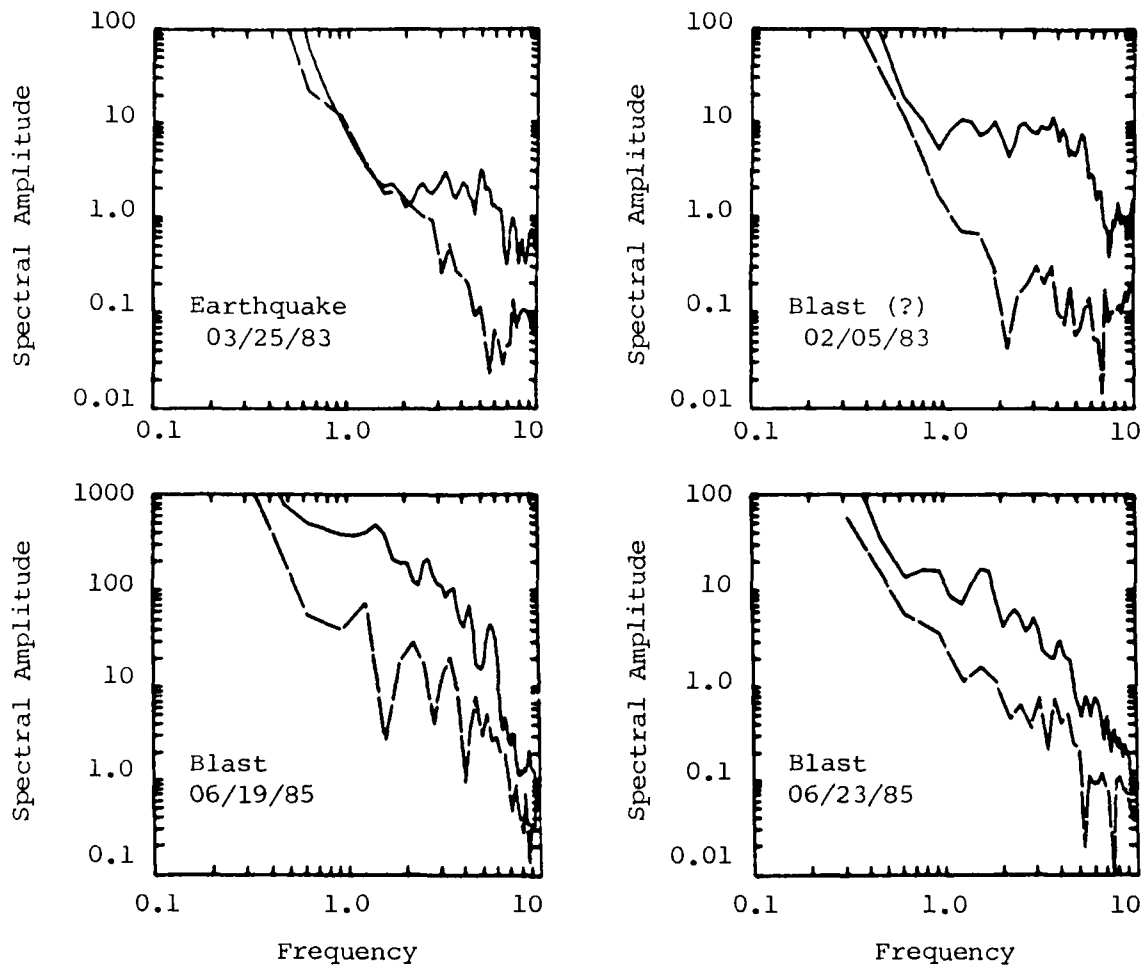
Figure 10. P_g spectra (solid line) and noise (dashed line) for the four events from Figure 8.

quarry blasts recorded on an almost daily basis by RSCP (and some of the other RSTN stations), the regional signals recorded by these stations appear to provide a good data source for investigating the distinctive characteristics of regional phases from quarry blasts in continental platform environments comparable to the Soviet Union.

2.3 Analysis of ECTN Data

The Eastern Canadian Telemetered Network (ECTN) is a relatively-broadband, high-frequency dense network of high-quality stations located in a high-Q region. The network routinely records earthquakes and quarry blasts in the region up to a Nyquist frequency of 30 Hz. Typical events in the magnitude range of 2 to 3 may be recorded at several stations at distances less than 300 km. Therefore, this network provides a good research database to develop and test regional seismic monitoring procedures.

We have converted data for 36 events from ECTN data files to CSS format. The data were kindly provided by the University of Toronto. The 36 recovered events have magnitudes ranging from 0.1 to 5.1 and include 6 or 7 quarry blasts. There are on average about 10 stations recording each event.

Table 3 lists origin data provided by the University of Toronto. Events 20, 23, 34, 35, 36, and 37 were identified as probable quarry blasts. We suspect that event 7 may also be a blast based on the assigned depth of 1 km. Only 8 of the 37 origins have unconstrained depths. The rest of the depths have been assigned by a "Geophysicist". The magnitudes are a mix of "MB", "ML", and "MN". "MB" is the teleseismic m_b magnitude, "MN" is an L_g magnitude, while "ML" is a local Richter magnitude. Eleven of the events have been studied by Chun et al. (1987) with the two station L_g method and Chun et al. (1989) give additional L_g magnitude calibration information for 12 of the events.

The ECTN instruments are relatively broadband instruments recording at 60 samples per second, except GAC which is recording at 30 samples per second. Instrument responses are shown in Figure 11 for the ECTN Mark-I, Mark-II stations (vertical only) and the GAC installation (three components). The station locations are provided in Table 4.

24

Table 3

Origins for Available ECTN Data

DATE			O.T.	N-LAT.	E-LONG.	H(KM)	MAG	#
Oct	04	1983	17:18:40.	43.45	-79.8	2G	3.1MN	1
Oct	07	1983	10:18:46.	43.94	-74.26	13G	5.1MB	2
Oct	07	1983	10:39:39.	43.95	-74.26	8G	3.5MB	3
Oct	11	1983	04:10:55.	45.20	-75.75	14G	4.1MB	4
Oct	16	1983	03:00:47.	45.62	-75.05	12.	3.1MB	5
Oct	16	1983	03:00:47.	45.62	-75.05	12.	3.1MB	6
Oct	24	1983	01:00:06.	48.14	-77.97	1G	3.1MB	7
Oct	03	1983	12:14:15.	44.14	-74.34	18G	2.8MB	8
Nov	01	1983	10:16:52.	45.67	-73.90	18G	3.4MB	9
Nov	16	1983	12:13:56.	47.00	-66.60	5G	3.2MB	1
Nov	17	1983	15:32:18.	47.00	-66.60	5G	3.7MB	11
Nov	18	1983	10:28:40.	47.00	-66.60	5G	3.0MB	12
Nov	27	1983	09:49:24.	46.80	-78.77	18G	2.8MB	13
Dec	04	1983	10:48:25.	45.19	-69.10	18G	3.1MB	14
Dec	08	1983	12:23:05.	45.11	-67.19	7.	3.0MB	15
Dec	09	1983	05:45:14.	44.48	-56.59	18G	3.6ML	16
Dec	09	1983	05:45:14.	44.48	-56.59	18G	3.6ML	17
Dec	01	1983	02:58:58.	44.53	-73.41	18G	2.7MN	18
Dec	01	1983	07:43:55.	45.70	-74.77	11.	2.8MN	19
Dec	11	1983	05:53:42.	45.12	-72.11	1G	2.4MN	20†
Dec	11	1983	01:52:03.	46.70	-76.27	18G	3.1MN	21
Dec	19	1983	20:00:36.	45.24	-66.77	5G	2.1MN	22
Dec	21	1983	15:04:44.	45.21	-73.96	10G	3.0MN	23†
Dec	28	1983	12:24:22.	47.07	-76.28	18G	3.5MN	24
Jan	15	1984	00:49:55.	46.54	-72.10	18G	2.5MN	25
Jan	15	1984	00:49:55.	46.54	-72.10	18G	2.5MN	26
Jan	02	1984	01:52:44.	47.53	-70.03	5.	0.1ML	27
Feb	02	1984	11:15:34.	44.66	-56.38	18G	4.2ML	28
Feb	11	1984	04:27:46.	46.49	-70.03	8.	1.0ML	29
Feb	11	1984	04:27:46.	46.49	-70.03	8.	1.0ML	30
Feb	13	1984	08:23:12.	46.91	-71.42	20G	2.2ML	31
Feb	13	1984	10:23:10.	46.88	-71.35	18G	2.1MN	32
Feb	15	1984	07:34:29.	47.50	-70.05	12.	0.7ML	33
Jul	07	1984	10:20:01.	46.88	-83.17	1G	2.9MN	34†
Jul	21	1984	09:28:00.	49.79	-82.31	1G	2.8MN	35†
Jul	21	1984	09:36:00.	47.94	-80.67	1G	2.8MN	36†
Sep	25	1984	04:00:00.	46.01	-71.37	1G	3.1MN	37†

† Probable Blasts

ECTN INSTRUMENT RESPONSES
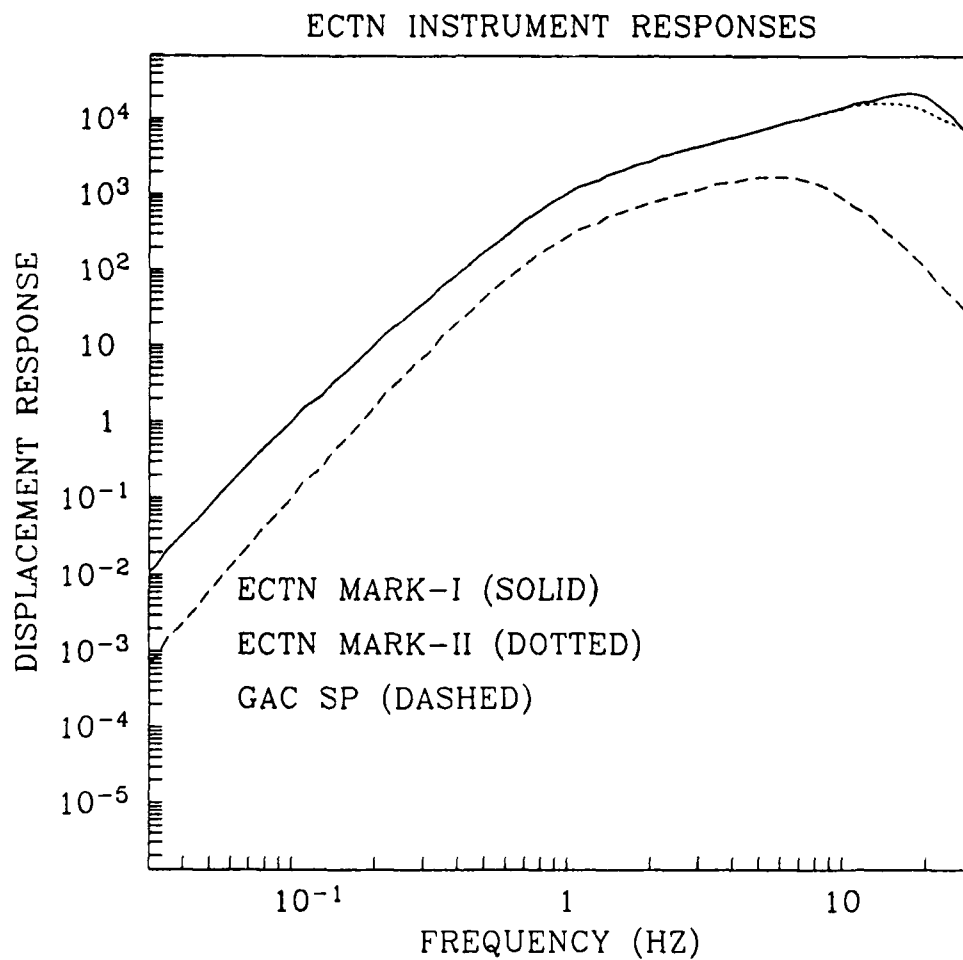
Figure 11. Instrument responses for the MARK-I, MARK-II and GAC systems at ECTN.

26

Table 4

ECTN Station Locations

STA	N-LAT	E-LONG	ELEV(M)	LOCATION
CKO	45.9940	-77.4500	190	CHALK RIVER ONTARIO
EBN	47.4620	-68.2420	195	EDMONSTON N. B.
EEO	46.6411	-79.0733	398	ELDEE ONTARIO
GAC	45.7030	-75.4779	62	GLEN ALMOND QUEBEC
GGN	45.1170	-66.8220	30	ST. GEORGE N. B.
GNT	46.3628	-72.3722	10	GENTILLY QUEBEC
GRQ	46.6067	-75.8600	290	GRAND-REMOUS QUEBEC
GSQ	48.9142	-67.1106	398	GROSSES-ROCHES QUEBEC
HTQ	49.1917	-68.3939	123	HAUTERIVE QUEBEC
JAQ	53.8022	-75.7211	366	LA GRANDE-3 QUEBEC
JBQ	53.6103	-75.6053	381	LA GRANDE-3 QUEBEC
KAQ	53.9833	-73.5230	472	LA GRANDE-4 QUEBEC
KLN	46.8433	-66.3717	411	MCKENDRICK LAKE N. B.
LMN	45.8520	-64.8060	363	CALEDONIA MTN N. B.
LPQ	47.3408	-70.0093	126	LA POCATIERE QUEBEC
MNQ	50.5333	-68.7744	610	MANICOUAGAN S. QUEBEC
MNT	45.5025	-73.6230	112	MONTREAL S. QUEBEC
OTT	45.3939	-75.7158	83	OTTAWA S. ONTARIO
SBQ	45.3783	-71.9263	265	SHERBROOKE QUEBEC
SUO	46.4027	-81.0068	252	SCIENCE N. SUDBURY ONTARIO
TRQ	46.2222	-74.5556	858	MONT-TREMBLANT QUEBEC
VDQ	48.2300	-77.9717	305	VAL-D OR QUEBEC
WBO	45.0003	-75.2750	85	WILLIAMSBURG ONTARIO
WEO	44.0186	-78.3744	149	WELCOME ONTARIO
SCP	40.7950	-77.8650	352	STATE COLLEGE PA. (DWWNSSN)
RSNY	44.5483	-74.5300	357	ADIRONDACK N.Y. (RSTN)
RSON	50.8589	-93.7022	357	RED LAKE ONTARIO (RSTN)

A map is shown in Figure 12 with station and event locations. Stations are indicated with triangles and the three stations SCP, RSNY, and RSON are plotted for reference. Events are plotted as crosses and the probable quarry blasts are indicated with a circle around the cross.

Among the various issues that we wished to address with this data, was the reliable estimation and interpretation of cepstra to be used in discrimination between earthquakes and quarry blasts. Several researchers in recent years have reported the detection of ripple-firing in recordings of quarry blasts (c.f. Baumgardt and Ziegler, 1988; and Smith 1988b). In addition, Alexander and Borkowski (1988) report the use of cepstral methods to estimate pP-P and sP-P times from regional seismograms. With the exception of Alexander and Borkowski, most cepstral analysis has been performed on a single station or a small array of stations. With its density of coverage in a high-Q area, the ECTN has the capability of giving multiple estimates of cepstra and allowing us to gauge the robustness of single station estimates. Also of interest is the bandwidth of the network since cepstral analysis requires the maximum available bandwidth. The ECTN stations have a Nyquist frequency 50 percent higher than the RSTN, DWWSSN, or NORESS array stations. Although the NORESS high-frequency station has a greater sampling rate than the ECTN, it is only one station.

First, we review cepstral analysis and some of the statistics of the estimation procedure. We make several observation about the process of cepstral estimation,

- Cepstral analysis is not an objective model independent analysis.

- There are no published criteria for judging the statistical significance of a cepstral peak.

- Bandwidth is critical to cepstral analysis and most data available does not have enough bandwidth to resolve the smallest time delays associated with ripple firing.

Given these considerations, we derive some statistical criteria for the evaluation of the significance of cepstral peaks and show that there is a maximum likelihood estimator for the combination of network data. The network stacking method of Alexander and Borkowski is related to this maximum

28
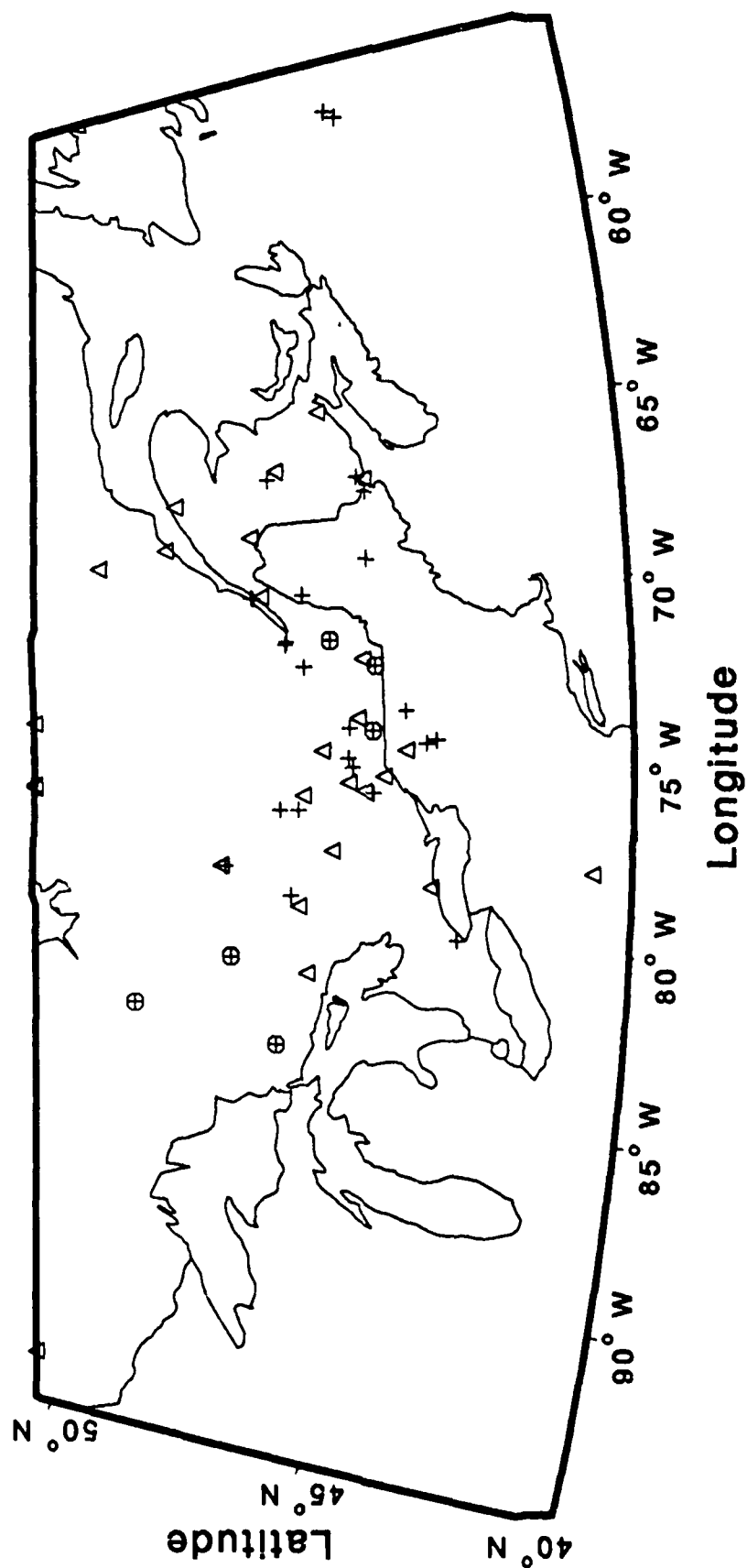
Figure 12. Map of ECTN stations and events. Stations indicated with triangles, events with crosses, and probable quarry blasts with circled crosses.

likelihood network estimator. Given that cepstral estimation is a model dependent procedure, we propose a procedure that balances bandwidth resolution against model dependence by use of a well-defined smoothing operator. Finally, the results for several probable quarry blasts and earthquakes are shown and discussed.

2.3.1 A Review of Cepstral Theory

The cepstrum is defined as the Fourier transform of the log of the power spectrum of the signal (Oppenheim and Schafer, 1975). If $s(t)$ is the time domain signal and $P(f)$ is its power spectrum then the cepstrum, $C(\tau)$, is the spectrum of $\ln(P(f))$. If we write the Fourier transform operator as $F[.,f]$ and the time domain taper as $\theta(t)$ then we have that

$$P(f) = |F[\theta(t)s(t) , f]|^2 = |\Theta(f) \times S(f)|^2$$

$$C(\tau) = F[\ln(P(f)) , \tau] = F[\Pi(f) , \tau]$$

where $\times$ is the convolution operation. The intent of cepstral estimation is to analyze the modulation of the power spectrum. With the use of some algebra, simple identities related to Fourier spectra, and a Taylor series expansion for $\ln()$, it can be be shown (see Flinn et al. , 1973) that if the signal contains an echo of relative amplitude b with time delay τ_0 described by

$$s(t) = a(t) + b\, a(t + \tau_0),$$

then the cepstrum is

$$C(\tau) = F[\ln(P(f)), \tau)] + F[\ln(1 + b^2 + 2b\cos(2\pi f\tau_0)), \tau]$$

$$\approx F[\Pi(f), \tau] + 2bF[\cos(2\pi f\tau_0), \tau]$$

$$\approx \pi(\tau) + 2b\delta(|\tau - \tau_0|).$$

Therefore $C(\tau)$ will have a peak located at $\tau = \tau_0$ and $\tau = -\tau_0$. The size and resolution of the peak will be determined by the relative amplitude of the

30

echo, b, and the shape of the log-power spectrum $\pi(\tau) = F(\Pi(f), \tau)$. This interfering term is the Fourier component of the shape of the log-power spectrum without the echo. Since we are usually interested in small time delays, we are concerned with the shape of the spectrum over large bandwidths. Since no realistic seismic signal has a flat spectrum, it is necessary to remove any trends and general shape of the log-power spectrum prior to estimating the cepstrum. Some model for $\Pi(f)$ is assumed (or fit) in order to remove the interfering effects of the broadband shape of the log-power spectrum. This is analogous to a trend removal and taper in the time domain prior to estimating the power spectrum. As the analogy suggests, this pre-whitening of the log-power spectrum introduces artifacts into the cepstrum just as tapering affects the estimation of the power spectrum. For example, smoothing of the log-power spectrum will introduce a multiplicative response into the cepstrum. We can not escape the fact that the processing at this step is nonlinear and model dependent.

To be precise, we may either add (or subtract) a correcting function, $\zeta(f)$, to the log-power spectrum, multiply (or divide) the log-power spectra by a correcting function, $\kappa(f)$, or convolve a smoothing operator, $\gamma(f)$, with the log-power spectra. The result of adding a correction is,

$$\tilde{C}(\tau) \approx F[(\zeta(f) + \ln(P(f)) + 2b\cos(2\pi f\tau_0)),\tau]$$

$$\approx Z(\tau) + \pi(\tau) + 2b\delta(|\tau - \tau_0|).$$

The result of applying a multiplicative correction is,

$$\hat{C}(\tau) \approx F[\kappa(f)(\ln(P(f)) + 2b\cos(2\pi f\tau_0)),\tau]$$

$$\approx K(\tau) \times [\pi(\tau) + 2b\delta(|\tau - \tau_0|)].$$

And the result of convolving a smoothing operator is,

$$C'(\tau) \approx F[\gamma(f) \times (\ln(P(f)) + 2b\cos(2\pi f\tau_0)),\tau]$$

$$\approx \Gamma(\tau)[\pi(\tau) + 2b\delta(|\tau - \tau_0|)].$$

31

In practice, all three things are done to the power spectrum in order to prepare it for cepstral estimation and we have,

$$C(\tau) \approx \Gamma(\tau)K(\tau) \times [Z(\tau) + \pi(\tau) + 2b\delta(|\tau - \tau_0|)].$$

Generally, the log-power spectrum is pre-whitened by the removal of a trend which is equivalent to assuming the power spectrum is proportional to frequency raised to some power, f^{-a}, where -a is the slope of the log-power spectrum. Since most seismic spectra have this form at high frequencies, this may be a good model. However, since most seismic log-spectra are also concave downward (due to corner frequency and attenuation), the effect of a simple slope correction is to introduce a cepstral signal with broad bandwidth and significant cepstral power at low quefrency. If a signal with 20 Hz Nyquist and 10 Hz corner frequency is subjected to a detrending, a 10 Hz modulation will remain in the log-power spectrum and show up as a 0.1 sec quefrency peak in the cepstrum. This will be true even if the bandwidth from 0 to 20 Hz has infinite signal-to-noise ratio.

The effects of limited bandwidth are even more subtle. If signal-to-noise ratio is such that the bandwidth is limited to a simple window in the frequency domain, such as f_1 to f_2, then the cepstrum will contain the Fourier transform of the spectral bandwidth (boxcar from f_1 to f_2) and a false peak may occur at $1/|f_2 - f_1|$. For example, suppose the 20 Hz Nyquist signal is limited to 2 to 15 Hz, then we can only expect to resolve quefrencies longer than 1/13 seconds. A number of researchers have attributed quefrency peaks shorter than 0.2 seconds to multiple sources with data limited to a 20 Hz Nyquist and bandwidths significantly less than 0 to 20 Hz.

An additional misconception may arise due to padding in the frequency domain. The power spectrum is defined from $-f_N$ to f_N and the cepstrum is computed using a total bandwidth of $2f_N$ that implies an apparent resolution of $\delta\tau = 1/2f_N$. In fact this is misleading, since the power spectrum contains the symmetry, $P(f) = P(-f)$, and the doubling of the power spectrum is only equivalent to a sinc interpolation. The best possible resolution is limited to $\delta\tau = 1/f_N$. As the previous discussion makes clear, practical resolution is limited to the reciprocal of a spectral window for which we have adequate signal-to-noise

ratio, $\delta\tau = 1/|f_1 - f_2|$. Furthermore, it is well known that Fourier estimation of low frequencies is a very difficult problem unless the window includes two or more cycles. These low frequencies (quefrencies in this case) are very sensitive to the de-trending algorithm and leakage from other quefrencies. Consequently, it is unwise to take much stock in detections of quefrencies less than $3/f_N$. For a 20 Hz Nyquist signal this is 0.15 second quefrency or 0.1 second for a 30 Hz Nyquist.

Since pre-whitening is necessary, the procedure is model dependent and the model assumptions must be examined as part of the procedure. It is possible to view the detection of multiple shots as a fitting procedure to the spectra. This is in effect proposed by Smith (1988b) who claims that bandwidths of at least 35 Hz will be required in order to make reliable detections of ripple firing with group delays of 100 to 200 milliseconds. From the point of view of cepstral analysis, this amounts to the $\tau > 3/f_N$ criteria stated above.

Finally, we can examine the detection of cepstral peaks using extensions of statistical methods traditionally applied to the detection of spectral peaks in power spectra. Assuming that the pre-whitening model has been applied correctly then we have $\Pi(f) = \ln(P(f)) + W(f)$ where $W(f) = \ln(w(f))$ is the deterministic pre-whitening correction. We note that $P(f)w(f)$ is distributed χ^2 with two degrees of freedom assuming that $w(f)$ correctly pre-whitens the spectrum (Shumway, 1988). Therefore $\Pi(f) = \ln(P(f)w(f))$ is zero-mean normal with unit variance except for any modulation due to the interference of multiple sources. Then $|C(\tau)|^2$ is the power spectrum of a Guassian white-noise process plus the spectrum of the modulation. We can establish a 95 percent detection criteria for peaks of $C(\tau)$ assuming that $|C(\tau)|^2$ is distributed χ^2 with 2 degrees of freedom in the absence of modulation due to multiple sources. Any peak greater than the 95 percent significance level is considered to be true modulation of the log-power spectrum.

Now in order to pre-whiten the log-power spectra, we choose to subtract a correction spectra derived from the convolution of a smoothing operator (low-pass filter) with the log-power spectrum. In this way we try to minimize the model errors associated with the pre-whitening of the log-power spectrum. We give up resolution of the smallest quefrencies to attain a better (unbiased) estimate of the cepstra for $\tau > \tau_L$. We choose τ_L to be in the neighborhood of $3/f_N$.

33

Figure 13 shows a flow chart that describes the process. The smoothing operator (low-pass filter), $\gamma(f)$ is applied so that the cepstral estimator is given by,

$$C(\tau) = F[2\ln(|F[s(t)\theta(t)),f]| \times (1 - \gamma(f)),\tau],$$

$$= F[2\ln(|S(f) \times \Theta(f)|) \times (1 - \gamma(f)),\tau],$$

$$= F[2\ln(|S(f) \times \Theta(f)|),\tau](1 - \Gamma(\tau)).$$

$\Gamma(\tau)$ decays to zero for $\tau > \tau_L$ such that the cepstra above τ_L are undisturbed.

We have discarded the lowest quefrencies as unreliable. These quefrencies are expected to be diagnostic of the ripple firing usually associated with delays measured in the 0.1 to 0.01 second range. However, if we reexamine the tapered signal as a sum of N subsignals of size b_k with time delays τ_k then

$$s(t) = \theta(t)\sum_{k=1} t_o N b_k a(t + \tau_k)$$

$$P(f) = |\Theta(f) \times A(f)|^2(1 + 2\sum_{k=1} t_o N b_k \cos(2\pi f\tau_k) + \sum_{k,j=1} t_o N b_k b_j \cos(2\pi f(\tau_k - \tau_j)))$$

$$\Pi(f) = \ln(P(f)) \approx 2\ln(|\Theta(f) \times A(f)|)$$

$$+ 2\sum_{k=1} t_o N b_k \cos(2\pi f\tau_k)$$

$$+ \sum_{k,j=1} t_o N b_k b_j \cos(2\pi f(\tau_k - \tau_j)) + \ldots$$

$$C(\tau) \approx F[2\ln(|\Theta(f) \times A(f)|),\tau](1 - \Gamma(\tau))$$

$$+ 2(1 - \Gamma(\tau))\sum_{k=1} t_o N b_k \delta(\tau - \tau_k)$$

34

CEPSTRAL ESTIMATION WITH CONVOLUTIONAL PRE-WHITENING
AND SIGNIFICANT PEAK DETECTION

TIME SERIES
S(t)

APPLY TAPER
T(t)S(t)

POWER
SPECTRAL
ESTIMATION
P(F)

CONVOLVE
WITH
-G(F)

LN(P(F))

SUM

RMS

POWER
SPECTRAL
ESTIMATION

WHITE
NOISE
MODEL

CEPSTRA
C(t)

PEAK
DETECTION

SIGNIFICANCE
LEVELS
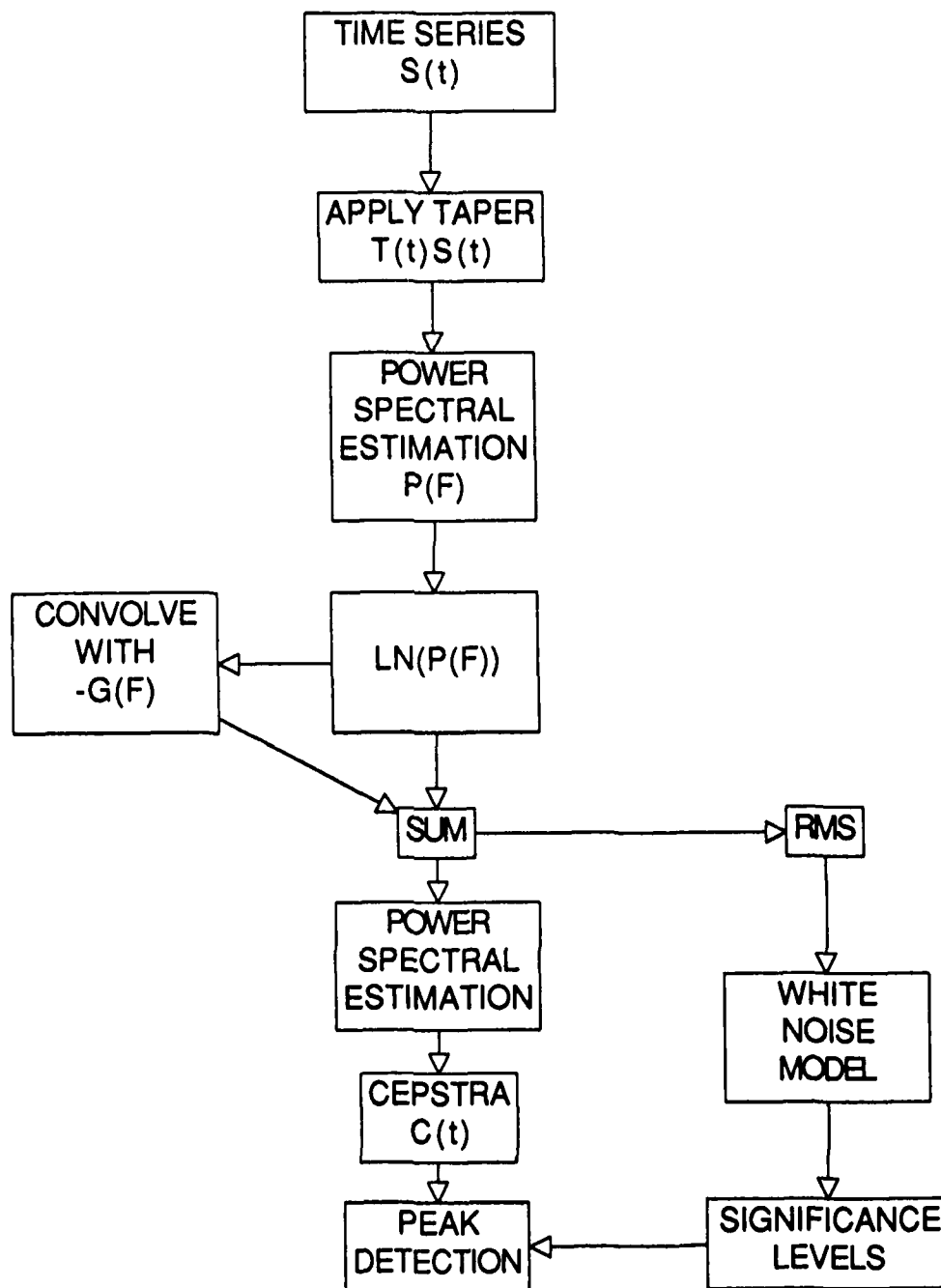
Figure 13. A flow chart describing the estimation of cepstra
using a low-pass smoother $\gamma(f)$ to derive a baseline
log-power spectrum to prewhiten the log-power spec-
tra prior to estimation of cepstra.

$$+ (1 - \Gamma(\tau)) \sum_{k,j=1} t_o N b_k b_j \delta(|\tau - (\tau_k - \tau_j)|) + \ldots$$

Depending upon the shot array $(\tau_1,\ldots,\tau_N)$ the last term may make significant contributions for delays approaching the duration of the shot array. Since the shot arrays are often designed to "stretch-out" the shot duration (Dowding, 1985) in order to minimize high-frequency near-field accelerations, the contribution to the cepstrum of all of the delay differences can not be ignored. A synthetic example is shown in Figure 14 (left). The synthetic shot array consists of 100 shots, 10 rows of 10 shots each. Rows and columns are detonated at 50 msec intervals and a 5 msec standard deviation is assumed for each blasting cap (Dowding page 242). The cepstra are "perfect" in that they do not include any blurring effects due to limited bandwidth, tapering, spectral smoothing, or incoherence between shots that may occur if the individual explosion sources are not identical. Note that significant cepstral peaks occur at multiples of the 50 msec delay between shots. However, a shot pattern may be chosen that shows no isolated peaks. A synthetic 10x10 shot array with 30 and 50 msec delay times is shown in Figure 14 (right). Note the absence of isolated cepstral peaks. Isolated cepstral peaks by themselves may not be sufficient to identify ripple firing.

In order to verify that peaks in the cepstra are significant most researchers have either examined cepstra from different stations or different phases at the same station. Baumgardt and Ziegler (1988) using NORESS data examined the cepstra of different phases. Alexander and Borkowski (1988) used several regional stations and stacked the cepstra from independent stations within the network. Alexander and Borkowski used both a linear (mean) and a non-linear (product) stacking procedure for the cepstra. Given that the cepstra are distributed χ^2, which is approximately log-normal, the geometrical mean of the network is an appropriate averaging procedure. The geometrical mean would constitute a maximum likelihood estimate under these assumptions. Alexander and Borkowski used the product of the cepstra without taking the n'th root as would be required for a geometrical mean. As presented, the cepstral peaks in the work of Alexander and Borkowski are probably misleading with their apparent large signal-to-noise figure. In the following analysis, we compare stacking of the cepstra versus stacking of the power spectra. We find that stacking of the detrended power spectra from the network appears to give a
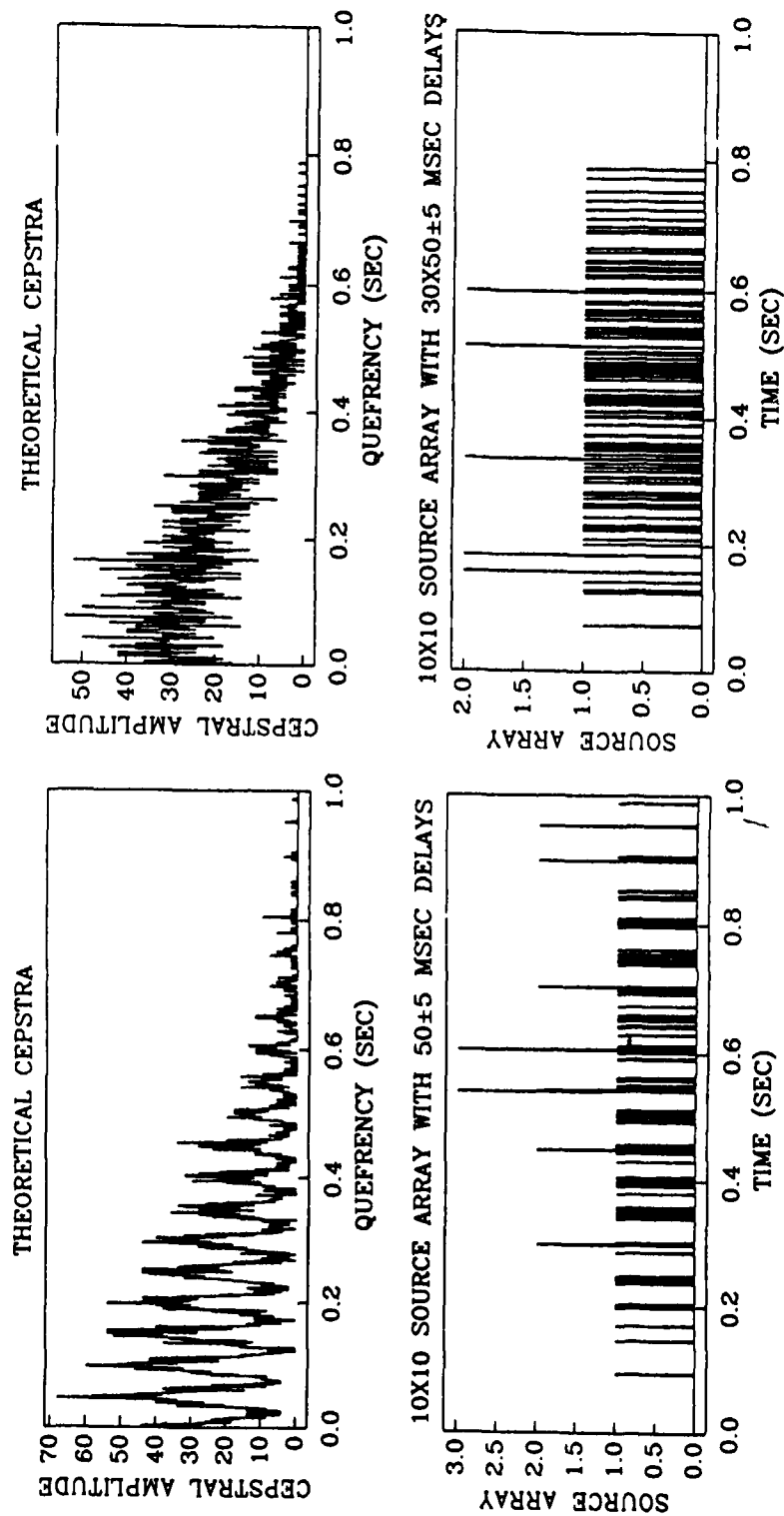
Figure 14. A synthetic rectangular source array of 10 by 10 shots with delays of 50 msec in both orthogonal directions (left) and delays of 50 msec and 30 msec in the two orthogonal directions (right) with 5 msec standard deviation assumed for the blasting caps. The ideal source is shown at the bottom and the theoretical cepstra at the top.

better estimate of the cepstra.

2.3.2 Cepstral Analysis of ECTN Data

Four events were chosen for preliminary analysis, two probable quarry blasts and two earthquakes. The four events had numerous good recordings at a range of distances and azimuths. Preliminary spectra indicated that the P and P_n signals had good signal-to-noise ratios above 20 Hz. The L_g and/or S_n had less predictable high frequency signal-to-noise ratios, so it was decided to concentrate on the P and P_n waveforms.

The average P-wave spectra for the four events are shown in Figure 15A, B, C, and D. The spectra from each station were adjusted to give the same average spectral level in the 4 to 7 Hz bandwidth and log-averaged. The standard deviation of the individual spectra are shown. Note that each network average spectrum appears to have somewhat regular spectral nulls. The earthquakes have corner frequencies in the 5 to 10 Hz range. While, the 12/21/83 quarry blast could be characterized with a corner frequency in the 5 to 10 Hz band, the 09/25/84 event has a broad minimum at 2 Hz and a broad maximum between 5 and 6 Hz. The detrended network average P-spectra are shown in Figures 16A, B, C, and D. They show the modulations apparent in the original network averaged spectra.

We have formed network estimates of the cepstra in two ways. We illustrate these two slightly different procedures with the 12/21/83 event. In the first way, analogous to the procedure of Alexander and Borkowski, we compute the cepstra for each station and then take a geometrical mean of the cepstra. Figure 17 shows the individual cepstra at the bottom and the geometrical mean above. For comparison, the "scaled" product of the cepstra (dashed line) is compared to the geometrical mean. As pointed out above, the product appears to have significant peaks but is deceptive in that it over emphasizes the three largest local maxima. Note the scatter in the individual station cepstra shown below. The 95 percent confidence level is established from the 95 percentile of a cepstrum computed from a Guassian white-noise log-power spectrum with the same rms level as the individual detrended log-power spectra.

38
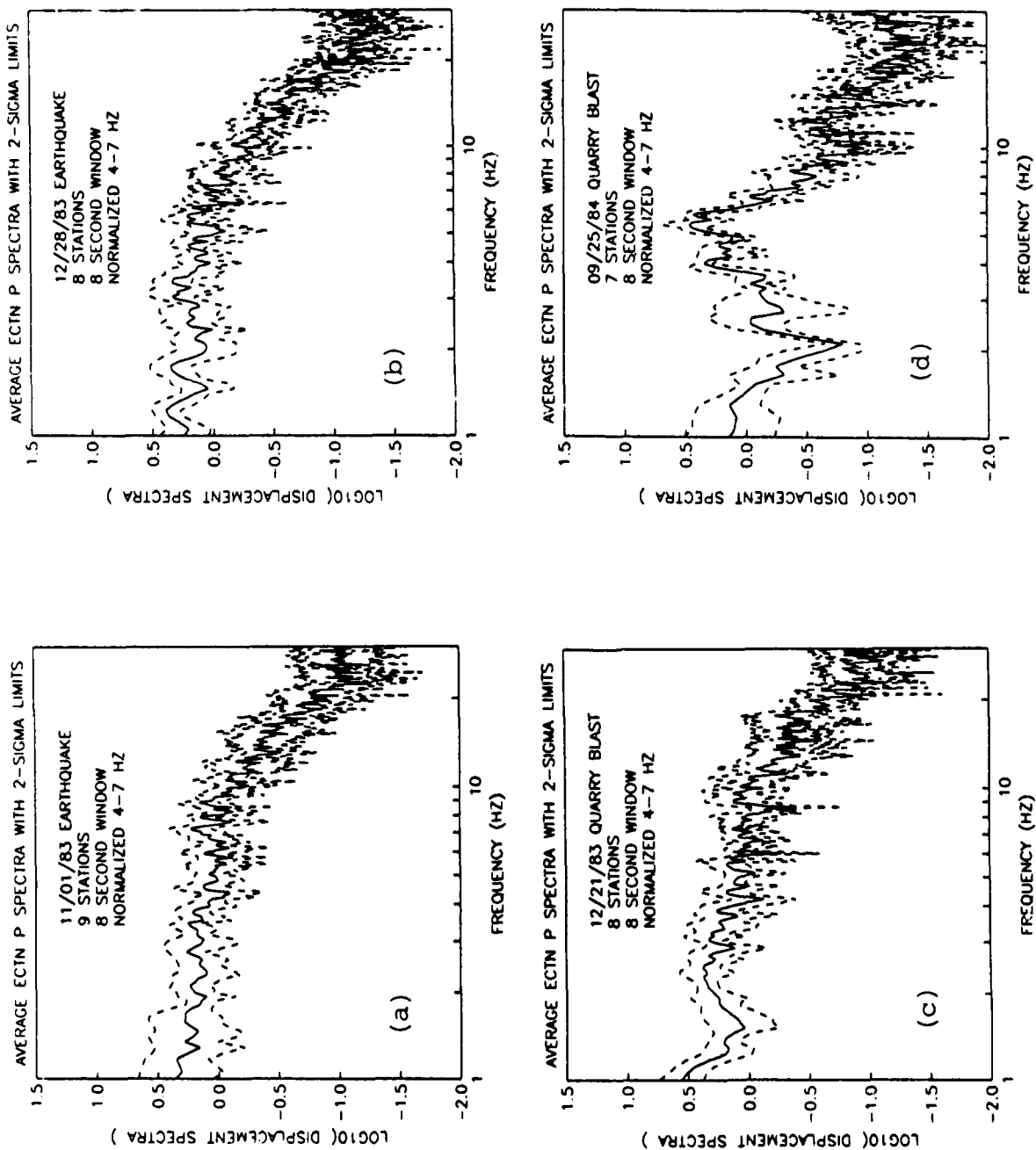
Figure 15. Network-averaged P-wave spectra for events of 11/01/83 (a), 12/28/83 (b), 12/21/83 (c), and 09/25/84 (d). Spectra were normalized in 4-7 Hz passband prior to averaging. Dashed lines indicate ± one sigma bounds.

39
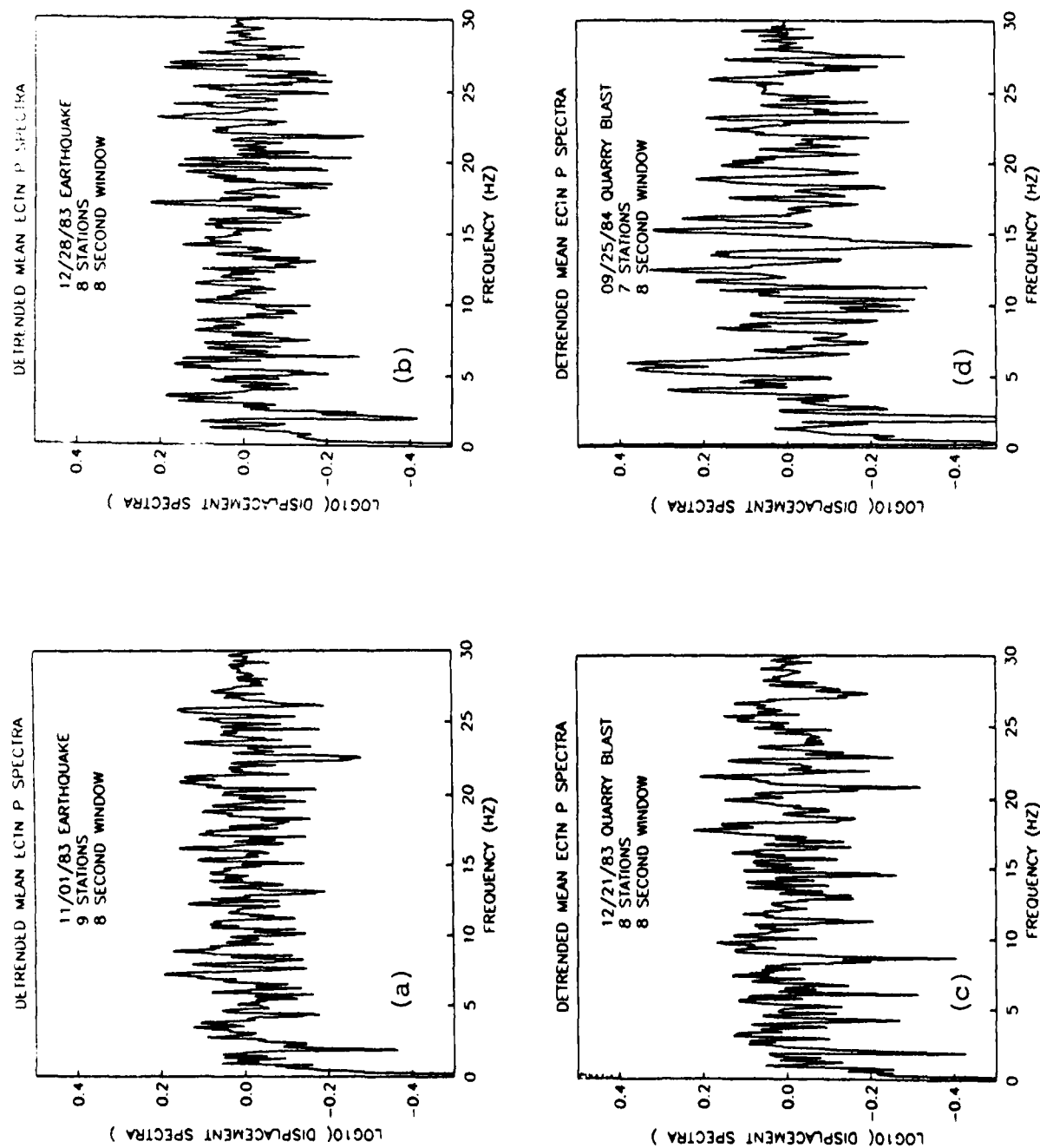
Figure 16. Detrended average P-wave spectra for events from Figure 15.

40
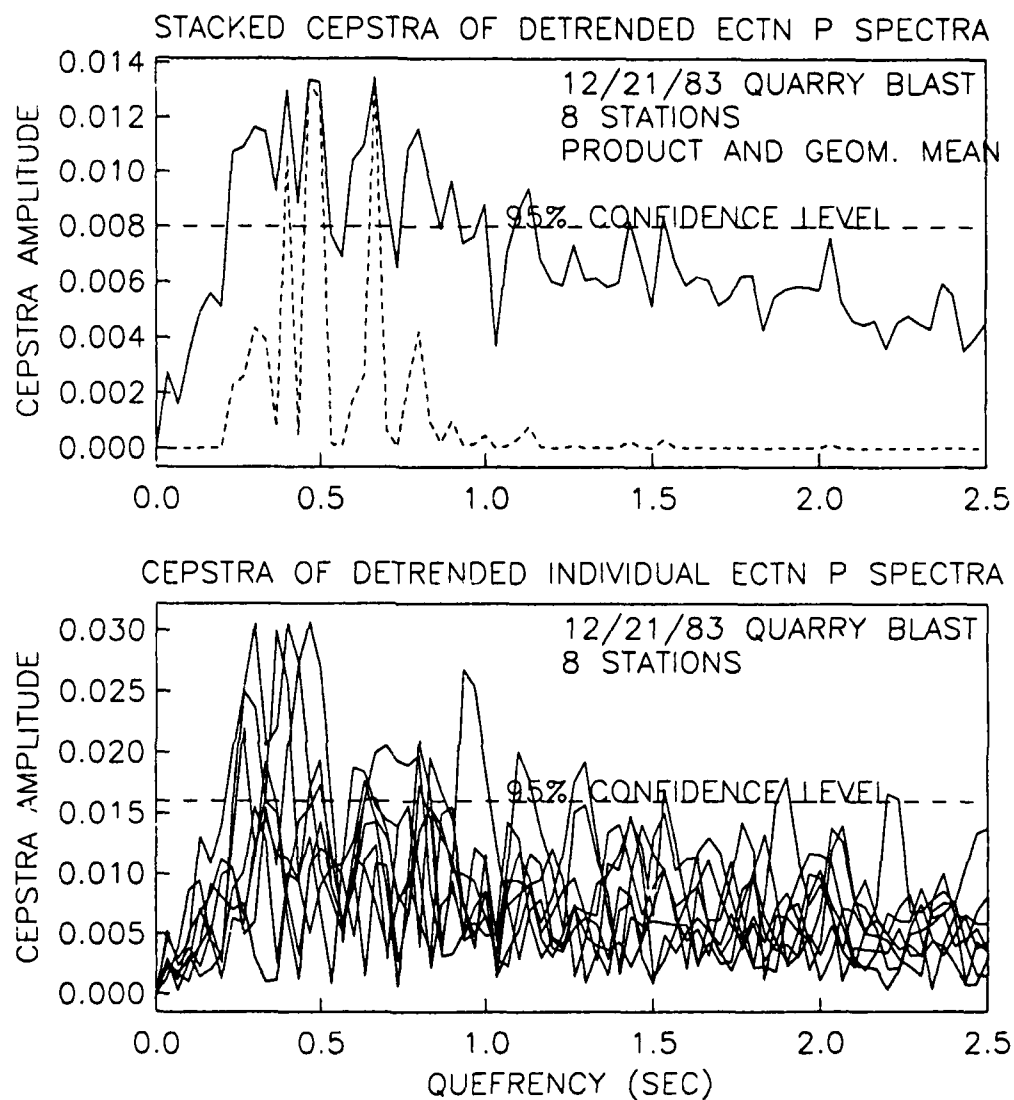
Figure 17. Individual cepstra for 8 different stations
for the 12/21/83 event (bottom). Geometric
mean of the 8 cepstra (solid line) and a
"scaled" version of the product of the in-
dividual cepstra (dashed line) (top).

As an alternative procedure, log-power spectra are averaged and then the cepstrum is computed. This network cepstral estimate is compared with the stacked cepstral estimate in Figure 18. The cepstrum of the stacked spectra (solid line) shows one very large peak at 0.5 seconds and numerous other well defined peaks at the 95 percent confidence level. The same peaks are apparent in the stacked cepstral estimate (dashed line) although the peaks appear to be broader and the background level is higher. There are no strong reasons at this point to prefer one of the two methods over the other; however, the second procedure appears to have a lower background level over a broader quefrency. The log-averaging of the individual power spectra appears to be more stable and lead to a more prewhitened log-power spectrum than the detrending of the individual log-power spectra. This would suggest that the second procedure is better.

Figures 19A, B, C, and D show the network cepstral estimates for the four events (two earthquakes and two probable quarry blasts). Note that all four events exhibit peaks at the 95 percent confidence level.

The two earthquakes have constrained depths of 18 km, and as such would be expected to have cepstral peaks with quefrencies of 5 or 6 seconds if the P+pP were responsible for the spectral modulation. The time window used to analyze the P waves was chosen to be 8 seconds, so we would not expect to reliably detect periodicity within the P waveform with quefrencies longer than 4 seconds. These events would have to be quite shallow to have periodicities caused by pP and sP with quefrencies near 1 second. It is not clear at this time what is responsible for these periodicities in the P waveforms. These periodicities are particularly puzzling, since the spectral modulations are present for a number of stations at different distances and azimuths from the event. Reverberations in the crustal structure could not be expected to be coherent across the network. It is possible that each P-wave path exhibits crustal periodicity and that these cepstral peaks then combine in a fashion not properly modeled by the statistical model proposed above. The null hypothesis that was used to define a significance level assumes that detrended log-power spectra are Gaussian white-noise time series in the absence of source multiplicity. The periodicities may be in the propagation paths. It may be that the proper null hypothesis more correctly assumes that each path has a set of randomly chosen periodicities with a spectrum defined by the range of crustal
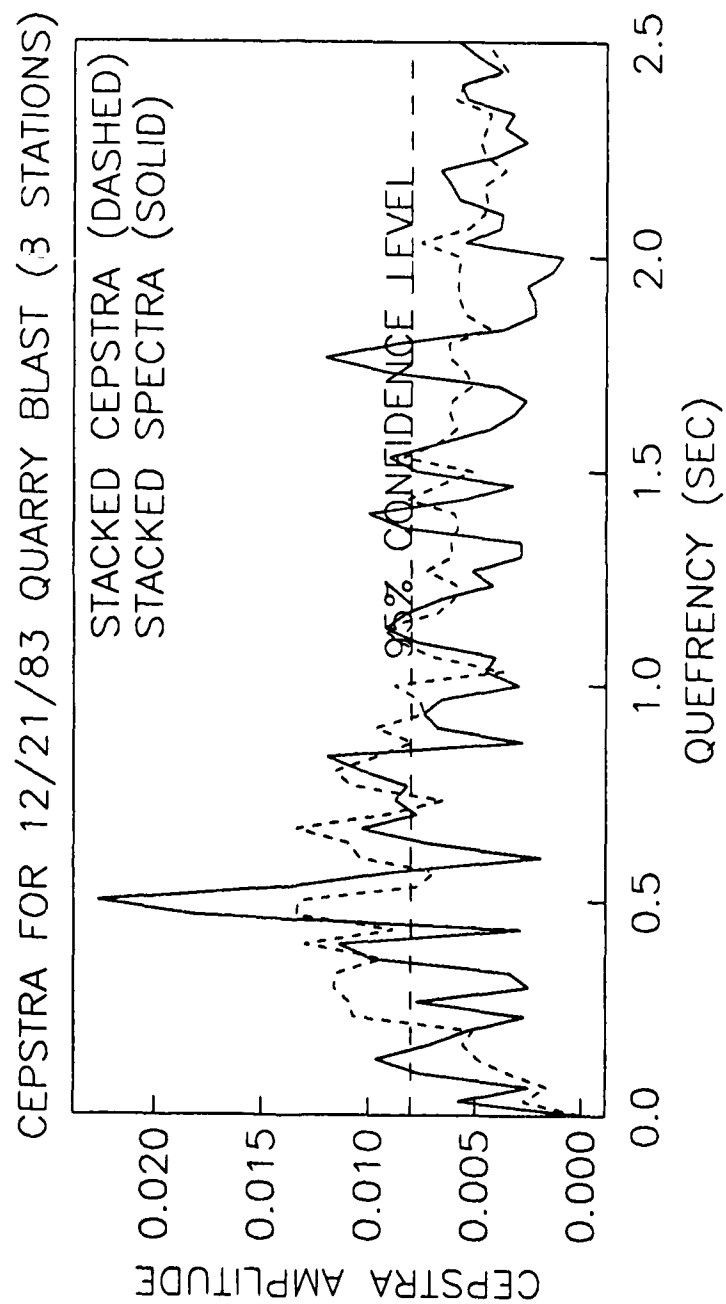
Figure 18. Comparison of the stacked cepstra from Figure 17 (dashed line) with the cepstra derived from the stacked log-power spectra (solid line).
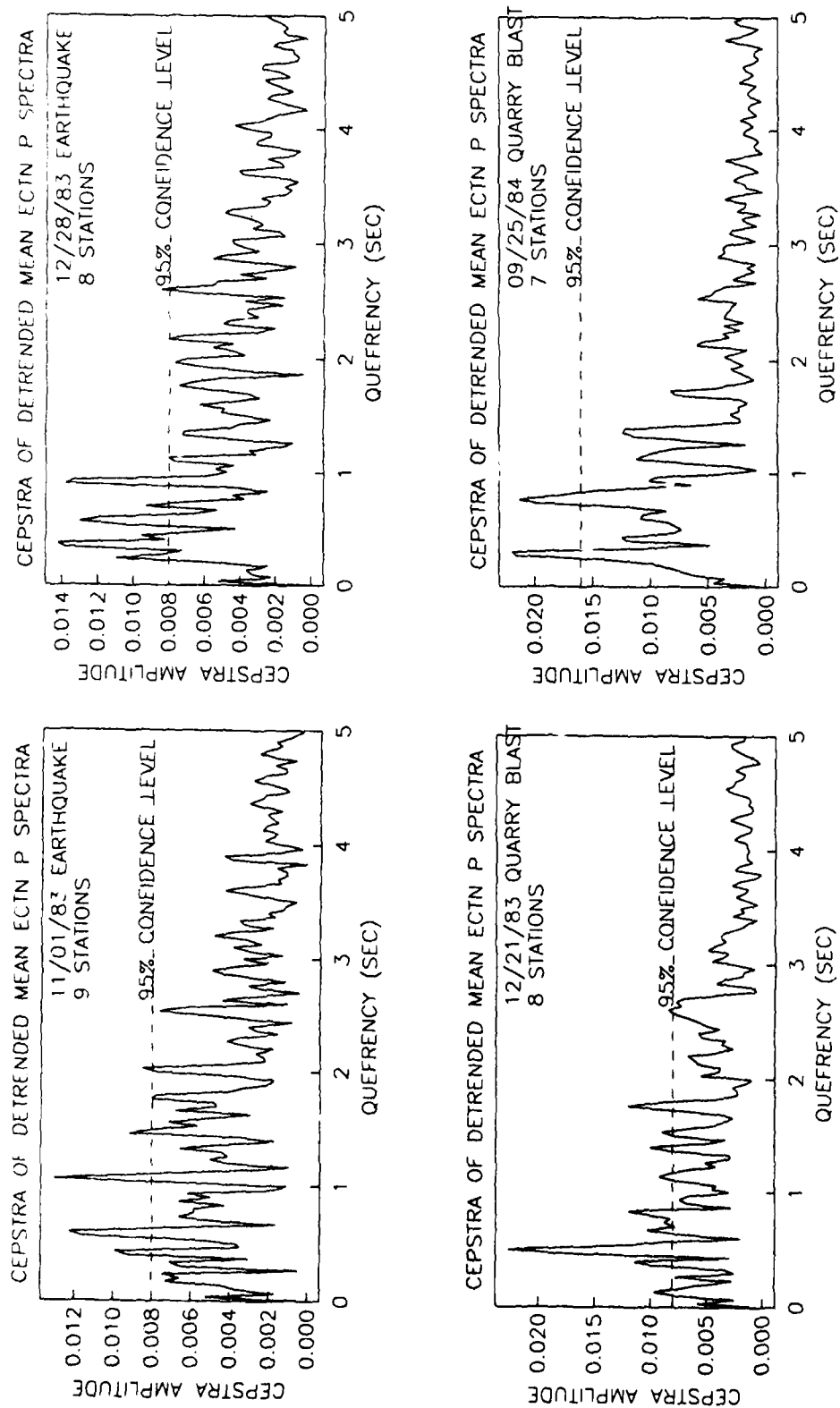
Figure 19. Cepstra from the detrended stacked log-power spectra of Figure 16 for events of 11/01/83 (a), 12/28/83 (b), 12/21/83 (c) and 09/25/84 (d).

structures in the region. One way to evaluate this hypothesis and establish confidence levels will require examination of synthetic P and P_n waveforms for a range of acceptable crustal models.

In summary, both earthquakes and probable quarry blasts recorded by the ECTN show evidence for deterministic modulation of the spectra as detected in cepstra. This spectral modulation requires a repetitive nature for both source types with quefrencies in the 0.2 to 1.0 second range. The cepstral peaks are observed at multiple stations in the network at a range of distances. Since the earthquakes had corner frequencies above 5 Hz, it is unlikely that these periodicities are related to source processes and are rather due to propagation effects. The null hypothesis used to test the significance of the cepstral peaks may be in error. An alternative hypothesis may be that crustal reverberations lead to spectral modulation that mimics multiple sources. This hypothesis could be explored with synthetic seismograms generated for a range of crustal structures.

In the light that false alarms are quite likely in cepstral analysis, the routine use of cepstral estimation may have limited utility for discrimination. The presence of cepstral peaks in the 0.2 to 1.0 second quefrency range is not in itself a reliable discriminant.

III. IDENTIFICATION OF SEISMIC SOURCES
IN THE SOUTHERN SOVIET UNION

3.1 Regional Observations from Soviet Events

To be considered truly reliable, regional discrimination procedures need to be tested on events from areas where the identification procedures are to be applied or, at least, calibrated for those areas. As noted above in Section II, regional seismic data have generally not been available for events in the Soviet Union. A few authors (e.g., Nuttli, 1986; Ringdal, 1988) have systematically measured L_g signal amplitudes at far-regional distances from East Kazakh underground nuclear explosion and used the results to compute L_g magnitudes for correlation with the explosion yield. However, in nearly all cases the paths to the stations used in these studies have been extremely long or tectonically complex resulting in very weak signals and requiring some assumptions about L_g propagation which may not be warranted for the paths involved. In particular, Ruzaikin et al. (1977) suggested that L_g signals were effectively blocked, and not normally attenuated, in crossing some of the tectonically active zones to the south of the Soviet test site. In previous work at S-CUBED, we reviewed the quality of regional phase signals including L_g recorded at SRO and other stations outside the southern Soviet border and concluded that the signals from Soviet explosions in both the East Kazakh and Caspian regions were weak and barely above noise level for most of the events. However, there was evidence that events from the same source regions typically produced stronger L_g signals at larger regional distances to stations in Scandinavia and northern Europe, even though the regional phases themselves were typically highly dispersed and not distinct.

It seems clear from these studies that the observed behavior of the signals and the propagation paths are atypical of the conditions which are anticipated for future in-country monitoring with regional seismic networks or stations. As pointed out above in Section II, the stable continental platform areas interior to the Soviet Union are expected to provide highly efficient propagation environments for regional phases, and particularly L_g, comparable to conditions in eastern North America. Highly efficient L_g transmission in Soviet platform

areas is certainly suggested by the far-regional observations in Scandinavia and northern Europe by Nuttli and Ringdal, which were cited above. However, the far-regional measurements do not truly represent normal regional monitoring which typically utilizes stations at ranges less than 2000 km and more often ranges less than 1000 km.

Only recently high-quality seismic data recorded at normal regional distance ranges from events near the Soviet East Kazakh test site have started to become available. These data are from two sources: the Chinese Digital Seismic Network (CDSN) and the joint Soviet/Natural Resources Defense Council (NRDC) temporary network surrounding the East Kazakh test site. The former has recorded numerous Soviet underground nuclear explosions and earthquakes at comparable magnitudes and ranges while the latter recorded mainly a large number of Soviet commercial blasts of small magnitude at nearer ranges. The data provide a good source for investigating the characteristics of regional phase propagation in more representative tectonic environments and for assessing the capabilities and problems which may arise for future in-country regional seismic monitoring around East Kazakh.

3.2 Analysis of Regional Signals from the CDSN

In analyzing the regional signals from underground nuclear explosions and earthquakes recorded by the CDSN, we focused on observations at station Urumchi (WMQ) which is the nearest station to the principal Soviet test site in East Kazakh (cf. Figure 20). Preliminary review of data from the WMQ site (cf. Bennett et al. , 1988) had indicated the potential of this station for recording good regional signals, including L_g, from East Kazakh explosions (R ≈ 970 km) and earthquakes at comparable ranges. Installation of the high quality digital station at WMQ in 1986 greatly enhanced the station's capability and made the waveform data easily accessible for analysis. In this study we attempted to recover the digital seismic signals from all East Kazakh underground nuclear explosions which occurred since the installation of the digital station. After reviewing the digital data from some of the earlier explosions, we found that there appeared to be a problem with station triggering which caused the recording system to shut off prior to arrival of L_g and not restart at the time of L_g even though the signal level was much higher than the background noise at the time of shutdown. As a result the L_g signals were missed. This was most
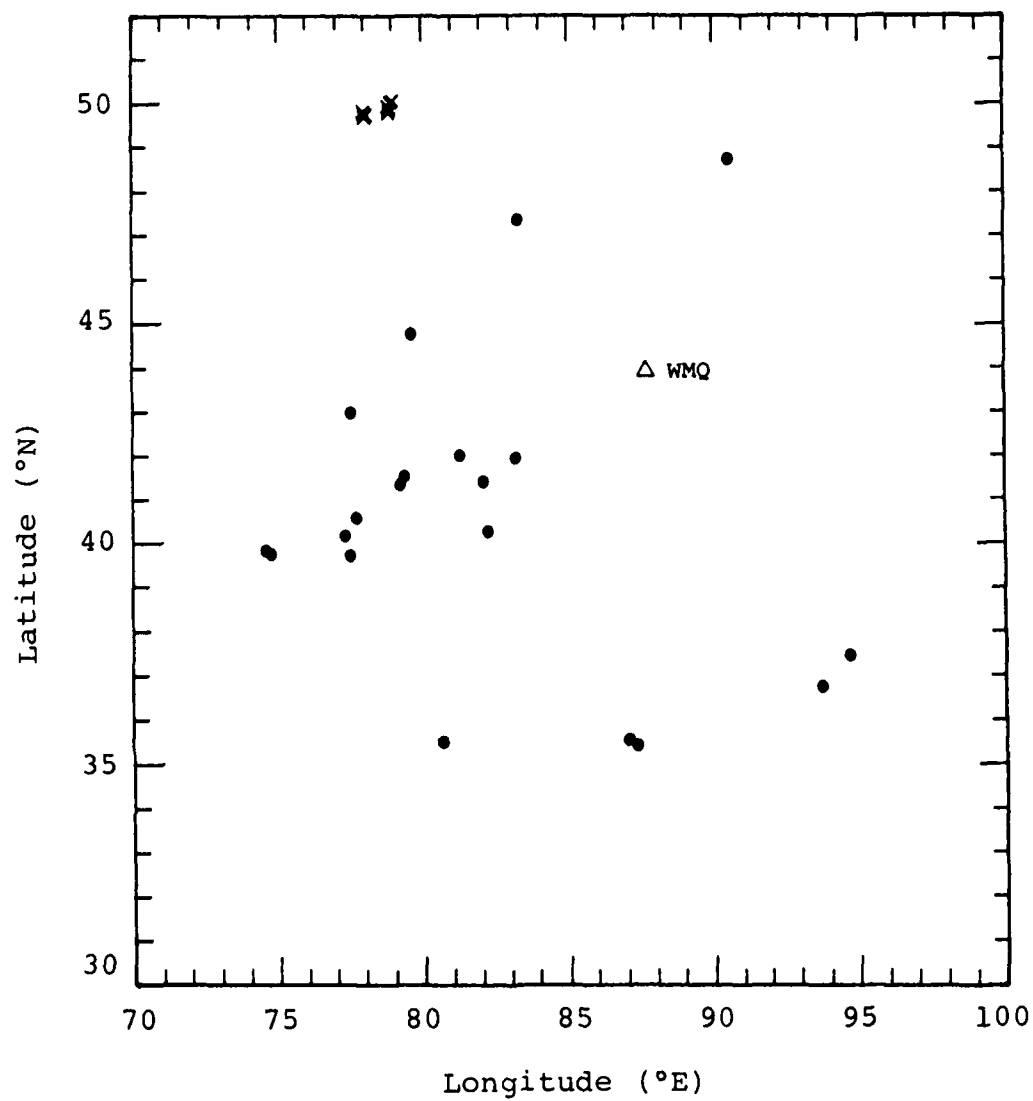
Figure 20. Locations of East Kazakh nuclear explosions (x) and regional earthquakes (●) in WMQ data-base.

problematic for the high sampling rate channels (40 samples/sec); in many cases the intermediate sampling rate channel (20 samples/sec) included the L_g signal window for these same events although even there the system occasionally shutdown before the end of the L_g signal. This triggering problem was ameliorated to some extent by a change to the detection algorithm, but we decided to use the intermediate channel in these analyses. We found that the intermediate channel provided a somewhat more complete event sample and still recovered most of the useful frequency band where signal-to-noise level was adequate at the ranges involved.

Figure 20 shows the locations of 12 underground nuclear explosions at East Kazakh for which the regional recordings at WMQ were analyzed. Table 5 provides the source information on these events. The magnitudes were between 4.7 and 6.2 m_b. The range of the explosions from WMQ was from 945 to 992 km with the nearer events located at Shagan River and the farther at Degelen Mountain. To develop a comparable earthquake sample, we searched the National Earthquake Information Service (NEIS) event list for events since the time that WMQ was converted to digital recording. In this search we attempted to identify earthquakes with magnitudes comparable to those of the explosions and located at distances from WMQ which encompass the distance range for the explosions. It is well known that the area surrounding the East Kazakh test site is virtually aseismic, so comparable earthquakes were not available which would have transmission paths close to those of the explosions. We were, therefore, forced to select from a more diffuse set of events. Figure 20 shows the locations of the 20 earthquakes for which regional signals from WMQ were recovered. The source information on these earthquakes is summarized in Table 6. The earthquakes had magnitudes between 4.5 and 5.9 m_b, and the distances from WMQ were between 423 and 1176 km.

Figure 21 shows representative examples of the vertical component records obtained at station WMQ for four explosions and four earthquakes. The regional records from both source types normally show strong, complex P and L_g phases. At this distance range the P waves from the explosions are typically dominated by early, high-frequency P phases which apparently correspond to paths in the deep crust or upper mantle. The P_g phase is not particularly distinct, appearing as a segment of increased amplitude coda

49

Table 5

East Kazakh Underground Nuclear Explosions

Date	Origin Time	Lat.(°N)	Lon.(°E)	Δ(km)	m_b
03-12-87	01:57:17.3	49.93	78.78	956	5.4
04-03-87	01:17:08.0	49.93	78.83	956	6.2
05-06-87	04:02:05.7	49.83	78.13	989	5.6
06-06-87	02:37:07.0	49.86	78.10	992	5.3
06-20-87	00:53:04.8	49.91	78.74	956	6.1
08-02-87	00:58:06.8	49.88	78.92	945	5.9
12-20-87	02:55:06.3	49.83	78.00	996	4.7
02-13-88	03:05:05.9	49.95	78.91	956	6.1
04-03-88	01:33:05.7	49.89	78.96	945	6.0
04-22-88	09:30:06.7	49.79	78.11	987	4.9
05-04-88	00:57:06.8	49.92	78.76	956	6.1
06-14-88	02:27:06.4	50.02	78.99	956	4.9

Table 6

Regional Earthquakes Recorded at WMQ

Date	Origin Time	Lat.(°N)	Lon.(°E)	Δ (km)	m_b
12-14-86	03:19:16.7	47.31	83.31	517	5.0
12-20-86	23:08:16.5	36.75	93.66	940	5.3
01-05-87	22:52:46.5	41.96	81.32	578	5.9
01-24-87	08:09:21.3	41.53	79.32	732	5.9
01-24-87	13:40:40.3	41.44	79.25	742	5.2
03-05-87	02:33:39.3	35.41	87.39	934	4.5
04-09-87	07:25:35.7	35.50	87.07	926	4.8
04-09-87	20:01:19.5	35.51	80.65	1102	4.9
04-30-87	05:17:37.0	39.76	74.57	1168	5.7
06-08-87	13:30:32.8	39.75	74.62	1176	5.1
08-05-87	10:24:21.1	41.36	82.11	534	4.8
12-03-87	23:51:42.9	39.66	77.48	967	4.7
12-06-87	16:20:45.2	37.44	94.61	912	4.7
12-17-87	12:17:25.6	41.94	83.20	423	5.1
01-02-88	22:02:36.0	40.06	77.34	956	4.9
03-25-88	02:07:55.8	44.71	79.60	656	4.5
05-02-88	02:13:26.3	40.26	82.20	600	4.9
05-25-88	00:05:22.8	40.57	77.62	912	4.9
06-17-88	13:30:45.0	42.94	77.50	834	5.3
07-23-88	07:38:09.9	48.72	90.51	589	5.5

51

m_b = 5.3, R = 992 km

m_b = 5.6, R = 989 km

m_b = 5.9, R = 945 km

m_b = 6.1, R = 956 km

50 sec

m_b = 4.9, R = 912 km

m_b = 5.5, R = 589 km

m_b = 5.7, R = 1168 km
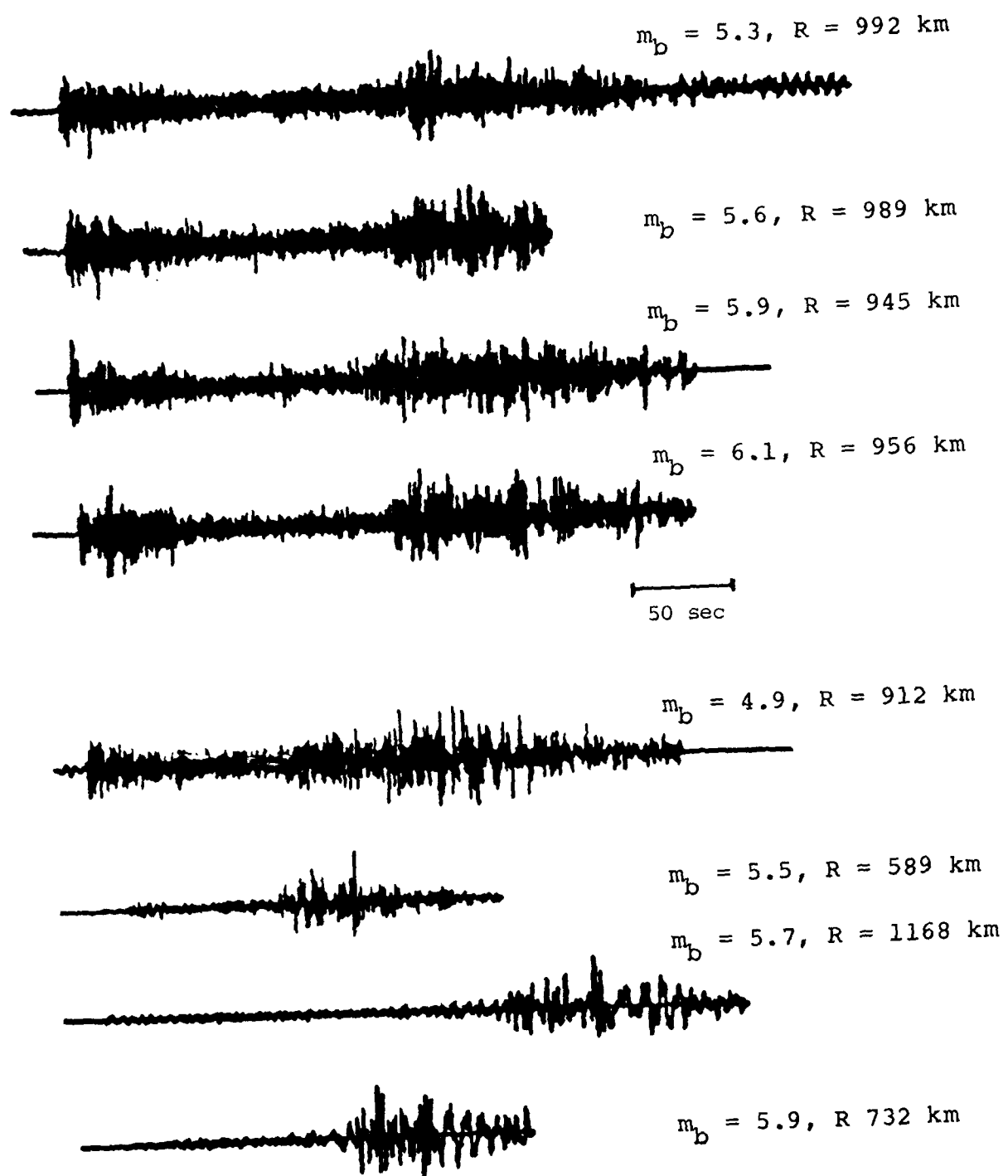
m_b = 5.9, R 732 km

Figure 21. Vertical-component records at WMQ from four nuclear explosions (top) and four regional earthquakes (bottom).

52

trailing the earlier P arrivals. L_g appears as a long-duration, complex phase with a peak amplitude which is frequently as large as the P phase on these broad-band recordings from the explosions. For the earthquakes the P phases are generally smaller in amplitude than the L_g phases, and multiple phases are frequently apparent depending on the epicentral distance. L_g signals are strong and of long-duration for the earthquakes and in some cases are preceded by an S_n phase which wasn't apparent in the explosion signals.

We made peak amplitude measurements of P and L_g signals from the broadband records of the explosions and earthquakes at WMQ. Figure 22 shows the S_{max}/P_{max} and L_g/P_g peak amplitude ratios for these events. The S_{max}/P_{max} ratio compares the peak amplitudes before and after S_n arrival time while L_g/P_g compares peak amplitudes in the appropriate group velocity windows (i.e., near 6 km/sec for P_g and less than 3.6 km/sec for L_g). In nearly all cases the S_{max} corresponded to the L_g peak, but as noted above P_{max} seldom corresponded to P_g. The ratio measurements provide fairly good separation between event types with generally larger ratios for earthquakes than for explosions. In order to clarify and possibly enhance these differences, we performed a band-pass filter analysis using a suite of seven narrow-band filters. The filter passbands were 0 to 1 Hz (center frequency $f_c = 0.5$ Hz), 0.5 to 2 Hz ($f_c = 1.25$ Hz), 1 to 3 Hz ($f_c = 2$ Hz), 2 to 4 Hz ($f_c = 3$ Hz), 3 to 6 Hz ($f_c = 4.5$ Hz), 4 to 8 Hz ($f_c = 6$ Hz), and 6 to 12 Hz ($f_c = 9$ Hz). Above and below the corners the filter response dropped off at 48 dB per octave. After filtering we recomputed the S_{max}/P_{max} (L_g/P_{max}) amplitude ratios for the various events as a function of the center frequency of the bandpass filter. Figure 23 shows the results of those measurements for the individual events. The L_g/P_{max} ratios in all cases start out well above 1.0 at low frequencies, but the ratios rapidly decay toward higher frequencies. The ratio measurements for both types of events start to level off at higher frequencies with the earthquakes leveling off at higher ratios. As a result, the ratios are observed to be somewhat intermingled with respect to event type at frequencies below about 2 Hz but completely separated at higher frequencies. The L_g/P_{max} ratios for the earthquakes are generally much higher than for the explosions above about 3 Hz. Figure 24 shows the average L_g/P_{max} ratios for the two event types as a function of frequency. Superimposed on these curves are the 95 percent confidence bounds on the means which were estimated using the data from Figure 23. The only area where the confidence bounds overlap is for the lowest center frequency
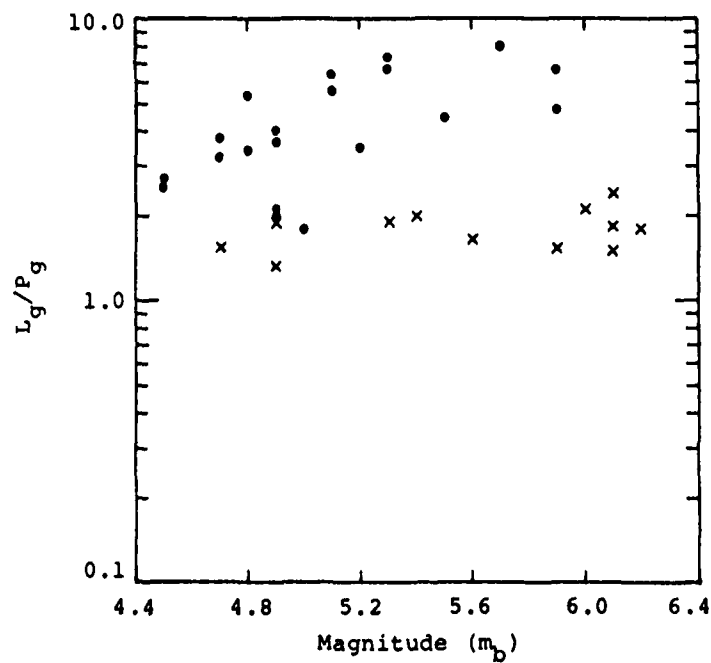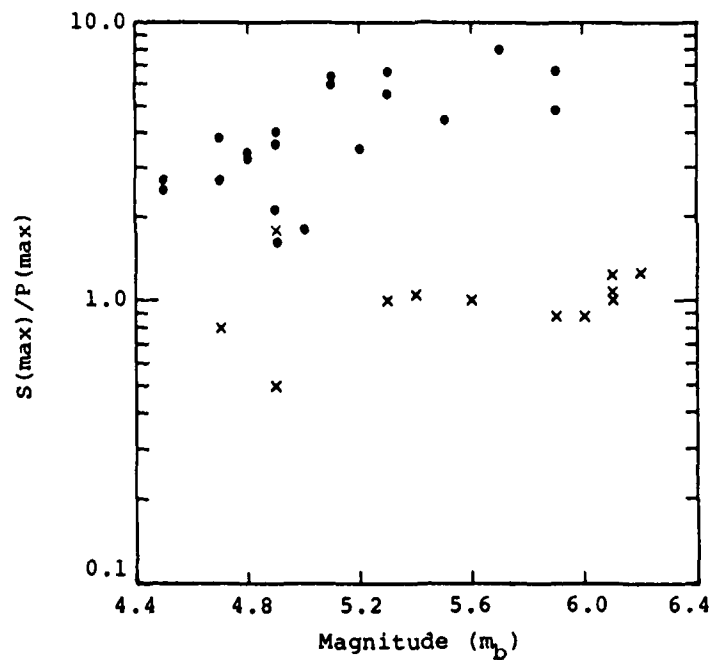
Figure 22. Peak amplitude ratios for S_{max}/P_{max} (top) and for L_g/P_g (bottom) measured from broad-band recordings at WMQ.
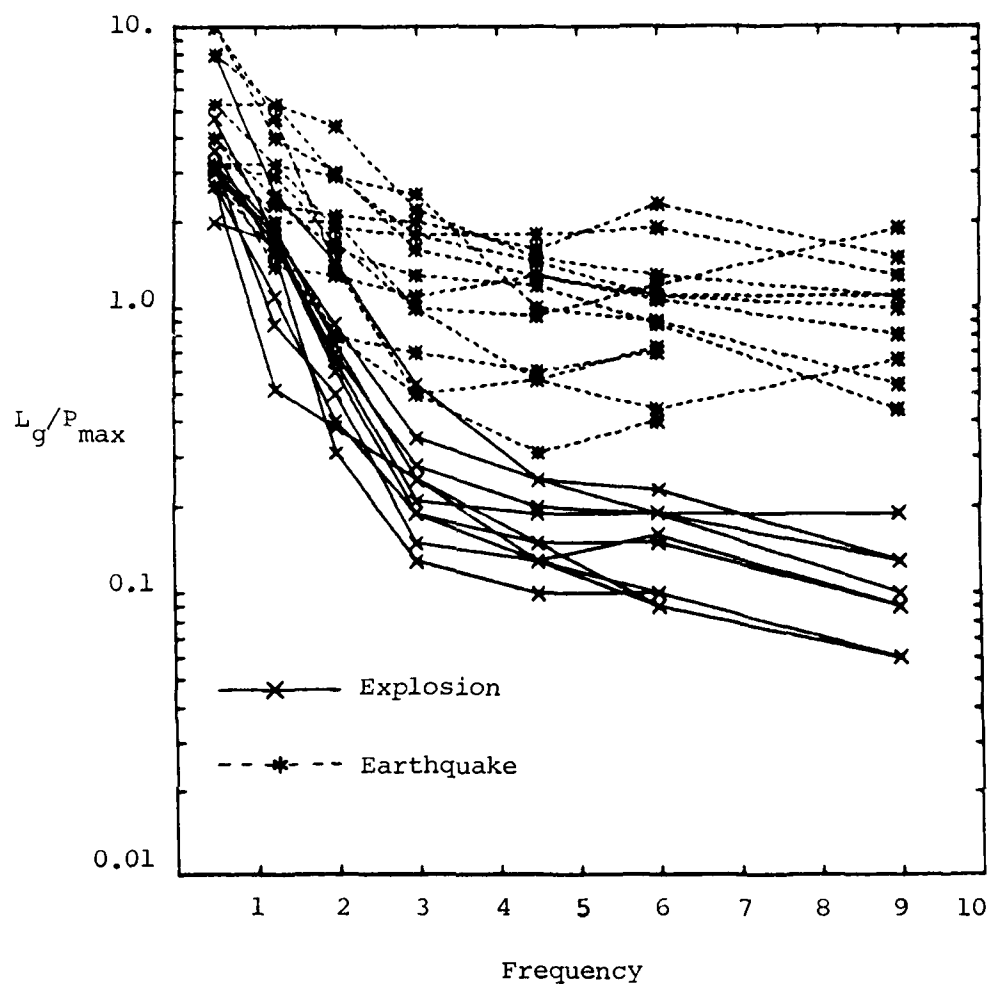
Figure 23. L_g/P_{max} ratios as a function of frequency for explosions and earthquakes recorded at WMQ.
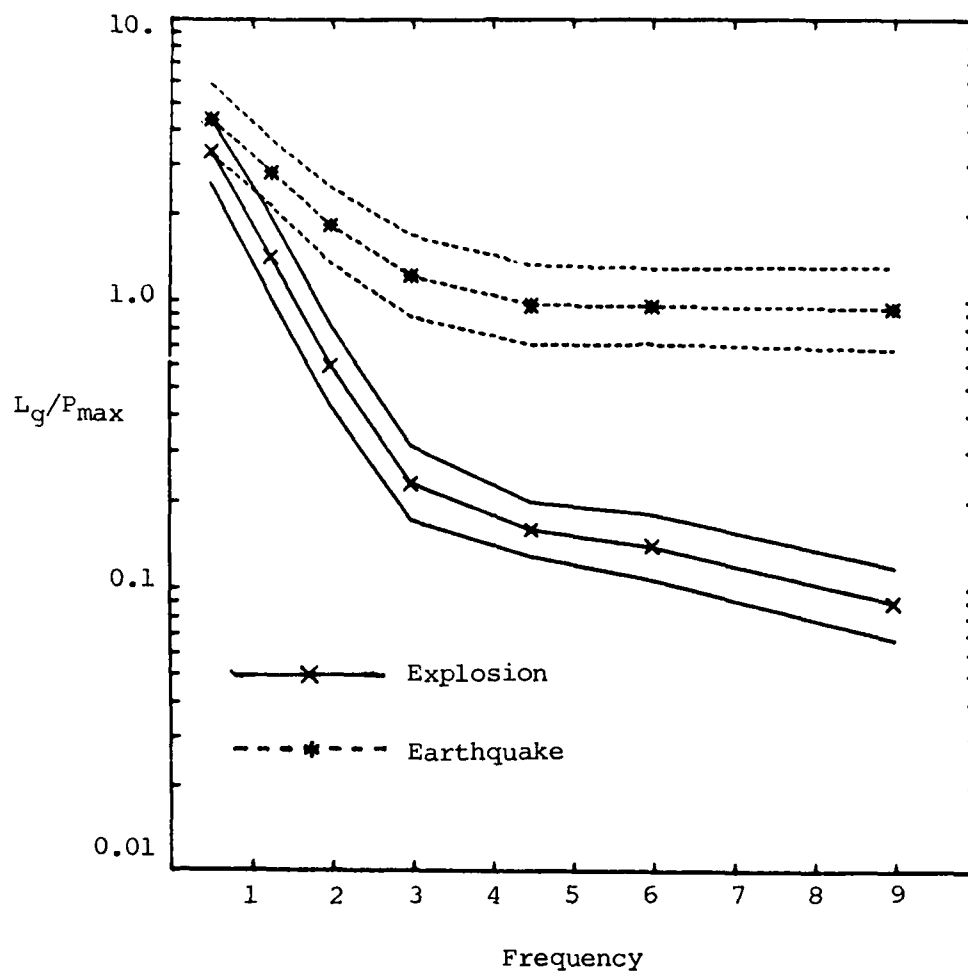
Figure 24. Average L_g/P_{max} ratios as a function of frequency for explosions and earthquakes recorded at WMQ.

(viz 0.5 Hz); at 1 Hz and above the L_g/P_{max} amplitude ratios are completely separated at the 95 percent confidence level. Furthermore, it appears that the separation between the measurements tends to increase toward higher frequencies. At the low-frequency end the average L_g/P_{max} ratio is about 4.4 for the earthquakes and about 3.3 for the explosions. The average earthquake curve levels off at a value near 1.0 above about 3 Hz. The average explosion curve falls off more rapidly out to 3 Hz and continues to fall off, at a somewhat slower rate, at higher frequencies. As a result, the average amplitude ratios are separated by almost an order of magnitude at higher frequencies.

Figures 25 through 27 show comparisons of the S/P amplitude ratio in two different frequency bands for various combinations of regional phases. Since the S measurement in virtually all cases corresponded to L_g, the different figures actually represent comparisons of the excitation of the different P phases relative to L_g. Figure 25 shows the S_{max}/P_{max} ratios for filter passbands of 3 to 6 Hz (top) and 0 to 1 Hz (bottom). The ratios are completely intermingled for the low-frequency band but well-separated for the high-frequency band. There is no apparent trend in the amplitude ratios with respect to magnitude. The results point out a need for care in dealing with observations obtained from seismic systems with sharply peaked response characteristics. Discriminants which rely on differences in a limited frequency band could provide false identifications at other frequencies. Figure 26 shows a similar plot for L_g/P_n ratios, where P_n is taken as the first arrival. In this figure the arrows indicate that the measurements represent either upper or lower limits on the actual ratios; in most cases this is only an artifact of the measurement procedure and could have been corrected by scaling the time histories differently. In any case, we again see some intermingling at the low frequencies and complete separation at high frequencies. It is interesting that for the lower-frequency passband the separation is actually better for the L_g/P_n ratio than for the S_{max}/P_{max} ratio in the previous figure. For the earthquakes the initial low-frequency P is normally quite small, and there is a tendency for P-coda phases to be somewhat larger. As a result the L_g/P_n ratios will tend to be larger than the S_{max}/P_{max} ratios for the earthquakes. This may also hold to some extent for the higher-frequency passband measurements. Finally, Figure 27 shows the same kind of plot for the L_g/P_g ratios. For the low-frequency (0 to 1 Hz) band the L_g/P_g peak amplitude ratios are about the same for earthquakes and explosions, but for the 3 to 6 Hz band the L_g/P_g amplitude ratios
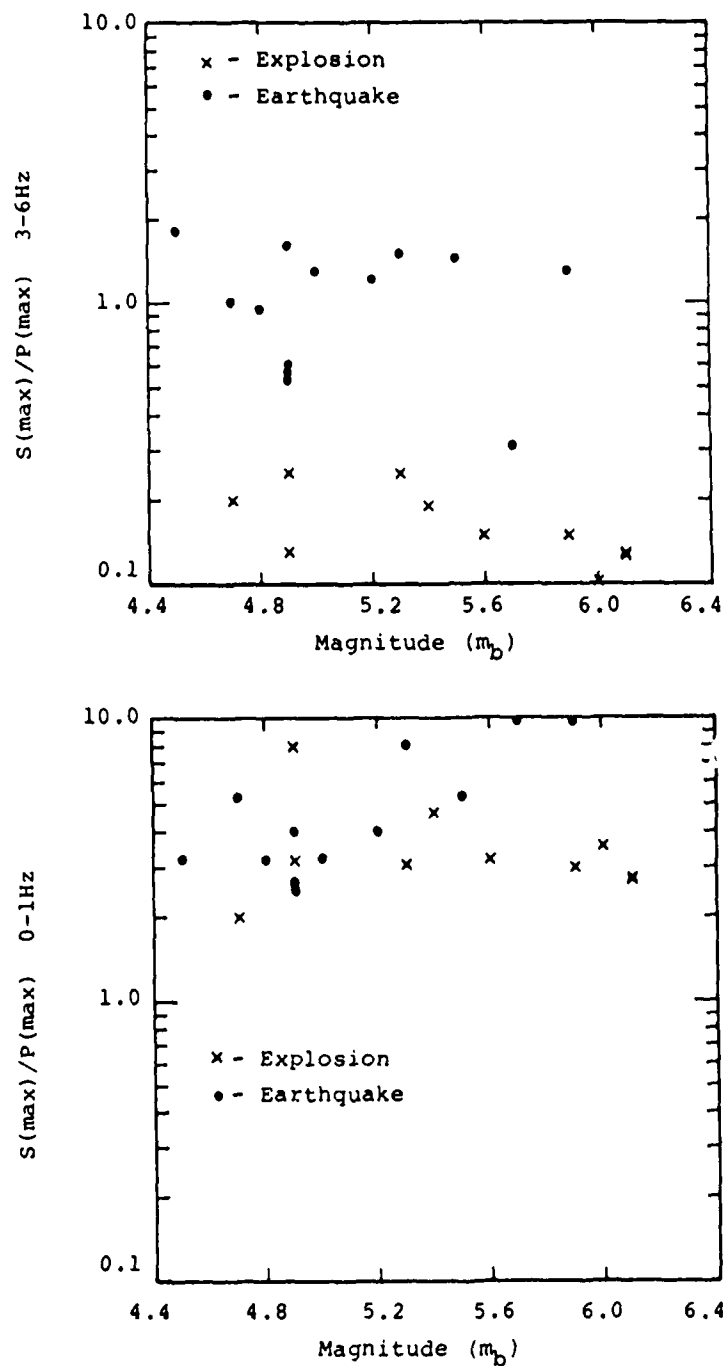
Figure 25.   Comparison of S_{max}/P_{max} ratios at WMQ
for 3-6 Hz passband (top) and 0-1 Hz
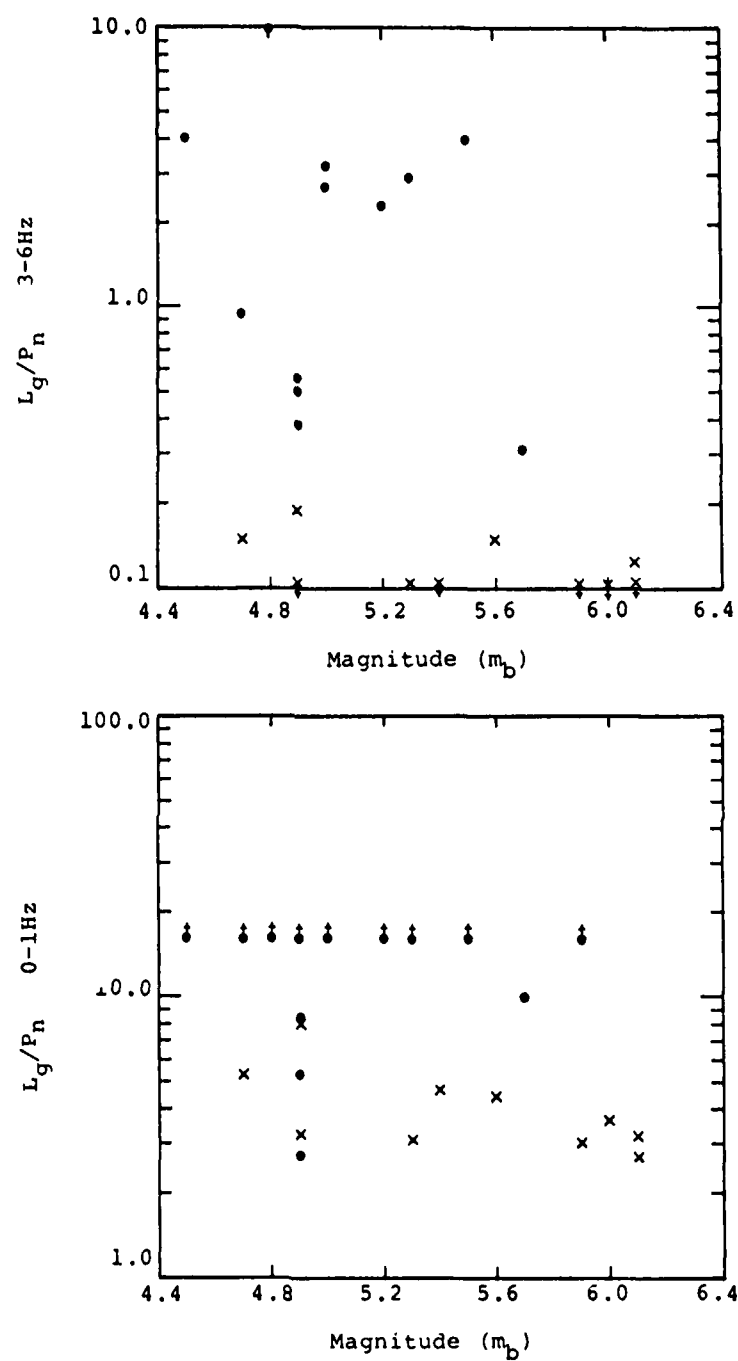passband (bottom).

Figure 26. Comparison of L_g/P_n ratios at WMQ for 3-6 Hz passband (top) and 0-1 Hz passband (bottom).
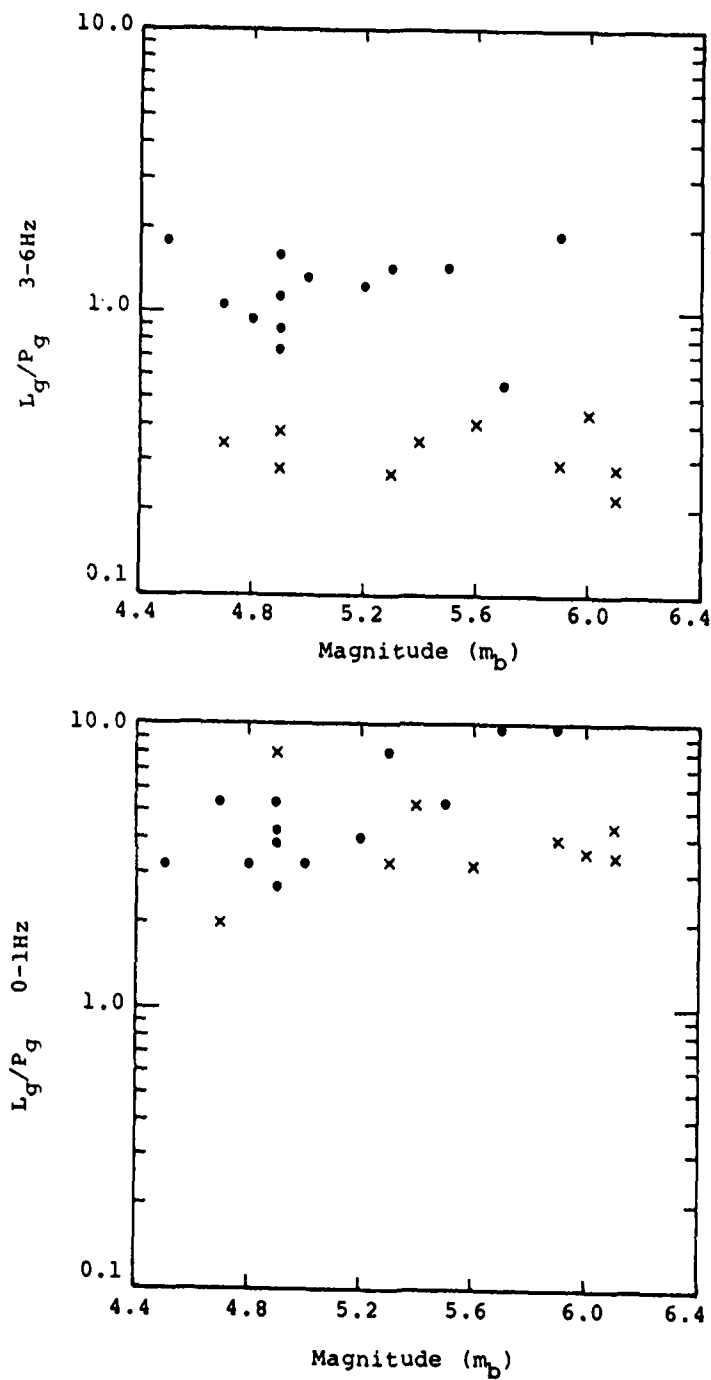
Figure 27. Comparison of Lg/Pg ratios at WMQ for
3-6 Hz passband (top) and 0-1 Hz pass-
band (bottom).

60

are larger for the earthquakes. At low frequencies the P_g signal is quite small for both earthquakes and explosions resulting in the large L_g/P_g ratios. At high frequencies the ratios are smaller and we have separation of the event types; but the measured signal in the P_g window may correspond to coda from earlier P phases and not the normal P_g. Again in Figure 27 there is no apparent trend in the ratio measurements with respect to magnitude.

One final comparison of the high- and low-frequency passband amplitude ratios is presented in Figure 28. Here we present the S_{max}/P_{max} ratios as a function of the epicentral distance at which the measurement was obtained. It was thought that this could be important because the explosions were concentrated in a very limited distance range from WMQ while the earthquake distances were more variable. First, for the lower-frequency passband there is little evidence of any dependence of the amplitude ratio on epicentral distance. The S_{max}/P_{max} ratios at all distances scatter about a mean value near four. For the high-frequency band there does appear to be some tendency for the S_{max}/P_{max} peak-amplitude ratios to decrease with epicentral distance. Focusing on the earthquake measurements, the ratios are generally greater than 1.0 at distances less than 800 km and show an overall decrease toward larger distances. However, the explosion S_{max}/P_{max} ratios would still fall well below any trend through the earthquake observations. So that even if the earthquake amplitude ratios were adjusted to a common range with the explosions using some average trend, the S_{max}/P_{max} ratios would still be separated by about a factor of four. One further caveat, which requires additional study, is that attenuation along the propagation path to East Kazakh may be different from the regional trend based on the earthquakes in Figure 28. We will return to this in subsequent discussions.

Our initial interpretation of the observed frequency dependence in the S_{max}/P_{max} amplitude ratio was that the observation was consistent with previous findings from the western U.S. Those studies (cf. Murphy and Bennett, 1982; Bennett and Murphy, 1986; Bennett et al. , 1988a) indicated that the earthquake L_g signals were richer in high frequencies than the comparable explosions, but the P_n signals had equivalent spectral content for explosions and earthquakes. Thus, the L_g/P_n amplitude ratios for those events would be expected to fall off more rapidly toward high frequencies for explosions than for earthquakes. Based on this interpretation it would than be anticipated that the
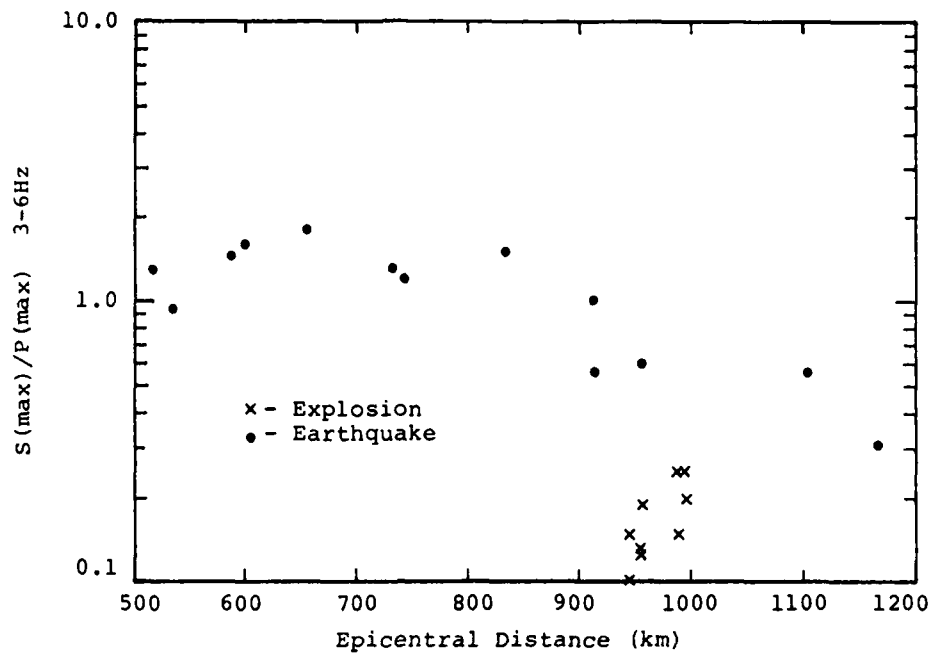
Figure 28. Dependence of S_{max}/P_{max} ratios at WMQ on epi-central distance for 3-6 Hz passband (top) and 0-1 Hz passband (bottom).
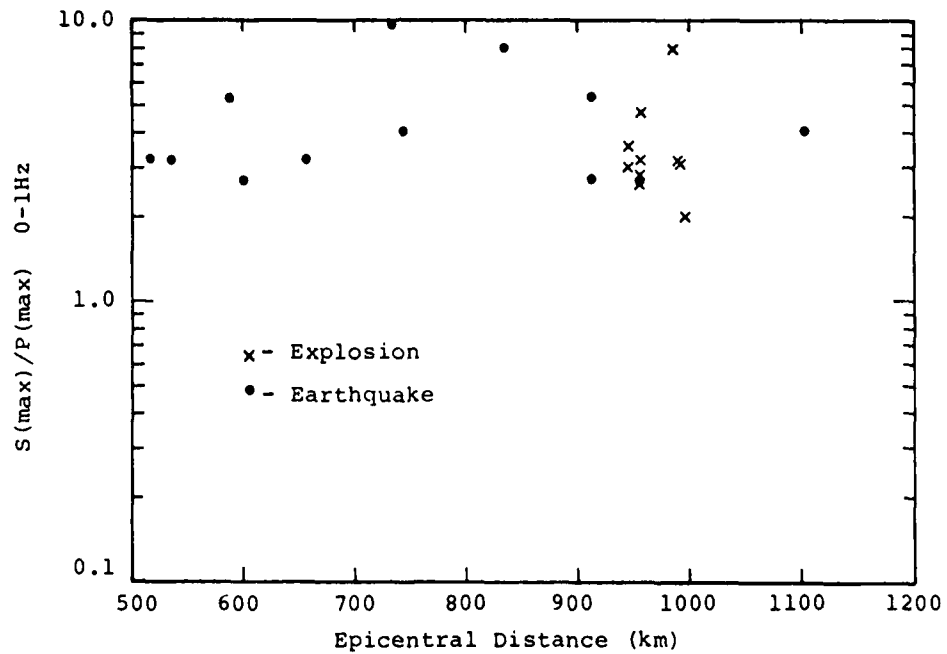
L_g spectral ratio discriminant might work on the events recorded at WMQ. To test this hypothesis we computed the L_g spectra for selected events from the WMQ database including seven explosions and seven earthquakes. The explosion magnitudes were between 4.7 and 6.1 m_b and the earthquake magnitudes were between 4.5 and 5.9 m_b. Epicentral distances were between 945 and 996 km for the explosions and between 732 and 1168 km for the earthquakes. Figure 29 shows the L_g spectra for the seven explosions after correcting for instrument response. The spectra show a nearly flat potion at lower frequencies and a relatively steep decay above an apparent corner frequency in the range from 0.6 to 1.0 Hz. In general, the corner frequency increases with decreasing magnitude as expected from simple source theory. The earthquake L_g spectra also showed a flat low-frequency segment and strong spectral decay above a corner frequency, but corner frequencies were somewhat more erratic with respect to magnitude. The apparent corner frequencies for the earthquakes were in all cases lower than the corner frequencies for the explosions with comparable magnitudes. Figure 30 shows schematic representations of the observed L_g spectra for the explosions and earthquakes observed at WMQ. Some of the variability in the low frequency level for the earthquakes may be attributed to epicentral distance differences; no correction has been applied for attenuation. However, in general the low-frequency L_g spectral level appears to be higher for the earthquakes than for the comparable explosions. If events with the same m_b are scaled to have comparable low-frequency spectral levels, then the explosions have higher corner frequencies and appear relatively richer in high frequencies. On the other hand, looking beyond the corner frequencies, the explosions appear to show a slightly steeper spectral decay than the earthquakes. Admittedly the latter is not a particularly strong difference and attenuation variations between the earthquake and explosion paths could be affecting the observations.

To obtain additional insight into the significance of potential attenuation differences on the L_g spectra, we applied Q corrections to the L_g spectra from a few selected events. The Q correction was applied in the form of a t^* operator, $e^{\pi f t^*}$, where $t^* = t/Q$; t is the travel time which we just took to be the epicentral distance divided by the L_g group velocity (approximately 3.5 km/sec). It is well known that Q varies significantly in the crust depending on the tectonic environment (cf. Nuttli, 1981, 1986). As a first approximation to Q for the path from East Kazakh to WMQ, we used the value determined by Bennett et al.

Figure 29.   L$_g$ spectra for seven East Kazakh underground
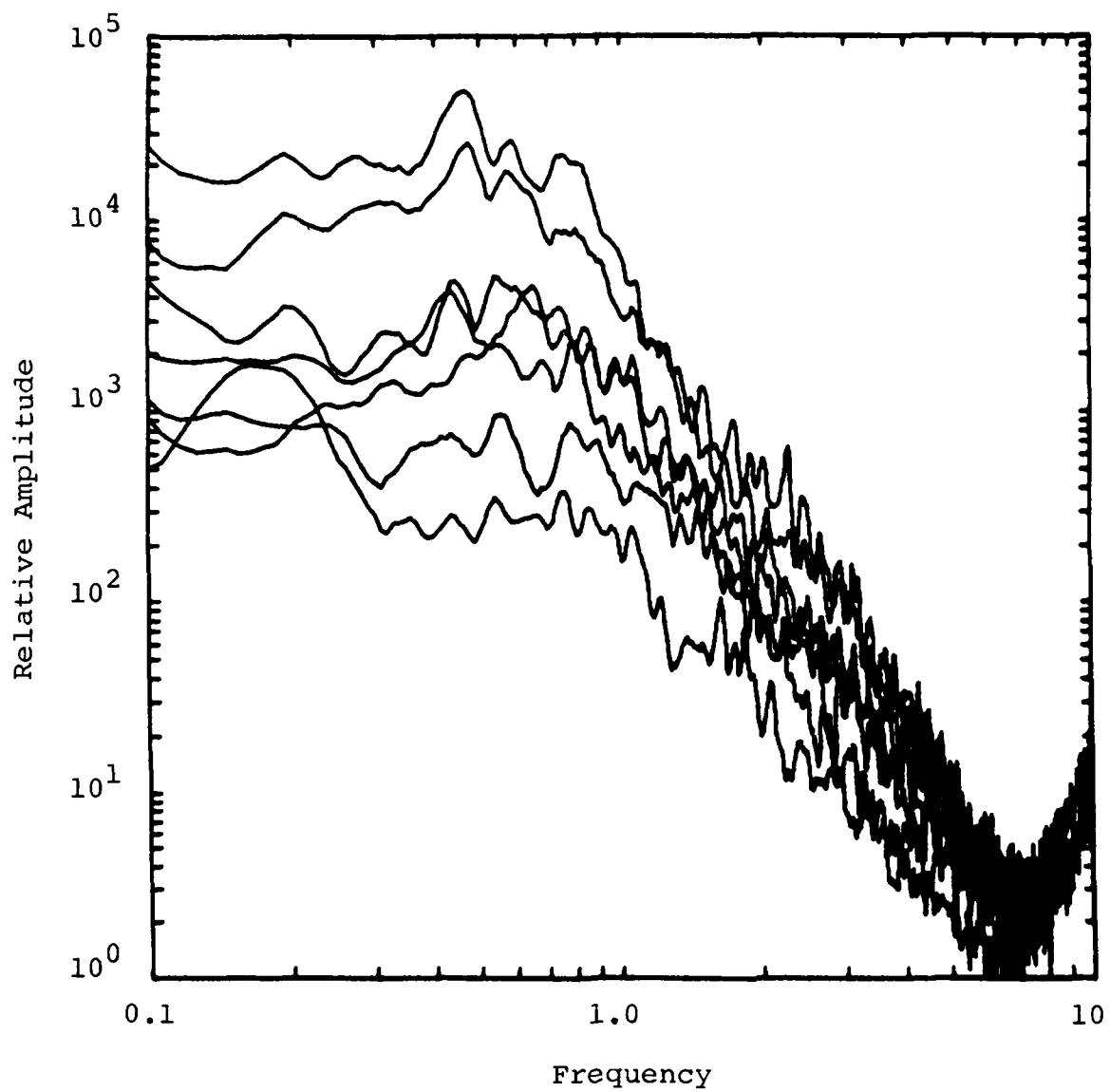nuclear explosions measured at WMQ.
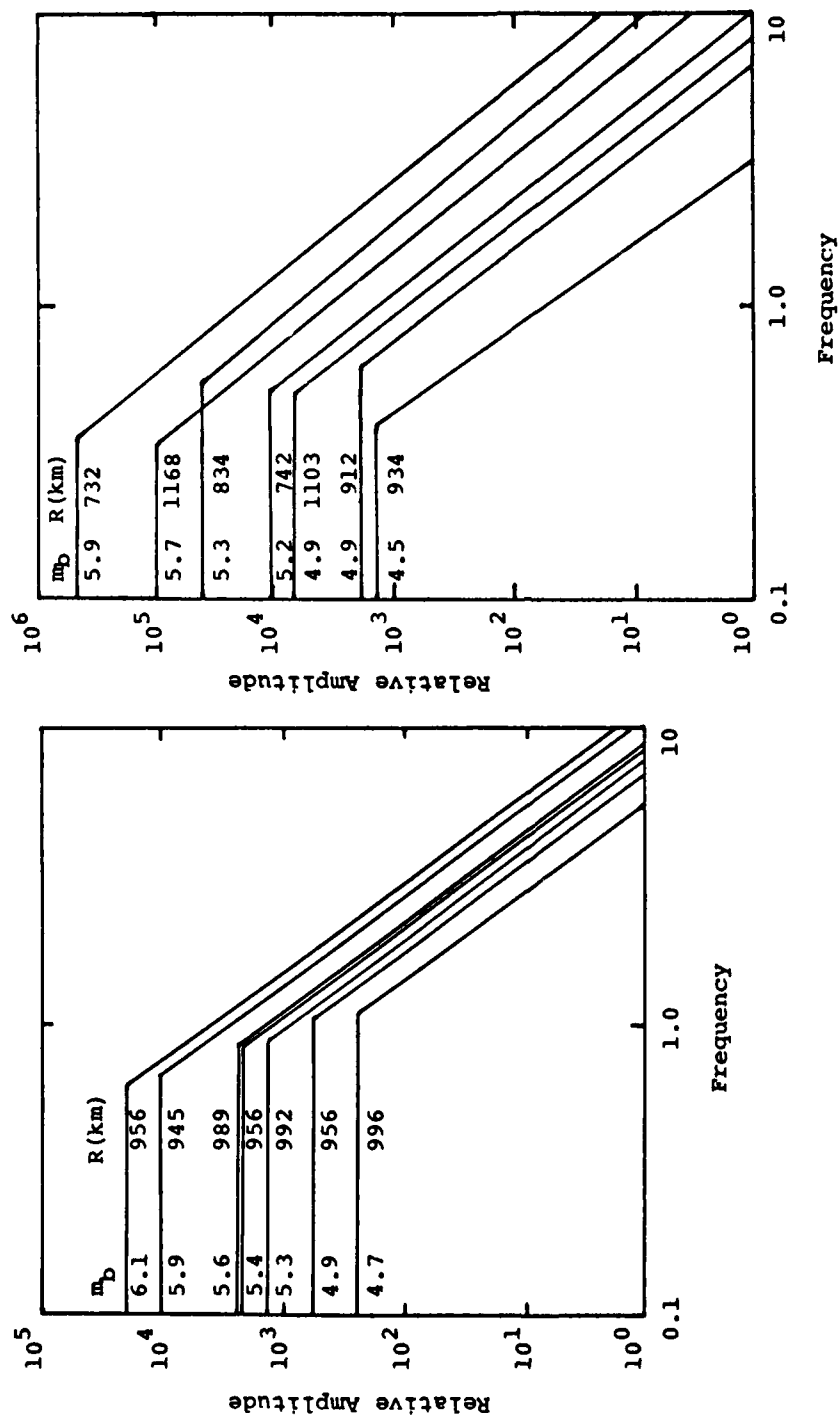
Figure 30. Comparison of schematic L_g spectra observed at WMQ for seven East Kazakh explosions and seven regional earthquakes.

65

(1988b) for the region around East Kazakh. They found an effective Q of 2000 for L_g. This Q value is considered fairly high, representative of a relatively efficient propagation path such as found in platform regions. It is believed that higher attenuation and lower Q values are appropriate in regions with increased tectonic activity, so that lower Q values may be more representative of the paths from many of the earthquake epicenters to WMQ. Figure 31 shows an example of the Q-corrected L_g amplitude spectrum for a magnitude 5.9 explosion at East Kazakh and a magnitude 5.9 earthquake. The earthquake range was 732 km. We applied the Q correction and then normalized the spectra to have equivalent values at 1 Hz. The plot on the left assumes that the explosion and earthquake had equivalent-Q paths with Q = 2000; while the plot on the right assumes the Q for the explosion path was 2000 but the Q for the earthquake path was only 1000. Comparing the spectral decays above the corner frequency, we see that for the equivalent Q assumption the slope of the spectral decay is practically the same for the explosion and earthquake. However, under the alternate assumption of a lower Q path for the earthquake, the slope is less steep for the earthquake. Figure 32 shows the same procedure applied to magnitude 5.3 events. The decay above the corner frequency is again seen to be about the same when the path Q's are assumed to be equal, but the decay is somewhat steeper for the explosion when a lower Q path is assumed for the earthquake. It seems reasonable from tectonic considerations to assume that the path to the earthquakes has lower Q. If this is in fact the case, it would follow that the Q corrected L_g spectra for the earthquakes would be relatively richer in high frequencies than the explosions with similar amplitude levels at 1 Hz. However, the precise Q corrections for the various source/station paths are unknown at this time and would require considerable effort to develop. Procedures exist for determining station-specific Q corrections to L_g (cf. Nuttli, 1986), but those have not yet been implemented for the paths involved here. One other interesting feature of the L_g spectra in Figures 31 and 32 is that the earthquake spectra at frequencies below 1 Hz appear to be relatively richer in low frequencies. This observation appears to conflict with L_g spectral observations from NTS (cf. Murphy and Bennett, 1982; Bennett and Murphy, 1986; Bennett et al. , 1988a; Taylor et al. , 1988), but it is unclear to what extent the spectral amplitudes at low frequencies can be relied on. Additional insight into the spectral behavior in this lower-frequency band might be gained from analysis of the L_g signals from a channel with better low-frequency response.
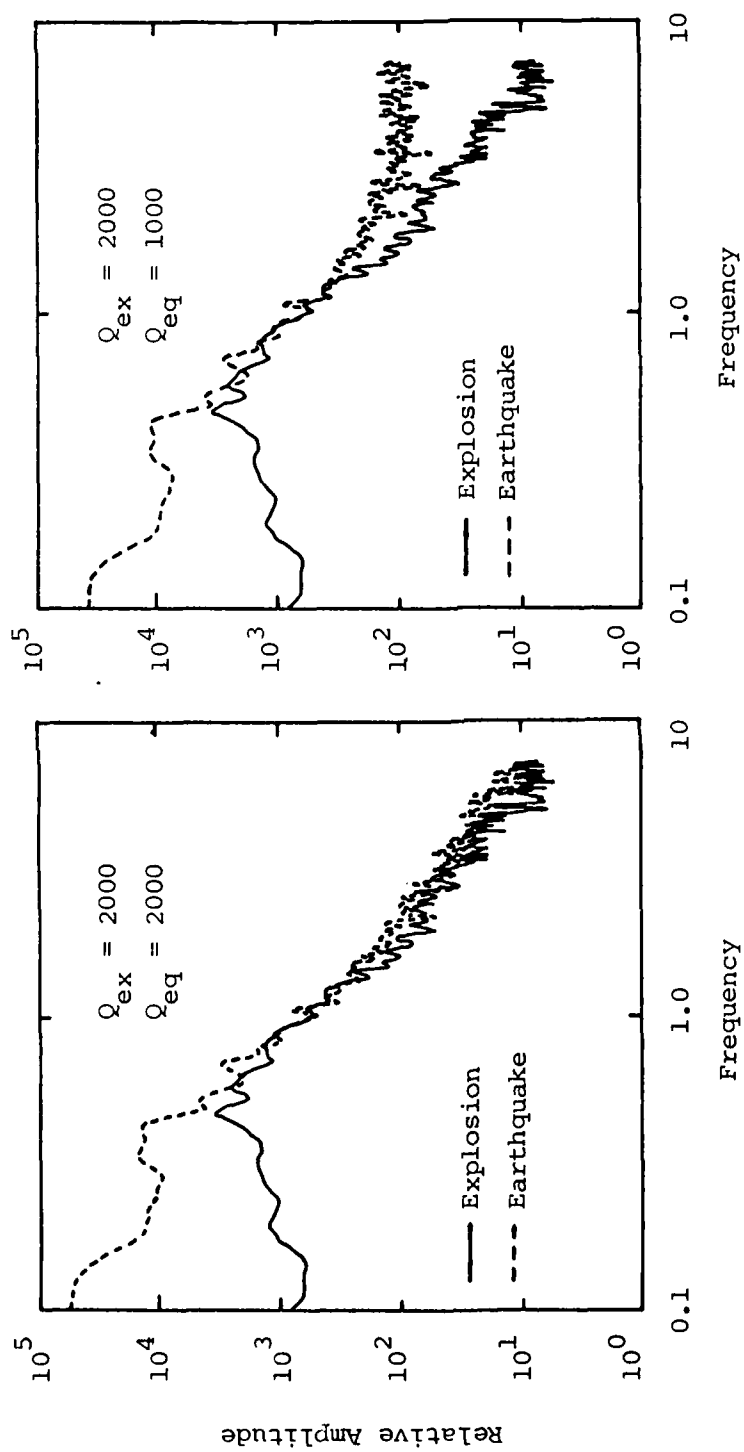
Figure 31. Comparison of L_g spectra at WMQ after Q correction for magnitude 5.9 m_b explosion and earthquake.
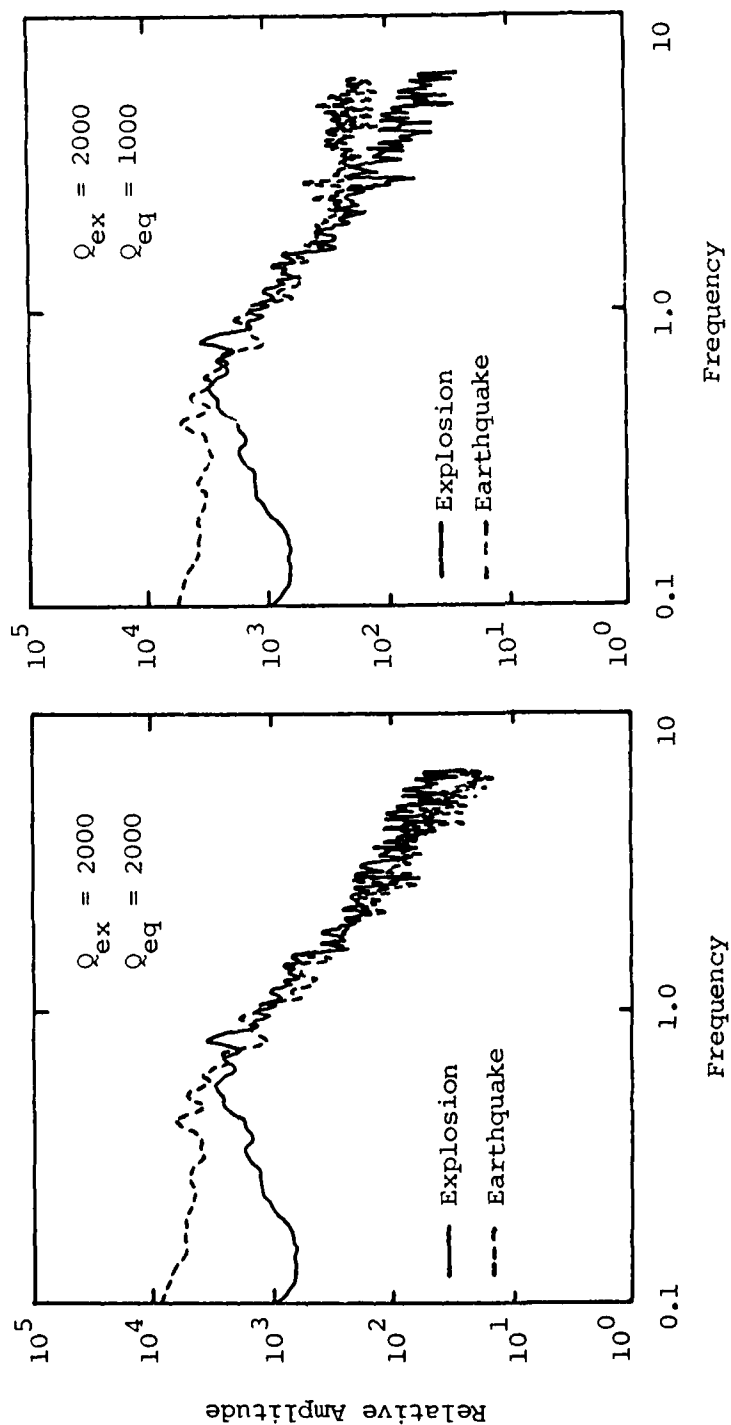
Figure 32. Comparison of L_g spectra at WMQ after Q corrections for magnitude 5.3 m_b explosion and earthquake.

68

In summary, the CDSN observations from East Kazakh explosions and regional earthquakes indicate some new possibilities for regional discrimination. Regional phases including L_g and several P phases are strong at this distance range and should provide useful signals for comparing different source types. Comparison of L_g to P excitation as a function of frequency appears to provide a promising discrimination method for these events, but additional investigation is needed to determine the significance of path differences on the measurements.

3.3 Identification of Events from the Vicinity of the East Kazakh Test Site Recorded by the Soviet/NRDC Network

The Soviet/NRDC seismic network in East Kazakh was installed during the summer of 1986 and monitoring continued episodically through early September of 1987. Seismic instrumentation in the network during the monitoring period was upgraded at several stages. In this report we will consider observations made during Phase II monitoring starting in March, 1987, which included both surface and borehole three-component seismometer installations at each of three stations surrounding the Soviet test site. Figure 33 shows the locations of the three stations at Karkaralinsk (KK), Bayanaul (BA), and Karasu (KS); the station locations in each case were hardrock sites (cf. Leith, 1987). The installations had a high digitizing rate of 250 samples per second enabling analysis of very high frequency signals although the frequency band was limited to frequencies below about 80 Hz by an antialiasing filter. Observations from the Soviet/NRDC network have been described in several previous reports (cf. Berger et al. , 1987, 1988; Bennett et al. , 1988b; Priestley and Walter, 1988; Smith, 1988a). In our previous report (cf. Bennett et al. , 1988b), we focused primarily on utilization of the teleseismic data to define P-wave bias of the region relative to NTS and on analysis of regional event signals to estimate attenuation and effective Q of the earth's crust in that area. The present analysis concentrates on the identification problem for the regional events recorded by the network.

Figure 33 also shows the locations of 362 regional events (including three network calibration explosions) which were located by CSS analysts in the region surrounding the test site using three-component single-station location methods. The stations were shut down, by prior agreement, during Soviet
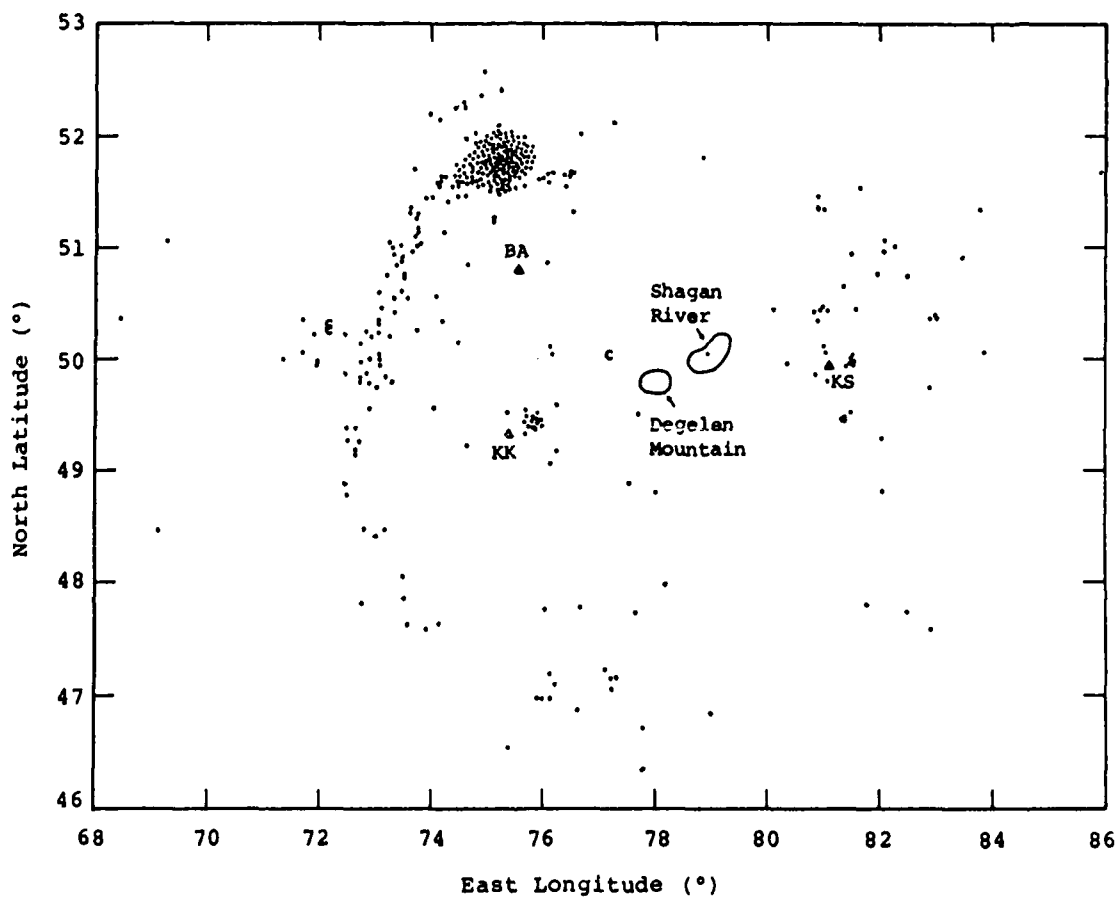
Figure 33. Locations of presumed mine blasts in East Kazakh recorded by the Soviet/NRDC network.

underground nuclear tests. As a result, the observations during Phase II, which extended from March 19, 1987 to September 5, 1987 actually included only 79 days of available data.

The observation of four to five locatable events per day of unknown origin in the region was initially somewhat surprising considering that the area around the East Kazakh test site is generally regarded as being naturally aseismic or as having a very low level of natural earthquake activity. This issue was clarified to some extent by Bennett et al. (1988b) who concluded that the majority of these events were probably blasts related to mining or construction activity in the area. This conclusion was based primarily on the fact that 92 percent of the events were concentrated during an eight-hour period of the time of day, suggesting a tendency to blast during daylight hours, which is similar to mining practice in the United States. We can also see in Figure 33 that many of the events tend to be clustered in specific areas (e.g., near 51.5°N, 75.0°E, near 49.8°N, 72.5°E, and near 49.4°N, 75.9°E). Several of these areas (e.g., Ekibastuz at 51.8°N, 75.3°E and Karaganda at about 50.0°N, 73.0°E) are centers of coal fields which are being actively strip-mined (Leith, 1988). However, except for the three calibration shots, we have no particular knowledge of the individual events in this sample, so it's possible that some of the events may not have been commercial blasts. This situation is comparable in many ways to that which we described above in Section II for eastern North America with regional stations detecting a large number of unknown events which would need to be identified if some low-level monitoring threshold were established.

In this study we have not attempted to conduct a comprehensive analysis of all 362 regional events in the database; however, we have sought to identify some of the salient features in the regional seismic signals from these events which may be useful in distinguishing them from other sources in the region. The signals recorded by the Soviet/NRDC network stations from these events frequently included strong P_g, L_g, and short-period fundamental-mode Rayleigh waves, R_g, to ranges of 400 km or more indicating efficient propagation paths for these small magnitude events. Figures 34 to 37 show several examples of the vertical-component signals at different ranges recorded at stations BA and KK from sources in two different zones: one to the north near Ekibastuz and a more diffuse zone to the south (locations around 47.0°N, 76.5°E). Although

71
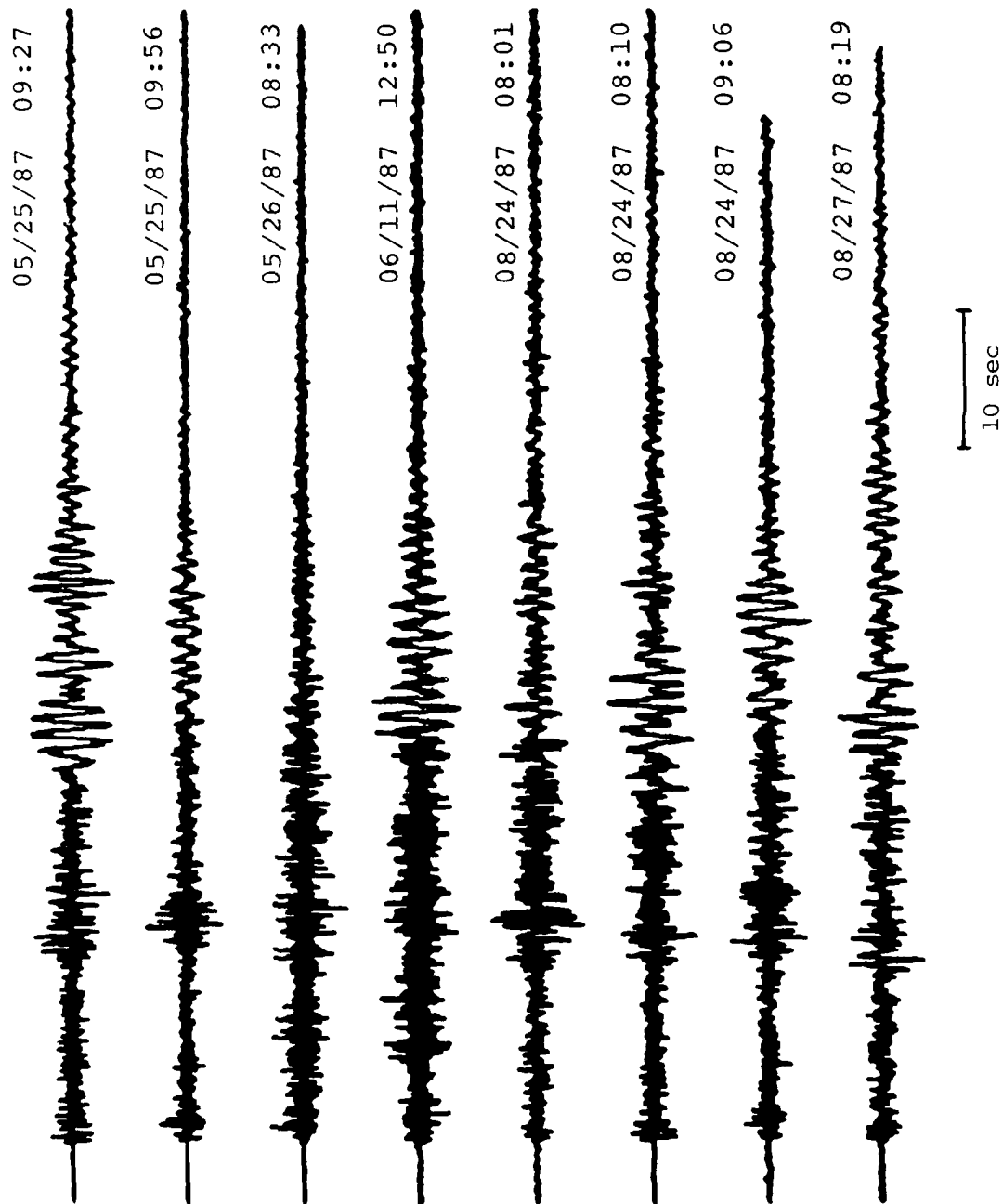
Figure 34. Vertical-component records at station BA from eight presumed mine blasts near Ekibastuz (R ≈ 100 km).

05/25/87 09:27

05/25/87 09:56

05/26/87 08:33

06/11/87 12:50

08/24/87 08:01

08/24/87 08:10

08/24/87 09:06

08/27/87 08:19

10 sec

72
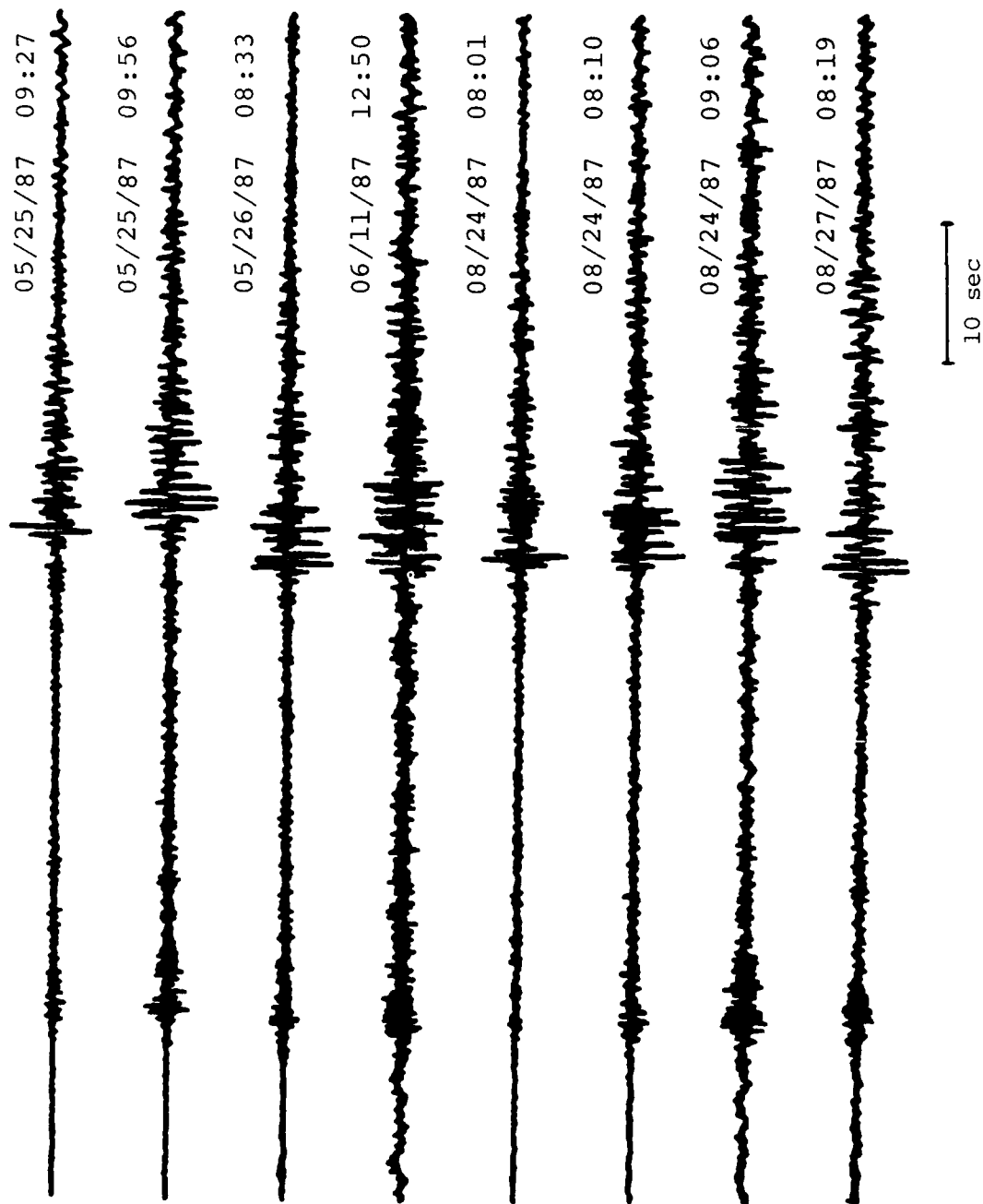
Figure 35. Vertical-component records at station KK from same eight presumed mine blasts near Ekibastuz (R ≈ 270 km).

The seismogram traces are labeled, from top to bottom:
05/25/87 09:27
05/25/87 09:56
05/26/87 08:33
06/11/87 12:50
08/24/87 08:01
08/24/87 08:10
08/24/87 09:06
08/27/87 08:19

10 sec

Figure 36. Vertical-component records at station KK from six presumed mine blasts from vicinity of 47.0°N, 76.5°E.

74
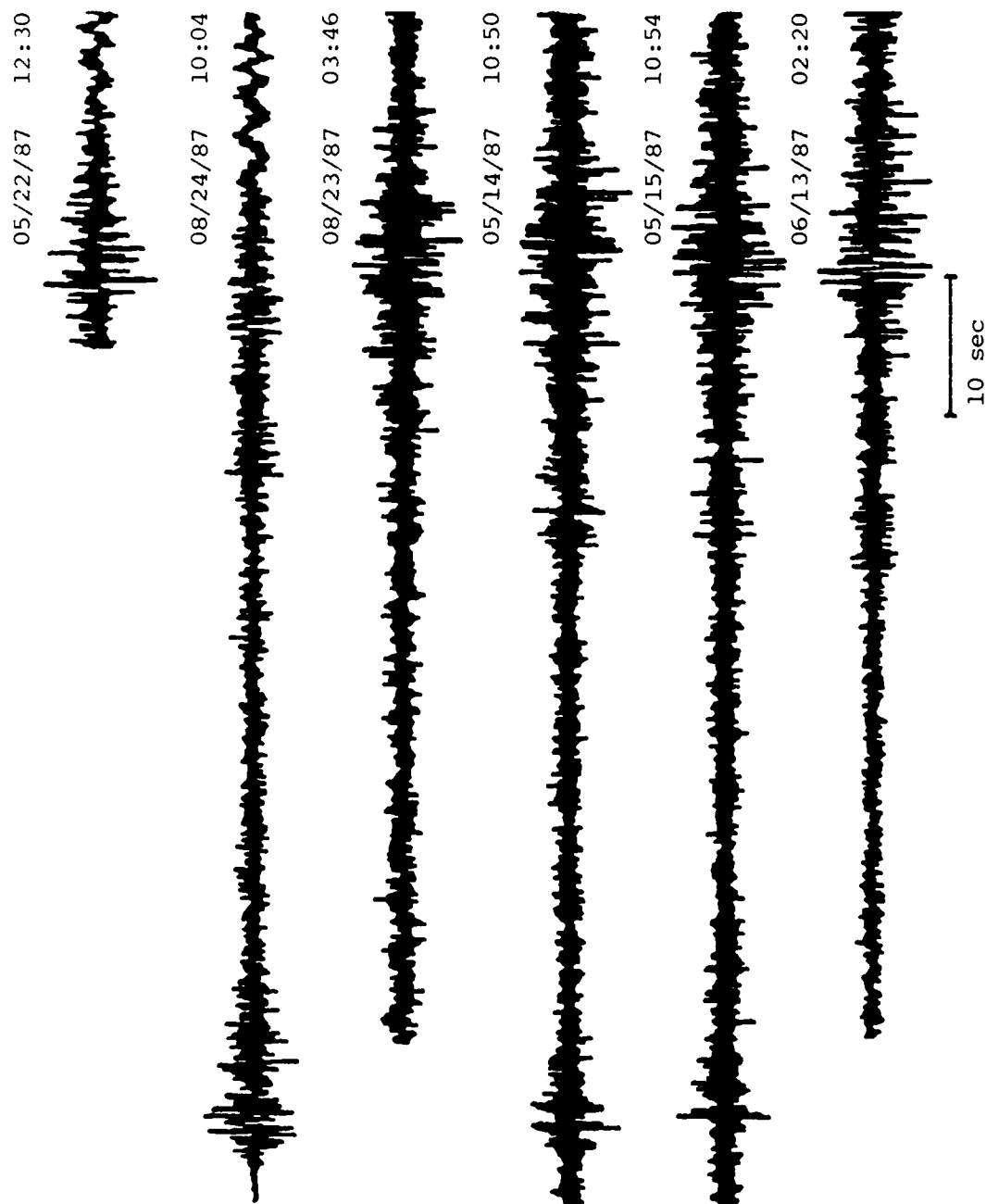
Figure 37. Vertical-component records at station BA from same six presumed mine blasts from vicinity of 47.0°N, 76.5°E.

the relative amplitudes of the P_g and L_g signals vary somewhat from event-to-event, the P_g signal amplitudes are generally less than or about equal to those of the L_g signals on the broad-band records. Furthermore, the signals from events in specific source zones have remarkable consistency from event-to-event. A notable exception in this regard can be seen by comparing the top two events in Figure 36. The 05/22/87 event has an L_g signal much larger than the P while the 08/24/87 event has an L_g signal much smaller than the P. Although the events within this source zone were clearly not all located at the same spot, the locations of the 05/22/87 event and the 08/24/87 event were essentially the same within the uncertainty of the single-station location method. Aside from the relative amplitude differences, the signals are quite similar in appearance for the P, L_g and R_g wave segments. Assuming that these two events were blasts located in close proximity, it seems reasonable to conclude that the differences in the relative amplitudes of P and L_g are most likely indicative of some change in shooting practice. This conclusion would imply that the effects of such changes in shooting practice on the relative amplitudes of P and L_g need to be understood before much reliance can be placed on such comparisons for discrimination.

Short-period, fundamental-mode Rayleigh waves, R_g, were frequently quite prominent on the Soviet/NRDC records from the presumed mining blasts in the East Kazakh region. These signals were particularly strong at the nearer distance ranges. Figure 38 shows three-component records at station KK for three presumed mining blasts at a range of 25 to 30 km. The R_g phase is strong on the vertical and E-W components and has a dominant frequency between 1.0 and 1.5 Hz. A similar fundamental-mode Love wave which is also controlled by the near-surface, low-velocity waveguide appears as a strong phase on the N-S component records for these blasts. Figure 39 shows similar R_g and Love wave phases recorded at station BA for two different presumed mine blasts, in this case located at ranges of 100 km. As noted above in Section II, these strong, short-period, fundamental-mode phases are associated with the seismic excitation of the low-velocity layer at the earth's surface by shallow-focus events. Unfortunately, we don't know whether any of the events surrounding the East Kazakh test site, which are in the Soviet/NRDC database, are earthquakes. Some of the events certainly produce somewhat weaker R_g signals, but this could also be caused by differences in shooting practice or attenuation which could be strong if the

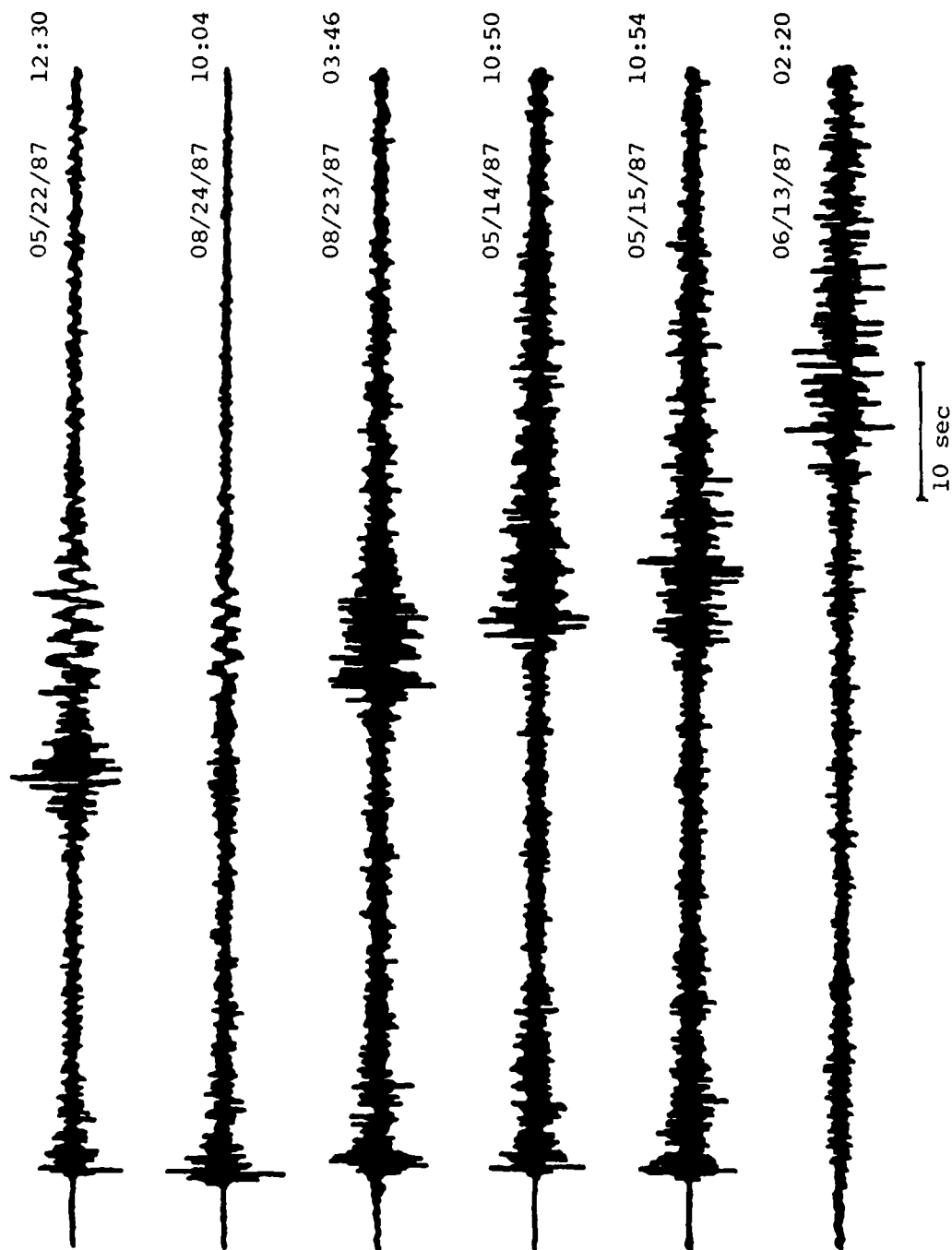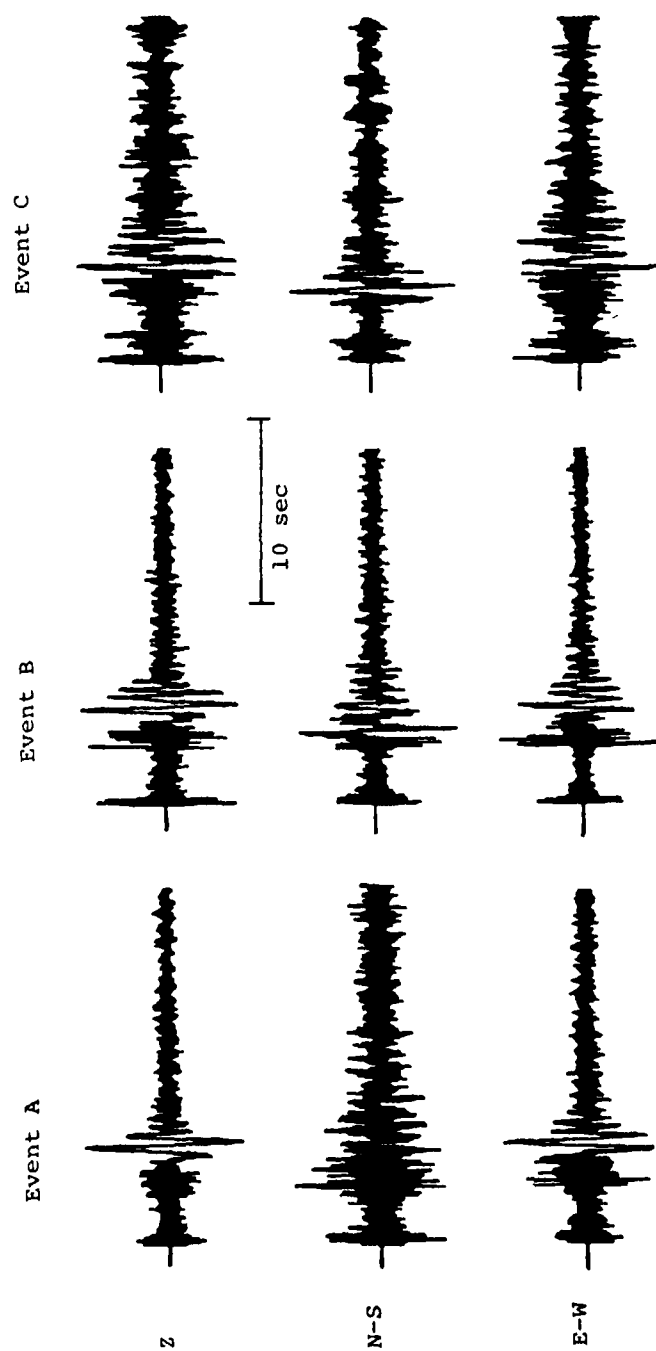Figure 38. Three-component records at station KK for three presumed mine blasts located 25-30 km to the east.

77
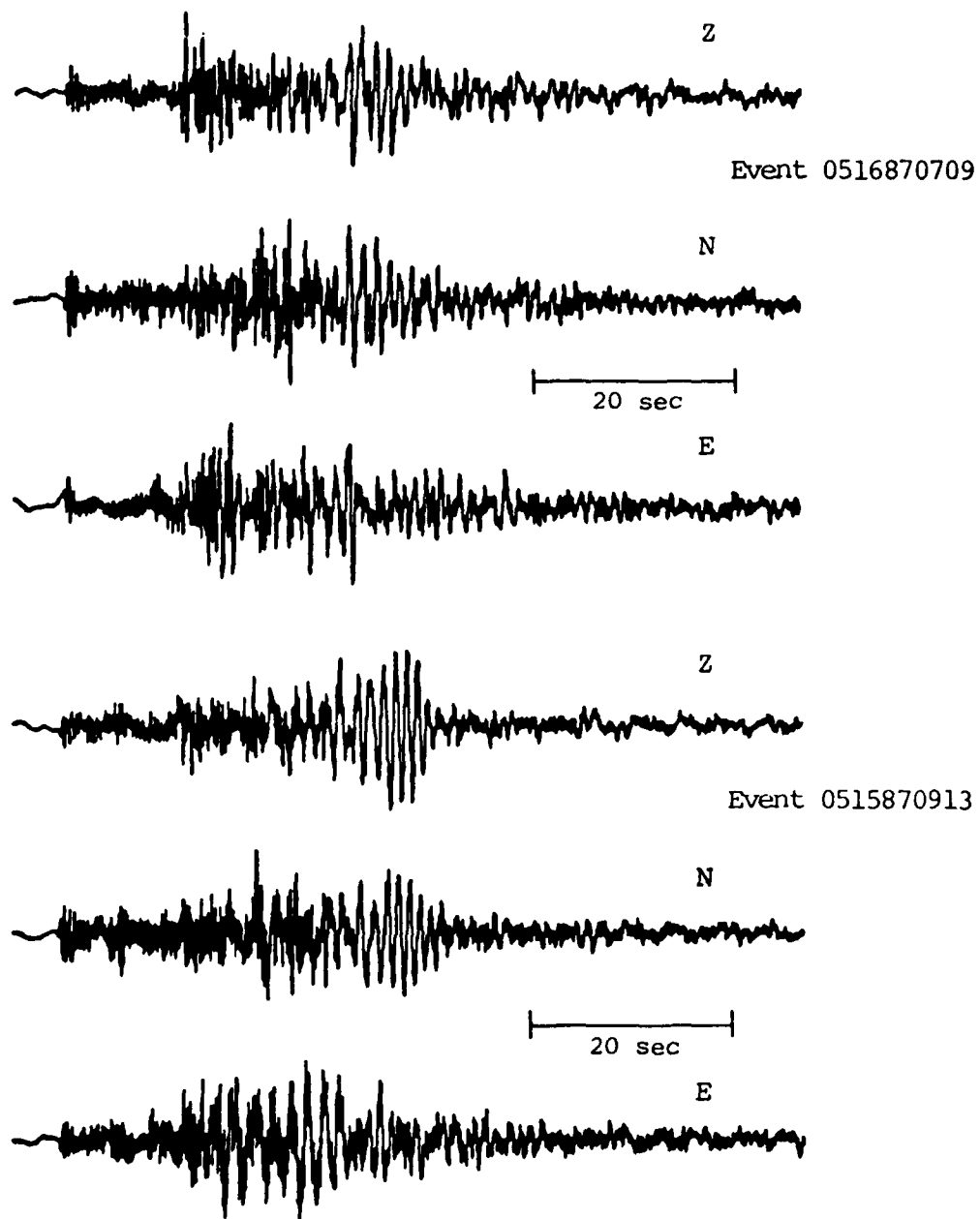
Figure 39.   Three-component records at station BA for two
presumed mine blasts located near Ekibastuz
(R ≈ 100 km).

waveguide is not continuous. So the lack of R_g cannot be regarded as an unambiguous indication of source depth which could be used to distinguish earthquakes from blasts.

On the other hand, the simple R_g waveforms observed for some of the presumed blasts recorded by the Soviet/NRDC network could be quite valuable for investigating regional crustal structure. To demonstrate this capability we analyzed the observed R_g signals recorded at station KK from the mine blasts located just east of the station at a range of 25 to 30 km. As shown above in Figure 38, these blasts produced strong, uncomplicated R_g signals at these relatively short ranges. It is well known from previous studies (cf. McEvilly, 1964; Herrmann, 1969; Kafka and Reiter, 1987) that the dispersed R_g wavetrain produced by such blasts is strongly dependent on the velocity structure in the upper few kilometers along the propagation path. Murphy (1981) and Murphy and Shah (1988) represented the near-surface explosion source as an axisymmetric vertical pressure acting on the surface of a multilayered half-space. They found for this source that the ground motion displacement was dominated by low-frequency, surface-wave components and that the Rayleigh-wave ground motion could be reasonably approximated as an Airy phase provided the source corner frequency, f_c , is less than the dominant frequency, f_o , associated with the site response. While we recognize that the individual shots in mine blasting are likely to have relatively high, source corner frequencies, it is believed that shot delays as well as non-linear interaction at the mine blast source will tend to lengthen the source duration and decrease f_c. Furthermore, although the actual mechanism of the mine blast is no doubt more complex than the model, the simplicity of the observed waveforms suggested that some insight could be gained from the relatively simple source description. Therefore, in analyzing the Rayleigh waves recorded at station KK from the mine blasts, we followed the approach of Murphy and Shah (1988) and assumed that f_c is less than f_o. Under this assumption Murphy and Shah found that the displacement spectral amplitude was sharply peaked primarily due to the Rayleigh wave site response term and that it could be represented as the product of a site response term, a propagation term and the source function all evaluated at f_o with

$$f_o = \frac{\bar{\beta}}{2.3H}$$

79

where $\bar{\beta}$ is the average shear-wave velocity above the first significant discontinuity in velocity at depth H. Then, for the vertical component Rayleigh wave, the peak amplitude of the ground motion was found to decrease as shear velocities in the structure increase, and the duration of the motion increased as the ratio of the shear velocity below to above the interface increased.

Figure 40 shows the vertical-component, displacement time history, corrected for instrument response, for a blast recorded on 05/23/87 at station KK. The signal is dominated by a somewhat weakly dispersed Rayleigh wave with a dominant frequency near 1.3 Hz. By comparison of the observed signal duration in Figure 40 with the results reported by Murphy and Shah for the dependence of the duration on the shear-velocity ratio, it appears that a velocity ratio with $\beta_2 / \beta_1 \approx 2$ matches closely the observed behavior. We therefore take $\beta_c / \bar{\beta} = 2$ where β_c is the shear velocity in the deeper crustal rock (i.e., half-space). Now, according to Leith (1987) the compressional velocity of crustal rock in the region is about 5.4 km/sec. Assuming a Poisson's ratio σ of 0.25, $\beta_c = 5.4/\sqrt{3} = 3.12$ km/sec. Thus, $\bar{\beta} = 1.56$ km/sec, and using the relation $f_o = \bar{\beta}/2.3H = 1.3$ Hz, we estimate H to be about 0.5 km. Murphy and Shah (1988) proceeded to show that the Rayleigh-wave vertical displacement time history for the model could be approximately represented by

$$W(r,\tau) = \frac{Ap \ e^{-\alpha\tau^{\frac{3}{2}}}}{r^{\frac{5}{6}}} \cos\omega_o \tau$$

where τ is time relative to the surface wave peak which has an amplitude Ap, $\omega_o = 2 \pi f_o$, and α is a parameter representing the decay in the wavetrain envelope with time. For the blast in Figure 40, we estimated α to be 0.89; then, the waveforms at the bottom of Figure 40 show the comparison between the Airy phase approximation to the blast Rayleigh wave and the observed signal. Obviously, the match is good near the peak and in adjacent cycles but not as good later as the signal becomes more dispersed. We conclude from this preliminary analysis that the dominant part of the vertical Rayleigh wave signal is adequately represented by the simple blast source for a layer over a half-space model. In the model the layer thickness is about 0.5 km, and the shear-wave velocity is 1.56 km/sec in the layer and 3.12 km/sec in the half-space. It seems clear that in a more exact treatment, we could probably do a

80
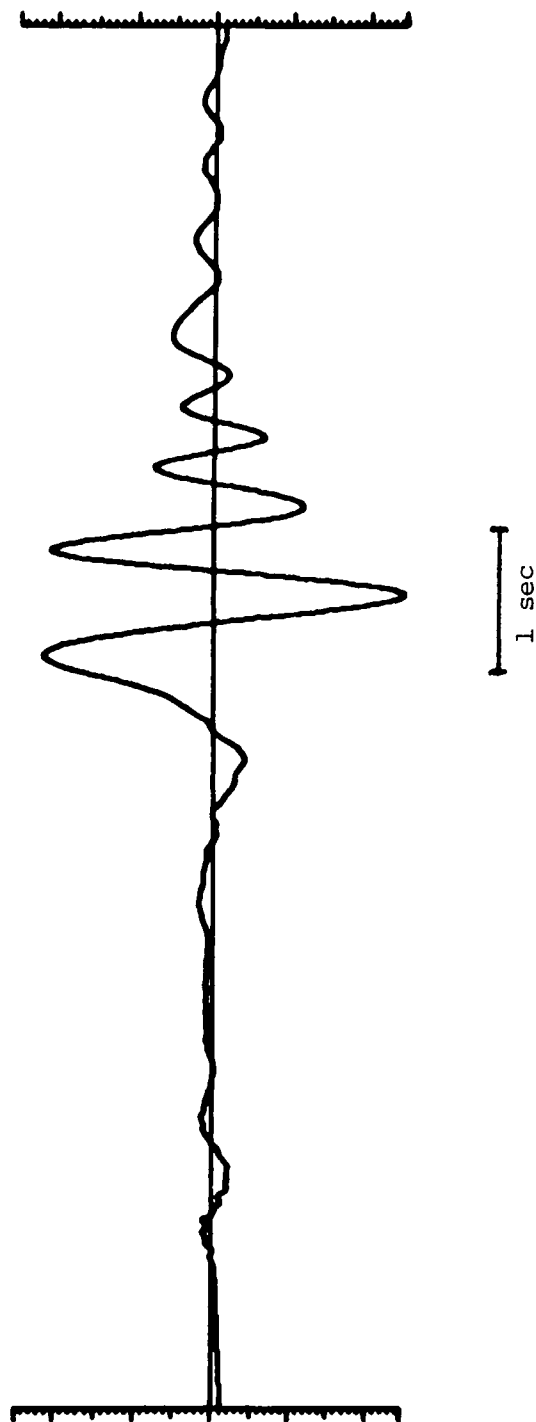
Airy Phase Approximation

$$\frac{Ap\,e^{-\alpha\tau^{3/2}}}{r^{5/6}}\cos\omega_o\tau$$

with $f_o \equiv \dfrac{\omega_o}{2} = 1.3$ Hz

$\alpha = 0.89$

Figure 40. Vertical-component displacement at station KK from presumed mine blast near East Kazakh (top). Comparison of observed R_g (solid line) and Airy phase approximation (dots) for an explosion source (bottom).

better job of matching some of the observed signal characteristics (e.g., dispersion). Nevertheless, the fact that the simple model agrees with the observations fairly well suggests that at least some signal characteristics may not be strongly influenced by the details of the blast mechanism. This could be demonstrated by analyzing observations from additional mine blasts with different shooting practices. Analyses of the dispersion characteristics of the short-period Rayleigh waves for the mine blasts in the other areas around East Kazakh might provide additional insight into variations in the near-surface geology across the region.

A final observation relating to discrimination of mine blasts using the Soviet/NRDC network data is the presence in the signals of characteristic indications of source multiplicity. It is well known that commercial explosions frequently consist of a series of delayed shots designed to reduce damaging vibrations and increase rock fracturing. Frantti (1963) and Willis (1963) provided some early insights into the potential influences of shot delays on seismic signals, but their studies focused on observations made fairly close to the source. Until recently little effort has been made to identify such effects in more distant seismic signals. This is partly because shot delays are rather short; and, therefore, the effects should be strongest at high frequencies, but seismic instrumentation has generally not been adequate in the past to investigate such effects. Simple theory indicates that the spectra of seismic signals from multiple shots will include a series of holes and another series of lobes at frequencies related to the delay times between shots. Dick et al. (1983) indicate that in surface blasting shot delays are normally between 25 and 100 msec, and similar practice is thought to extend worldwide. In order to resolve the spectral effects of these kinds of shot delays, it would be necessary to have fairly broad-band recording instruments with signal spectra extending from low frequencies to several tens of Hertz. In Section II above we noted that the frequency band of signals recorded at RSCP from mine blasts in the eastern U. S. was probably inadequate to identify such spectral scalloping. However, recent studies by Baumgardt and Ziegler (1988) and Smith (1988b) using broad-band seismic systems have found evidence of delayed shooting in some mine blast recordings at regional distances in Norway and northern North America.

82

Since the Soviet/NRDC network had a fairly high digitizing rate and the signal-to-noise level extended to high frequencies for many of the larger events, it is reasonable to expect that the regional signals from the mine blasts would show some evidence of the expected spectral scalloping. Figure 41 shows uncorrected spectra obtained at stations BA (R = 100 km) and KK (R = 270 km) for the L_g signal windows from one of the larger presumed mine blasts in the northern source zone near Ekibastuz (51.6°N, 75.0°E). We show the spectra out to 100 Hz although it appears that the spectrum at the more distant station has fallen to the noise floor at a lower frequency. At the nearer station BA, the L_g spectrum is seen to consist of a sequence of peaks and troughs which we interpret to correspond to the expected scalloping. The spectral lobes are rather broad, but the holes seem to be relatively sharp. The most obvious hole occurs at 11.5 Hz and we observe a sequence of successive holes positioned at odd multiples of the initial hole with intervening lobes as would be predicted by simple theory. Since the spectral scalloping is presumed to be related to the shot delays in the source, the theory would predict that the same scalloping should be observed at the other station. Although the holes are less definitive, we certainly see evidence of their presence at some of the expected frequencies. Again following the simple theory, the shot delay required to produce a hole at 11.5 Hz, and at the successive odd multiples, is just equal to the reciprocal of twice that frequency, or about 43 msec. Unfortunately, as noted earlier, we lack specific information on the shooting practice in these presumed blasts. The shot-delay explanation for the observed spectral behavior seems reasonable, but alternate causes may also be possible. Furthermore, it's clear from the spectrum at the more distant station in Figure 41 that the spectral scalloping in the regional signals may not be easy to discern at larger ranges except for much larger events. It is also clear in principle that variations in shot delays could complicate the spectrum to an extent that the regularity in the pattern expected from delayed shooting might go unnoticed. Therefore, detection of delay shooting characteristics in regional phase spectra from mine blasts may be useful for identifying some events but may not provide the panacea which will be required to eliminate the large number of commercial blasts at lower threshold levels.

83
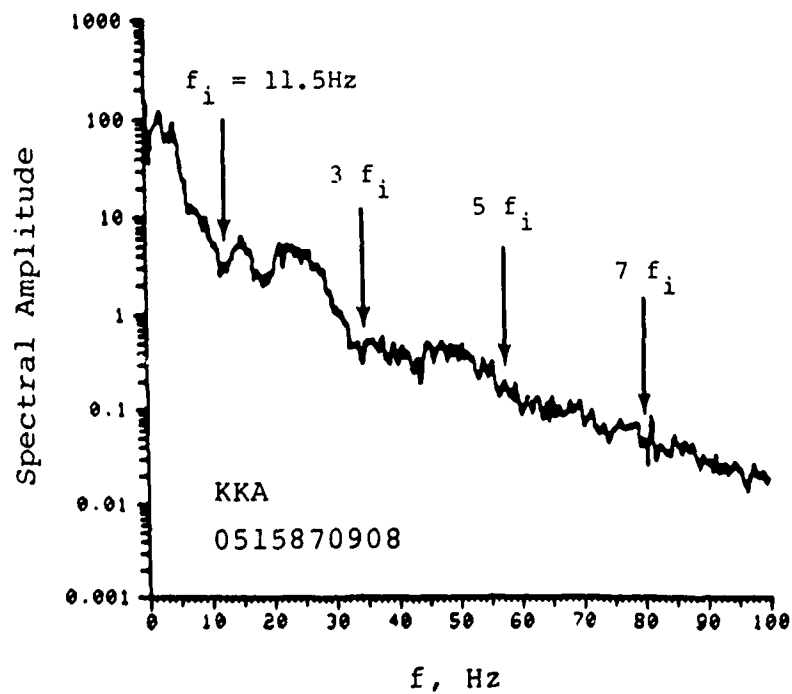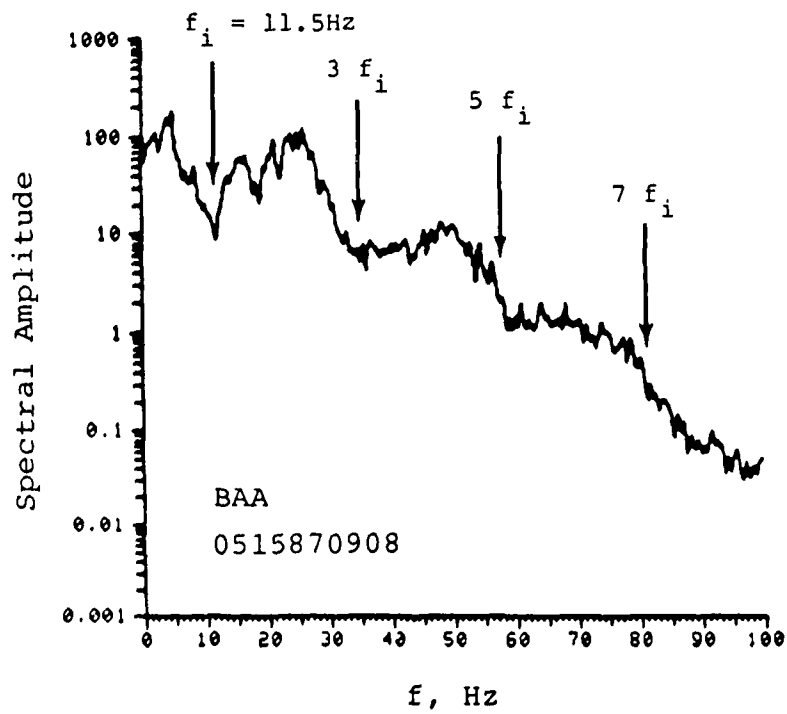
Figure 41.   Evidence of notches in L_g spectra from presumed
mine blast near Ekibastuz.

84

IV. NTS UNDERGROUND NUCLEAR EXPLOSIONS AND COMPARABLE EARTHQUAKES

4.1 Empirical Derivation of Techniques for Regional Discrimination of Nuclear Explosions

It is well known that the excitation and propagation of regional seismic signals is strongly dependent on the crustal properties of the source and receiver region. Therefore, a true test of regional discrimination capability in the Soviet Union should involve determination of the seismic signal differences between Soviet underground nuclear tests and nearby earthquakes of comparable magnitude. Several factors have precluded satisfactory empirical testing of this kind; these include, in particular, the general lack of natural seismicity in the Soviet platform region where most nuclear explosion tests have been conducted and the unavailability (prior to CDSN and the new IRIS sites) of data from seismic stations at regional distances from Soviet tests. This lack of a suitable database for testing regional discrimination in the Soviet Union has forced many previous investigators to take a more hybrid approach. This approach utilizes empirical results from regional seismic measurements for U.S. nuclear tests and comparable earthquakes and infers how source or propagation differences might influence the measurements in areas of intended application (viz the Soviet Union). An important feature in this methodology is the utilization of a controlled set of sources enabling analysis of the sensitivity of the measurements to a variety of source conditions.

Blandford (1981) found that, after careful correction for attenuation differences, the amplitude ratio of the regional signals before and after the predicted S times separated U.S. underground nuclear explosions from earthquakes with locations throughout the eastern and western U.S. However, Murphy and Bennett (1982) and Bennett and Murphy (1986) found considerable intermingling of small NTS explosions and nearby earthquakes when the relative amplitudes of P_n, P_g and L_g signals were compared using measurements at equivalent ranges from regional VELA array stations; but those studies also produced evidence of spectral differences in the regional phases from the explosions and earthquakes. Recent studies by Taylor et al. (1986,1988) and Glaser

85

et al. (1986) have investigated a wide variety of regional discriminant measures and found that some discriminants were more effective than others in separating the source types when applied to NTS explosions and earthquakes spread throughout the western U.S. Taylor et al. (1988) and Patton (1988) demonstrated sensitivity in the L_g signals from explosion sources to certain source parameters including depth of burial, material properties and spall. Because of the significance of using a controlled source sample to establish empirical regional discrimination techniques, a part of our efforts in this research has focused on analysis of a data sample from NTS underground nuclear explosions and western U.S. earthquakes. Our data sources in this phase of the research were primarily selected events from the Lawrence Livermore National Laboratory (LLNL) seismic network and several additional events recorded at greater regional distances at the RSTN station RSSD. These stations provided high-quality digital data with relatively high sampling rates.

4.2 Analysis of LLNL Data

In previous reports (cf. Bennett et al., 1987a,b), we described the results of analyses of the amplitude and spectral characteristics of the regional phases recorded by the LLNL network stations from a small sample of four underground nuclear explosions and four nearby earthquakes. Those data have subsequently been supplemented with records from six additional NTS explosions and four additional earthquakes with epicenters less than 100 km from NTS. The earthquake sample was selected from the larger LLNL database so as to minimize propagation differences by choosing those earthquakes with epicenters closest to NTS. The explosion sample was selected to provide events from a single source area (Yucca Flat) with depths both above and below the water table and with at least some explosions having equivalent magnitudes to the earthquakes which were being compared. The data themselves were generously supplied by Dr. Steven Taylor with the assistance of others at LLNL. Figure 42 shows the event locations relative to the LLNL network stations, and Table 7 summarizes the event source information. The explosions were all at Yucca Flat at ranges of about 225 km from MNV (Mina, Nevada), 290 km from KNB (Kanab, Utah), 310 km from LAC (Landers, California), and 400 km from ELK (Elko, Nevada). The magnitudes of the explosions in the sample were between 4.2 and 5.5 M_L; and the source depths were from 0.3 to 0.7 km.

86
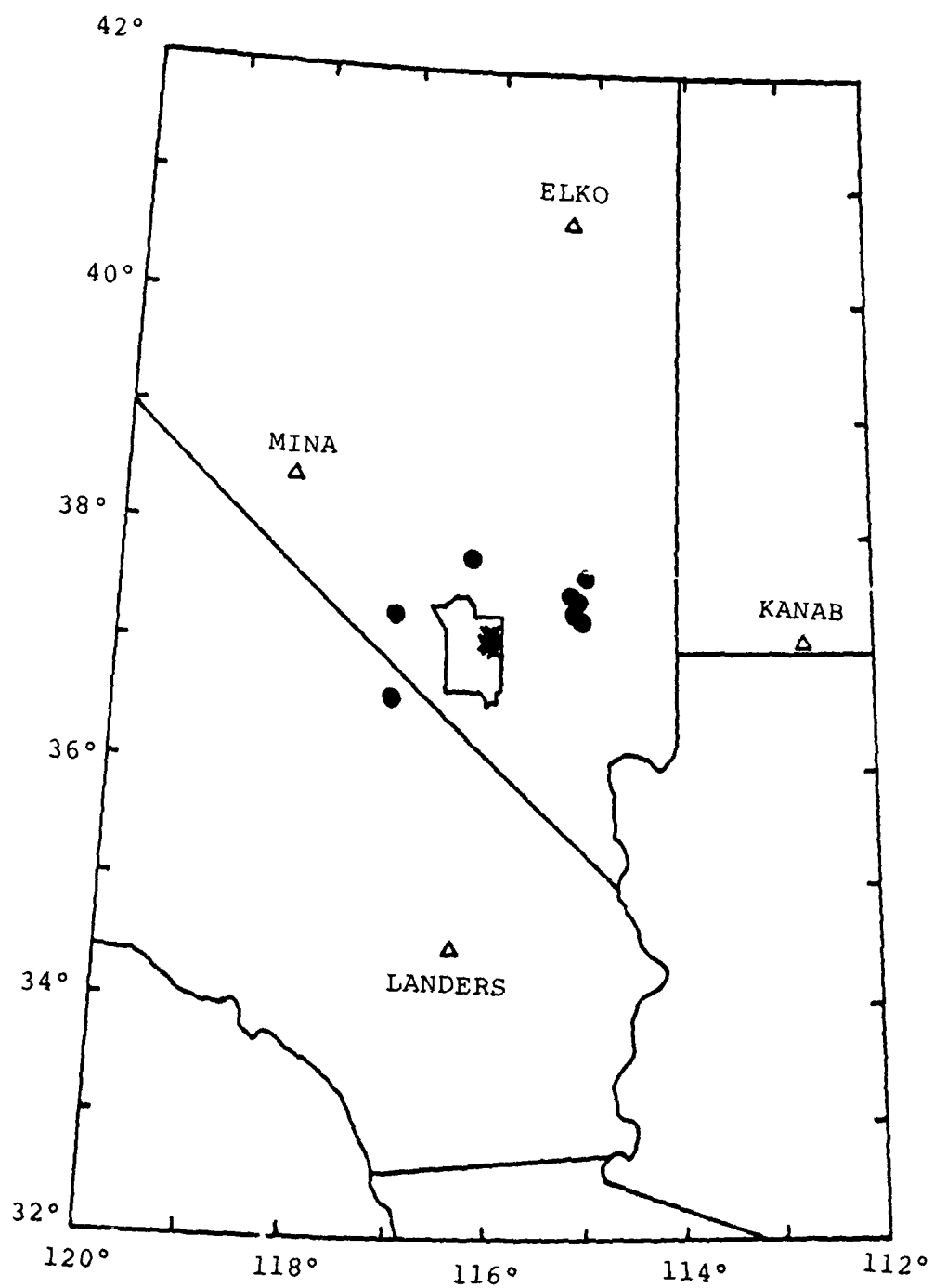
Figure 42. LLNL station locations and event sample from vicinity of NTS.

Table 7

LLNL Data Sample

NTS EXPLOSIONS

Date	Time	Lat.($^\circ$N)	Lon.($^\circ$W)	Depth(km)	M_L(BRK)	m_b	
03-31-84	14:30:00.0	37.15	116.08	0.32	4.2	4.1	AGRINI
08-11-83	14:00:00.1	37.00	116.00	0.32	4.2	4.4	SABADO
08-03-83	13:33:00.1	37.12	116.09	0.33	4.3	4.2	LABAN
01-31-84	15:30:00.0	37.11	116.12	0.39	4.4	4.1	GORBEA
09-27-78	17:00:00.0	37.08	116.05	0.44	5.0	5.0	DRAUGHTS
09-13-84	14:00:00.0	37.09	116.07	0.48	5.0	5.0	BRETON
04-14-83	19:05:00.1	37.07	116.05	0.53	5.5	5.7	TURQUOISE
04-27-77	15:00:00.1	37.09	116.03	0.59	5.1	5.4	BULKHEAD
03-23-78	16:30:00.2	37.10	116.05	0.64	5.5	5.6	ICEBERG
04-05-77	15:00:00.2	37.12	116.06	0.69	5.5	5.6	MARSILLY

EARTHQUAKES NEAR NTS

Date	Time	Lat.($^\circ$N)	Lon.($^\circ$W)	Depth(km)	M_L	$m_b(L_g)$
08-12-79	11:31:19.7	37.26	115.08	3	3.6	-
08-16-79	03:37:44.9	37.25	115.06	3	3.7	-
07-06-82	02:10:43.5	37.69	115.05	3	4.2	-
06-04-83	11:37:40.9	37.39	115.21	4	3.6	2.9
05-12-82	19:29:24.5	37.27	115.08	7	4.0	3.3
10-25-80	00:30:59.0	37.79	116.28	8	3.8	-
12-25-79	14:17:10.8	37.27	117.06	8	4.2	-
03-16-82	07:08:13.1	36.60	117.07	9	3.5	-

Earthquake locations surrounded the Test Site with ranges between 160 and 300 km from MNV, between 200 and 395 km from KNB, between 250 and 385 km from LAC, and between 340 and 485 km from ELK. The earthquake magnitudes were between 3.5 and 4.2 M_L, and the depths were between about 3 and 9 km.

In previous reports Bennett et al. (1987a,b) presented representative vertical component time histories for the smaller explosions in the database and several nearby earthquakes. Figure 43 shows representative time histories for several of the events from the LLNL database. The general characteristics of the regional phases from these events were described in the previous reports. The P_n, P_g, and L_g phases in most cases appear as clear signals except at those ranges less than the P_n-P_g crossover distance where P_n is buried in the P_g. The explosions are more repetitive in signal character from event-to-event at a fixed station than are the earthquakes; this in large measure reflects changes in propagation path and epicentral distance for the earthquakes but may also represent to some extent mechanism-dependent effects. Bennett et al. (1987a,b) showed that such differences could considerably modify the relative amplitudes of the P_n, P_g and L_g signals as is observed for the earthquakes. However, some differences have also been noted in the different explosions measured at common stations (cf. Bennett et al. , 1987a,b) suggesting the possibility that small changes in the explosion source parameters might significantly affect the relative amplitude of P_g and L_g and the frequency content of the signals.

In analyzing the more recent LLNL data sample, our studies have focused on the spectral behavior of the regional phases. Time windows encompassing the principal energy in the P_g and L_g signals were picked from the records. These were fairly consistent for events with similar source locations; but, in any case, small shifts in the window times produced only minor changes in the computed spectra. Window lengths were taken to be approximately 12.5 seconds for P_g and approximately 25 seconds for L_g. The spectra were also computed for noise windows approximately 6.3 seconds in length preceding the P wave. The window lengths were somewhat variable between events because the sampling rate of the LLNL network recording system was not always consistent. For most events the digitizing rate was 40 samples per second, but some events were recorded at a rate of 42 samples per second and several at a rate
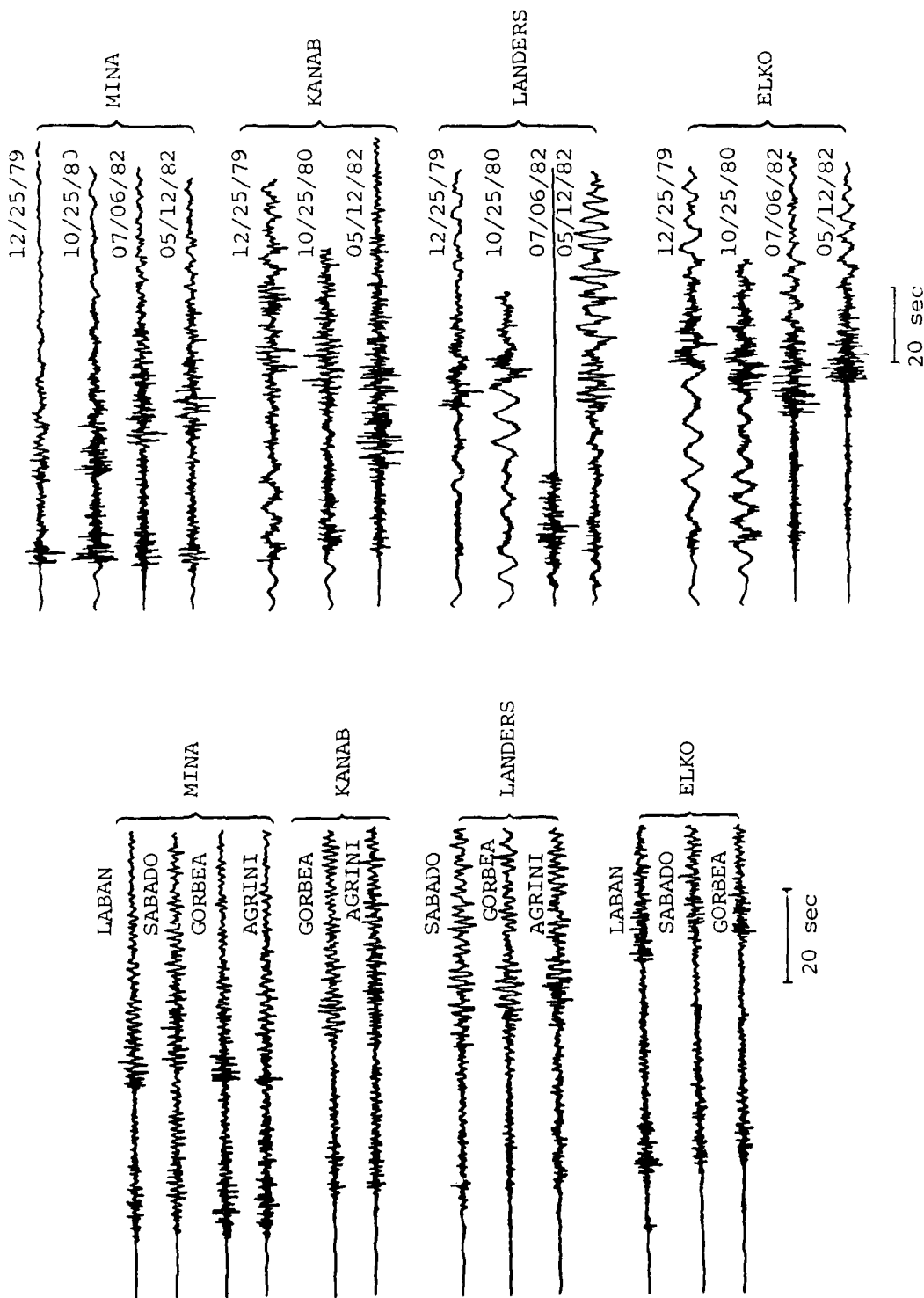
Figure 43. Typical vertical-component records at LLNL stations from NTS explosions (left) and regional earthquakes (right).

of 62.5 samples per second. Such differences are not expected to have a significant effect on the spectral amplitudes in the frequency band of interest because the spectra have been normalized by the window lengths and smoothing was applied to provide roughly comparable frequency resolution.

In a previous report Bennett et al. (1987b) showed that the signal-to-noise levels of L_g and P_g signals for most events in the LLNL database was good out to frequencies of 10 Hz or so. In some cases the L_g and P_g spectra have been found to flatten-out at levels well above the pre-P ground noise at frequencies less than 10 Hz apparently because of limitations on the dynamic range of the recording equipment. It was further noted that the L_g and P_g spectra for explosions tended to fall-off more rapidly at higher frequencies than the signals of earthquakes with comparable magnitudes. To check the latter observation with the enhanced LLNL database, the L_g and P_g spectra for all events were normalized to common amplitude levels at 1 Hz. Then the explosion and earthquake spectral shapes were averaged separately over the events from each source type out to those frequencies where spectral flattening associated with the dynamic range problem became apparent. Figure 44 shows the average earthquake and explosion spectral shapes for the L_g signals recorded at each station. In all cases we see that the average earthquake and explosion spectra match fairly closely out to about 2 Hz but the explosion spectrum falls-off at higher frequencies much more rapidly than the average earthquake spectrum. Figure 45 shows the mean plus and minus one standard deviation L_g spectral shapes. At all stations the L_g spectral shapes for earthquakes and explosions are observed to be totally separated at the one-sigma level above about 4 Hz. This observation is similar to the behavior of the L_g spectra previously found by Murphy and Bennett (1982) and Bennett and Murphy (1986) from analyses of the signals recorded at the VELA array stations. In those studies the spectral differences between the explosions and earthquakes could only be observed out to about 4 Hz because of recording instrument limitations. The results here suggest that even greater separation in the L_g spectra between the NTS explosions and nearby earthquakes is achieved at higher frequencies (viz out to at least 10 Hz). Thus, the L_g spectral ratio discriminant might be enhanced by observations at higher frequencies. Figure 46 shows similar average spectral shapes for the P_g phases recorded by the LLNL network stations. Like the L_g behavior, the explosion and earthquake spectral shapes are observed to match fairly closely at frequencies below about 2 Hz but then separate at higher
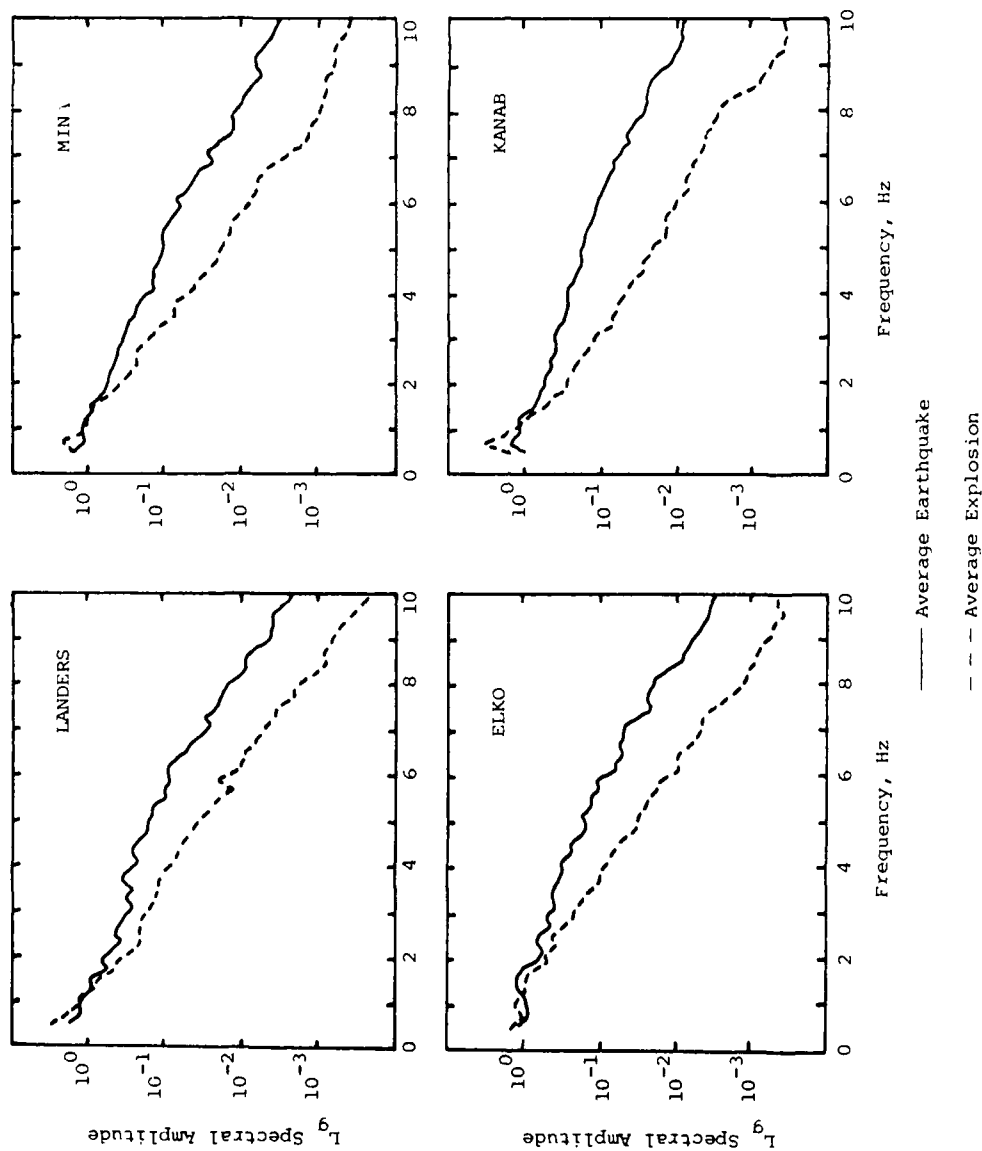
91

Figure 44. Comparison of average L_g spectral shapes for NTS explosions and nearby earthquakes recorded by LLNL stations.
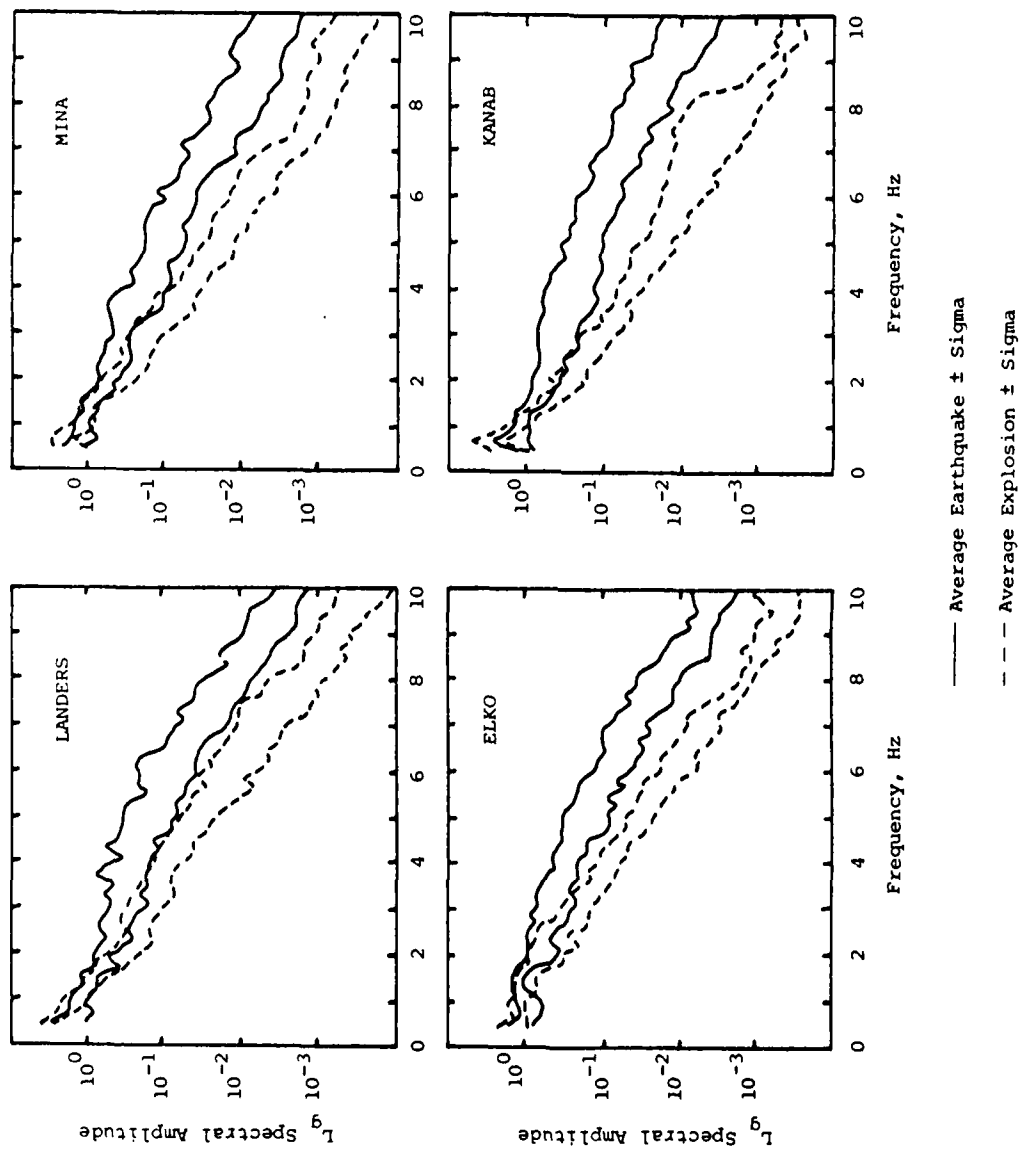
Figure 45. Comparison of one-sigma bounds on average L_g spectral shapes from Figure 44.
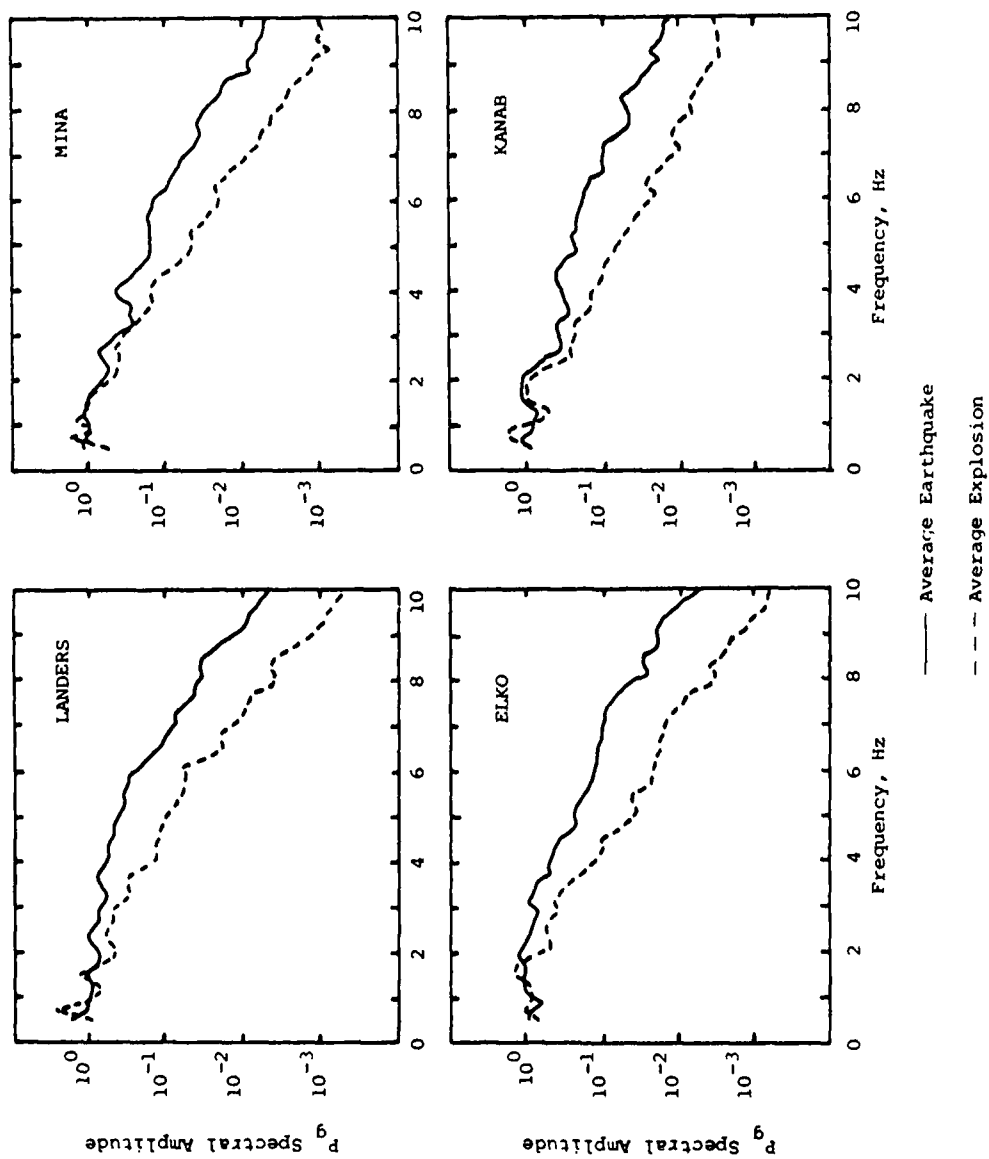
Figure 46. Comparison of average P_g spectral shapes for NTS explosions and nearby earthquakes recorded by LLNL stations.

frequencies with the earthquake spectra appearing relatively richer in high frequencies. The behavior is again in general agreement with the P_g spectra previously measured at the VELA array stations (cf. Murphy and Bennett, 1982; Bennett and Murphy, 1986).

One interesting characteristic of the regional signals which isn't obvious from the comparison of the L_g and P_g spectra in Figure 44 and 46, is that the relative enrichment of the high frequencies in the earthquake versus the explosion signals is more prominent for the L_g than for the regional P waves. This can best be seen from bandpass filter analyses of the time histories. Figure 47 shows the results of such an analysis applied to the regional signals from a small explosion (AGRINI) and an earthquake (06/04/83) recorded at the LLNL network station KNB. It can be seen that for the unfiltered trace and for the low-frequency band (0.2-4.0 Hz) the relative amplitudes of the L_g and P_g signals are about the same for the explosion and the earthquake. Bennett et al. (1987b) showed that L_g-to-P_g amplitude ratios measured from the unfiltered traces for these explosions and earthquakes were intermingled and had substantial scatter particularly for the earthquakes. However, in the higher frequency bands the L_g signal for the explosion drops off dramatically relative to the P waves. On the other hand, the L_g signal for the earthquake in higher frequency bands remains strong relative to the P_g phase. As a result, the L_g-to-P_g amplitude ratio at high frequencies is much larger for the earthquake than for the explosion. Figure 48 shows similar results for an additional explosion (BRETON) and earthquake (08/16/79) also recorded at station KNB. The main difference here appears to be that the P_n phase in explosion BRETON is stronger and the L_g phase in the 08/16/79 earthquake is stronger. Just as in Figure 47, the L_g-to-P amplitude ratio in the higher frequency band is much larger for the earthquake than for the explosion. Unfortunately, we have not yet systematically tested the consistency of this observation on a larger event sample; although some additional test cases at other stations for a few frequency bands have produced similar results (cf. Bennett et al. , 1987b). A careful comparison of the spectra in Figures 44 and 46 indicates that at high frequencies the L_g-to-P_g amplitude ratios on the average is larger for earthquakes than explosions measured at two of the stations, KNB and MNV; but this distinction is less obvious at the other two stations. The latter suggests that this observation could be associated with a radiation pattern effect which may be weak at some azimuths.
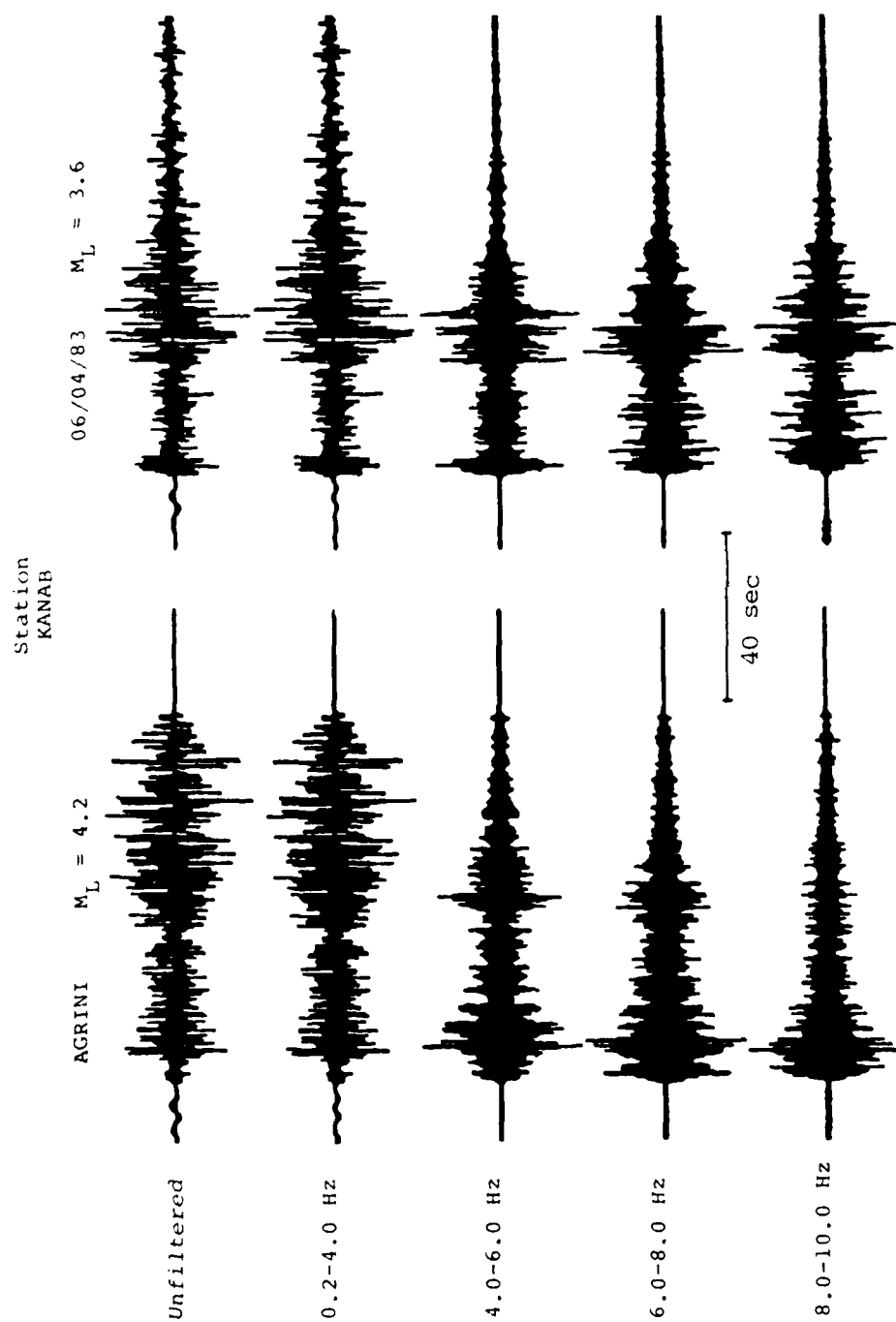
Figure 47. Bandpass filter analysis applied to explosion (left) and nearby earthquake (right) recorded at LLNL station KANAB.
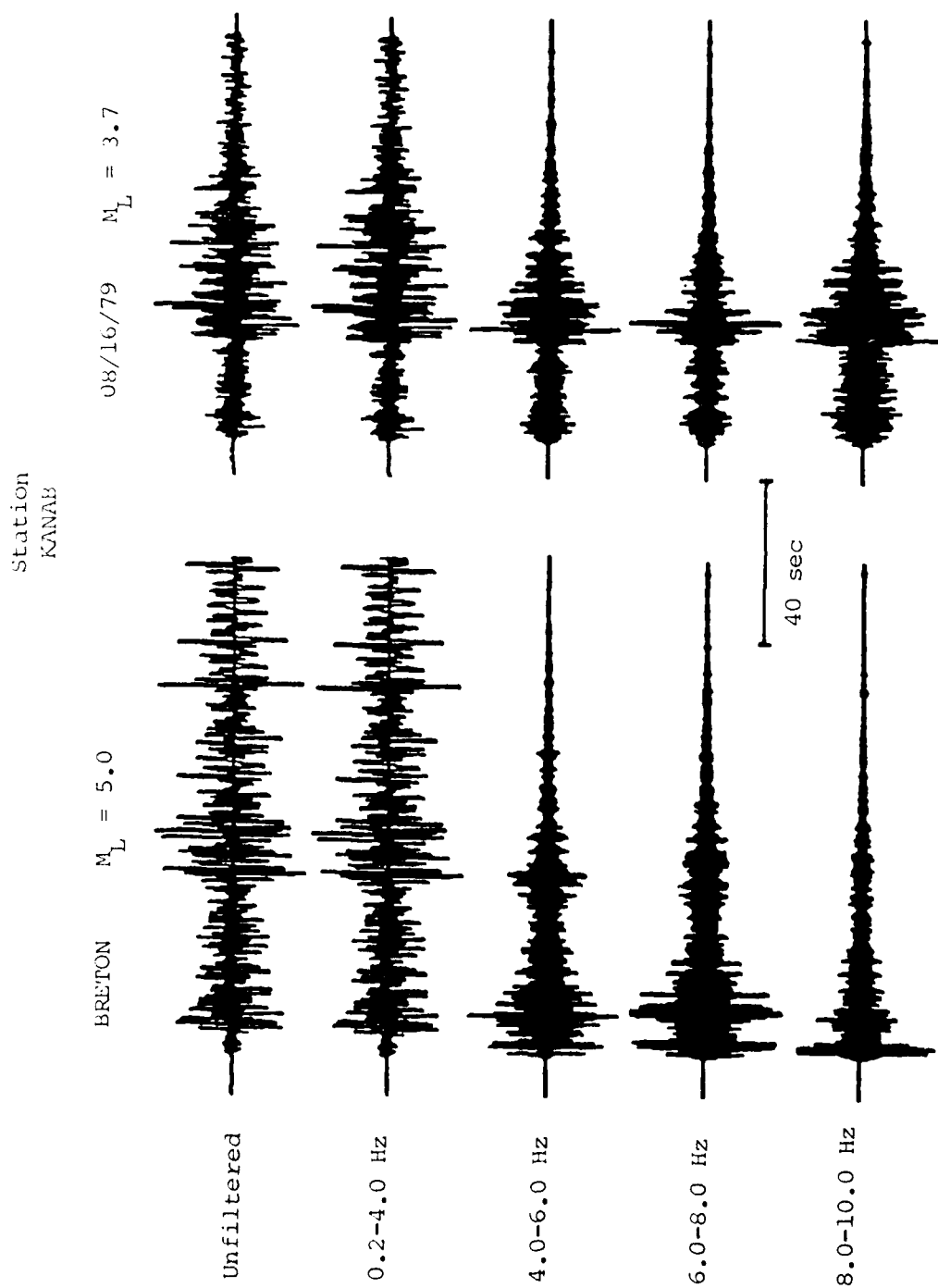
Figure 48. Bandpass filter analysis applied to different explosion (left) and earthquake (right) recorded at LLNL station KANAB.

97

As pointed out above, one goal in selecting the explosion database, which is a subset of the larger LLNL database, was to include a range of source depths. In particular, we sought a sample with source depths above and below the water table at Yucca Flat, so it could be determined whether this relatively strong contrast in material properties might be affecting the spectral behavior of the regional phase signals from NTS explosions. In a previous report Bennett et al. (1987b) found that explosions below the static water table tended to produce only slightly larger L_g-to-P_g amplitude ratios measured at station ANMO (R $\approx$ 900 km) than those above the water table. It was also found that the P_g and L_g spectra at ANMO for a small sample (three above and three below the water table) of Yucca Flat explosions appeared to show little effect of the water table to frequencies of 5 Hz. Taylor et al. (1988) found that more deeply buried NTS explosions tended to produce regional phases at LLNL stations which were relatively richer in high frequencies and suggested several mechanisms which might explain this observation. Patton (1988) also saw evidence of L_g coupling variations within Yucca Flat and, in particular, found that events above the water table showed more scatter in L_g magnitudes which he attributed to porosity effects. Of the ten Yucca Flat explosions in our LLNL database (cf. Table 7, above) only three had source depths below the static water table (viz the three deepest events). The corresponding average spectral shapes for the L_g and P_g signals are shown in Figures 49 and 50, respectively. In both cases there appears to be a slight tendency for explosions below the water table to be richer in high frequencies. This is opposite of the effect that would be expected from the decreased corner frequency associated with the larger magnitudes of these deeper events. The observation is in general agreement with the findings of Taylor et al. cited above, but they also suggested that deeply overburied explosions might confound a spectral discriminant of the type described.

Although the effect of burial below the water table seems to be a slight enhancement of the higher frequencies in the regional phase spectra, it isn't clear from the evidence presented here whether this would be adequate to diminish the effectiveness of the regional phase spectral differences between earthquakes and explosions as a discriminant. To obtain additional insight into the problem, we focused on the P_g and L_g spectra for only explosions below the water table for our LLNL sample (i.e., three events). Figures 51 and 52 compare the average P_g and L_g spectral shapes for these deeper explosions with the average earthquake spectral shapes at the four LLNL stations. The

Figure 49. Comparison of L_g spectral shapes for NTS explosions above and below the water table recorded by LLNL stations.

99

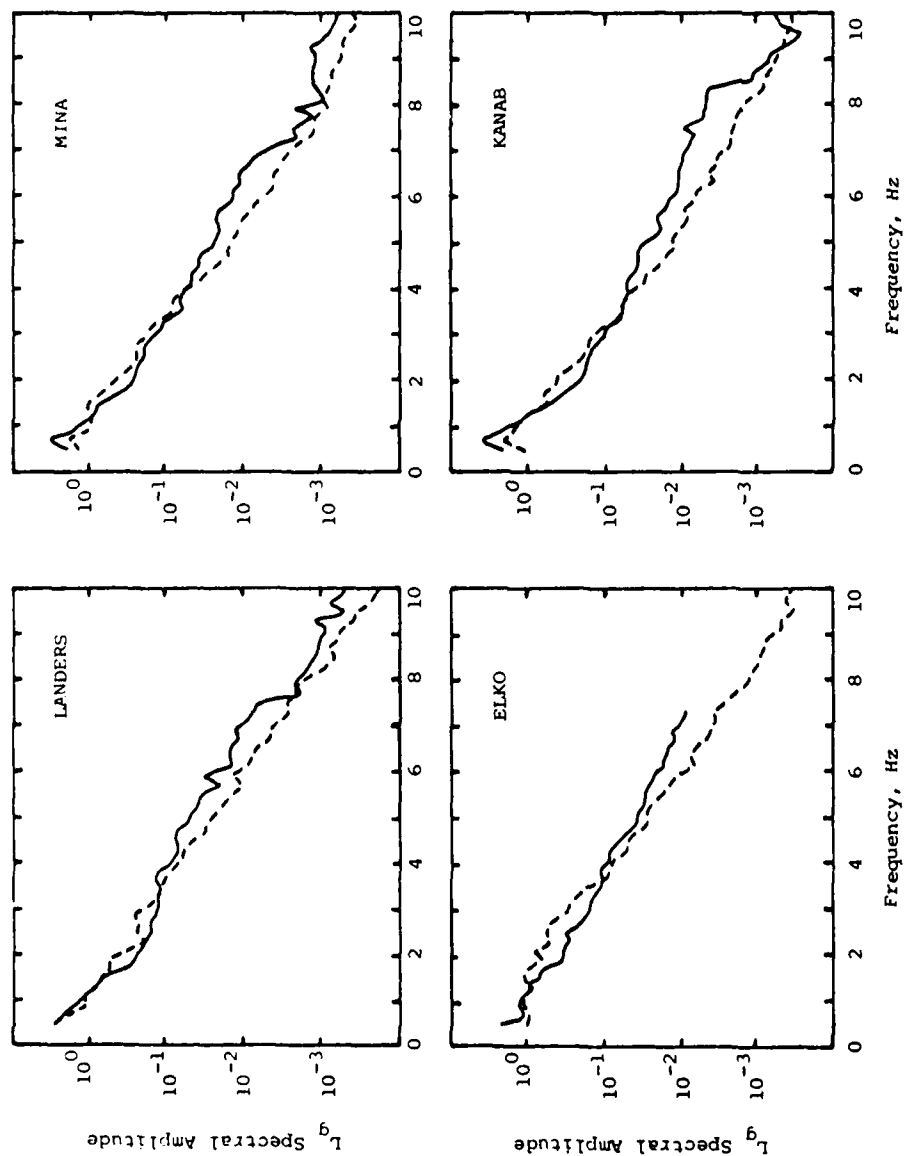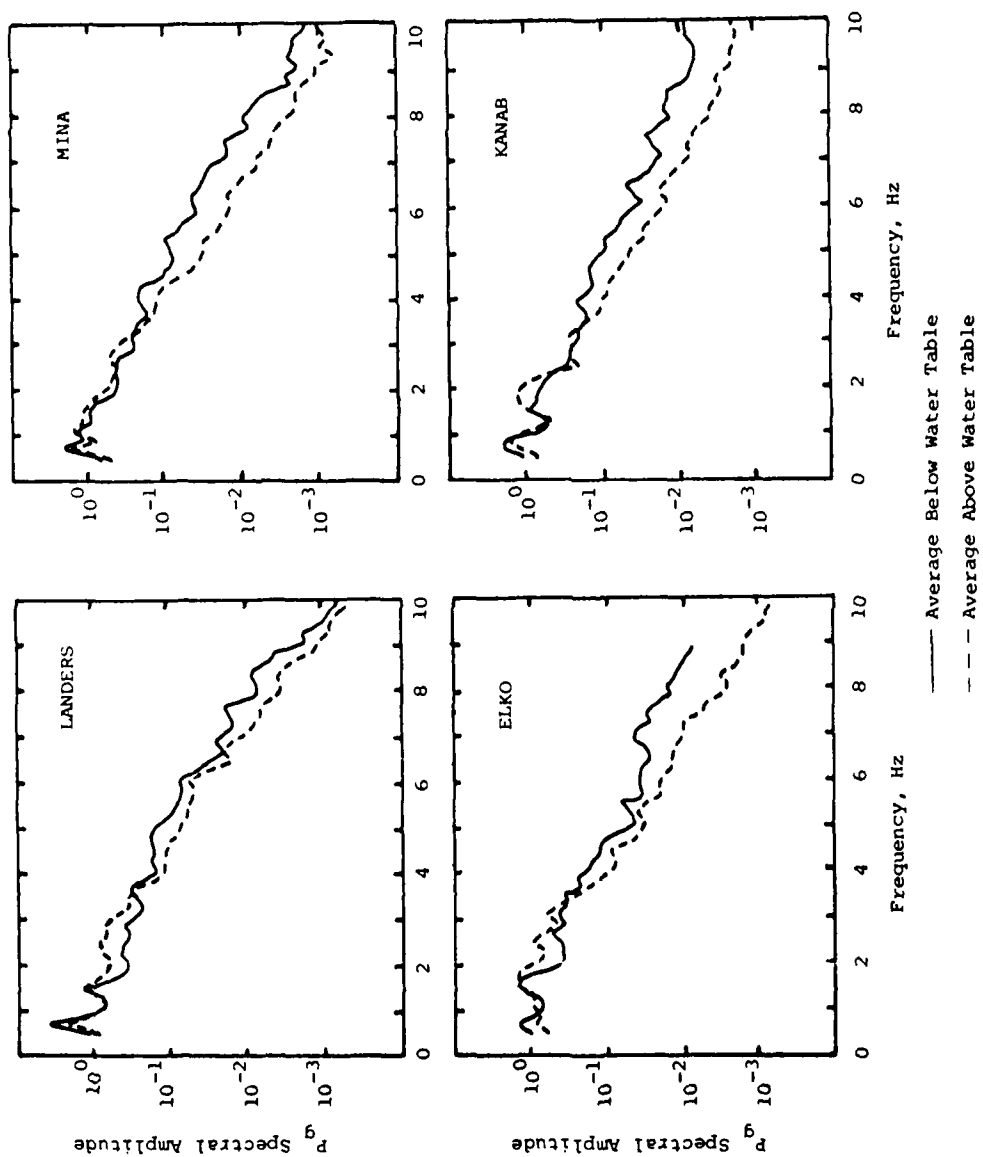Figure 50. Comparison of P_g spectral shapes for NTS explosions above and below the water table recorded by LLNL stations.
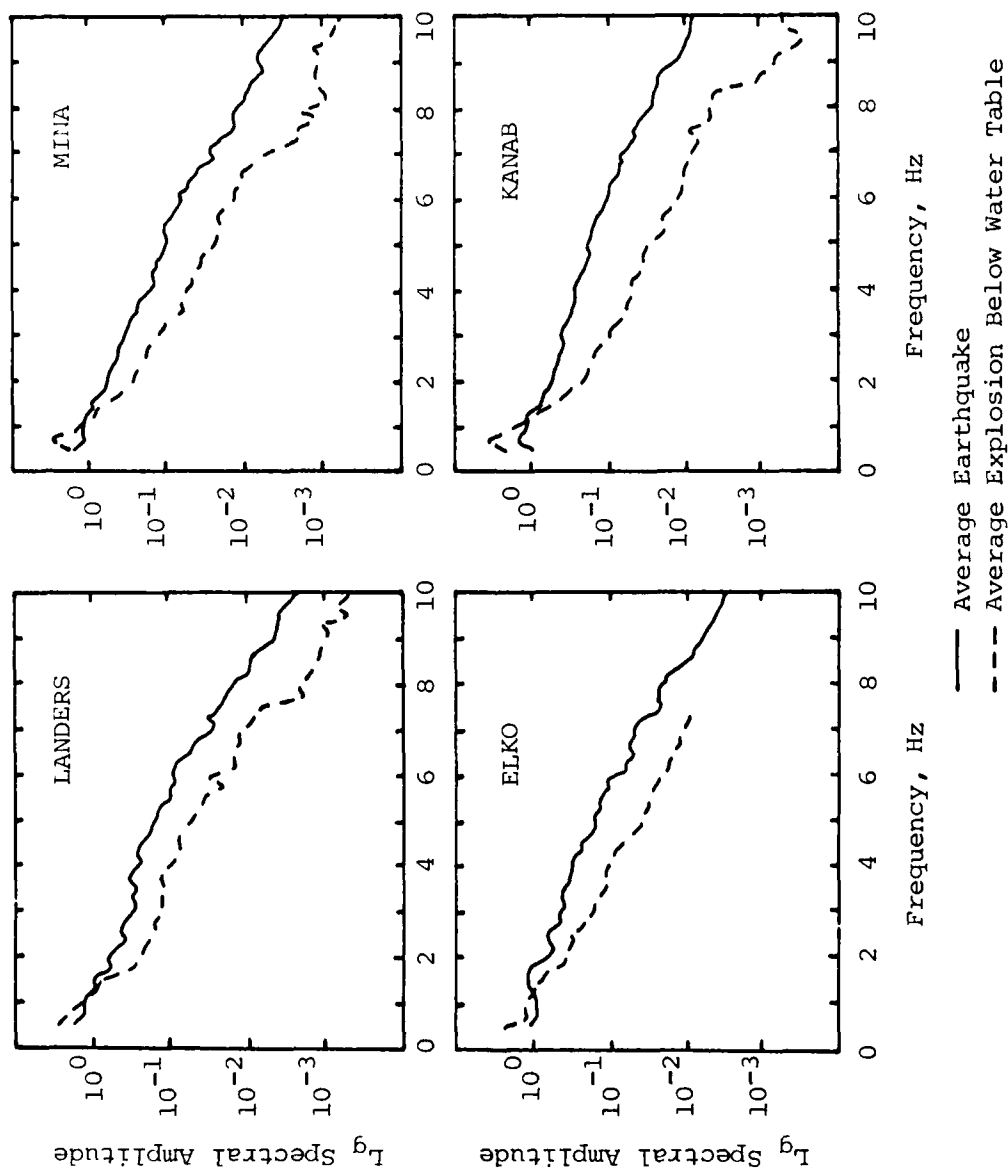
Figure 51. Comparison of L_g spectral shapes for average explosions below the water table and average earthquakes recorded by LLNL stations.

Figure 52. Comparison of Pg spectral shapes for average explosions below the water table and average earthquakes recorded by LLNL stations.
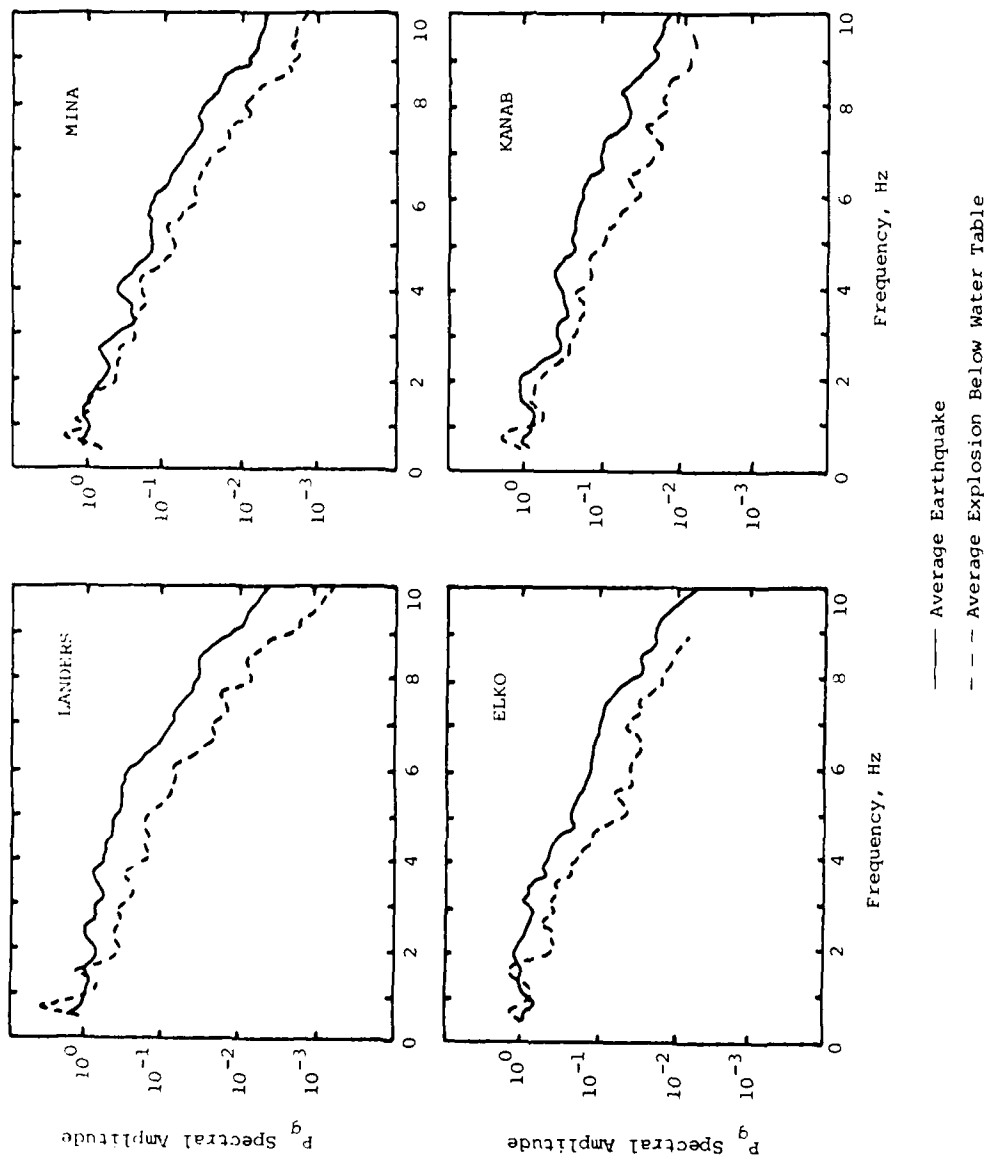
102

comparisons show that there is still substantial separation at higher frequencies between the earthquake and explosion spectra. One would intuitively expect from source theory that smaller magnitude explosions, at depths comparable to these three deeper explosions, would further reduce the spectral separation between explosions and earthquakes because of the corner frequency shift. However, there is no way of telling from our limited empirical database how significant these other effects of overburial will be in altering the L_g and P_g spectra from small explosions. In this regard it is interesting to note that the two overburied explosions described by Taylor et al. (1988) produced L_g spectral ratios only marginally lower than several other normally contained explosions of comparable magnitude. So, it is not clear to what extent the overburial or other unknown factors might be influencing the observed spectral ratios. The resolution of these questions will ultimately require improved theoretical understanding of L_g generation by explosion sources and additional observational results to confirm the theory. The LLNL network measurements should continue to provide an excellent data source for such investigations.

4.3 NTS Explosions and Earthquakes at RSSD

In Section III above we described the characteristics of regional phase signals from Soviet underground nuclear explosions in East Kazakh and comparable earthquakes. It was noted there that available stations for regional monitoring of those events were located at distances considerably larger than those LLNL network stations used in the preceding analysis of discrimination of NTS explosions. To get some idea of regional discrimination capabilities for NTS events using high quality stations at regional distance ranges more comparable to the Soviet experience, we have briefly reviewed the characteristics of regional phases recorded at the RSTN station RSSD from NTS underground nuclear explosions and earthquakes at comparable magnitudes, ranges and azimuths in the western U.S. The RSSD station is located in South Dakota about 1300 km northeast of the explosion source area at NTS. It is noted at the outset that attenuation of regional phases in the crust of the western U.S. is known to be relatively large; so that, even though the distances are comparable to the observations from Soviet events, some adjustments to the regional signals may still be appropriate before results from the two areas can be compared.

103

Figures 53 and 54 show the vertical-component, short-period records observed at RSSD for a sample of NTS explosions and several earthquakes. Figure 53 shows five Yucca Flat explosions with magnitudes between 4.8 and 5.9 m_b, and Figure 54 shows two Pahute Mesa explosions with magnitudes of 5.5 and 5.7 m_b and three California earthquakes with magnitudes from 5.6 to 6.1. The ranges of the earthquakes from RSSD were from 1430 km to 1670 km compared to explosion ranges between 1280 km and 1290 km. The ranges and paths are somewhat different; but, for the available database from RSSD, these events appear to provide the best comparisons. At these ranges the regional signals at RSSD appear to be dominated by early P phases and L_g. The early P phases are believed to be associated with upper mantle and deeper crustal propagation paths including P_n and P^*; the P_g phase following after these early P phases is less distinct at this range appearing as a coda segment of increased amplitude but smaller than the earlier P phases. The P signals from the NTS explosions are remarkably similar in character to those seen above in Figure 21 from Shagan River explosions recorded at station WMQ. In particular, the P signals in both cases include two or three distinct phases with apparent group velocities between about 7.6 and 6.3 km/sec. If the observation of these phases prevails at other far-regional Soviet stations (e.g., the new IRIS stations), detailed comparisons of the signal characteristics between the NTS shots and Soviet explosions may provide important source information. The L_g signals at RSSD appear on the short-period vertical records as strong signals roughly equivalent in amplitude to the P phases. The L_g-to-P amplitude ratio is generally near 1.0 or slightly less than 1.0 for the explosions and near 1.0 or slightly greater than 1.0 for the earthquakes.

To get additional insight into the characteristics of these regional signals at RSSD, Fourier spectra were computed for the P_n (viz initial P), P^*, P_g and L_g window segments for the explosion CAPROCK (m_b = 5.8, R = 1280 km) and the Round Valley earthquake near Mammoth Lakes, California (m_b = 5.6, R = 1435 km). These are shown in Figure 55; no instrument correction has been applied. The uncorrected spectra are all rather sharply peaked in the frequency band from 0.5 to 2 Hz and fall off rapidly to noise at higher frequencies. The spectra appear to reach a noise floor near 5 to 7 Hz for the various P phases and near 4 Hz for L_g. The overall spectral shapes of the individual phases are not greatly different for the explosion and earthquake, even though there appear to be some differences in spectral details. The most notable difference is that

104
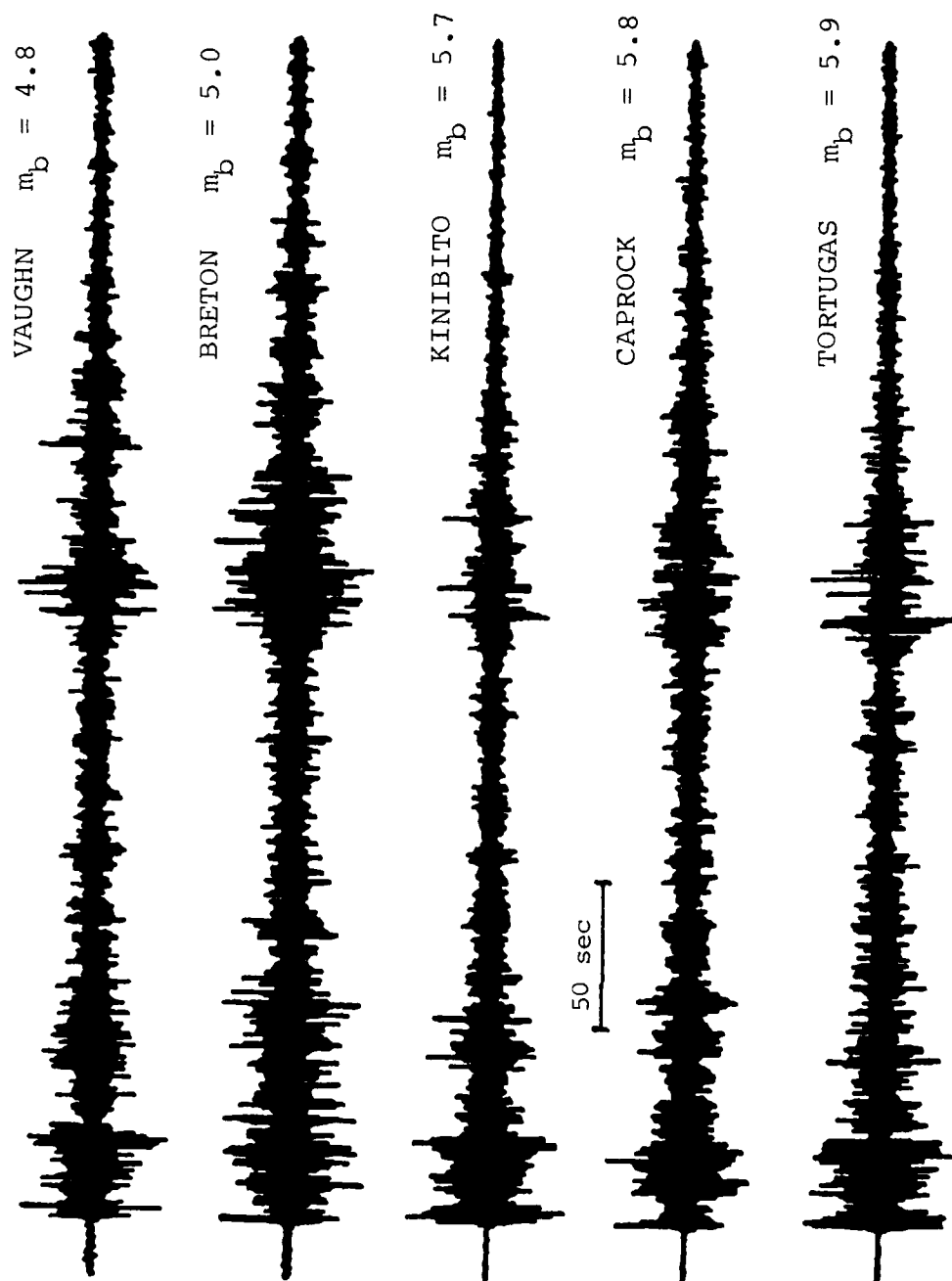
Figure 53. Vertical-component records at station RSSD from five Yucca Flat explosions.

VAUGHN m_b = 4.8

BRETON m_b = 5.0

KINIBITO m_b = 5.7

CAPROCK m_b = 5.8

TORTUGAS m_b = 5.9

50 sec

105

Figure 54. Vertical-component records at station RSSD from two Pahute Mesa explosions and three California earthquakes.

SALUT m_b = 5.5
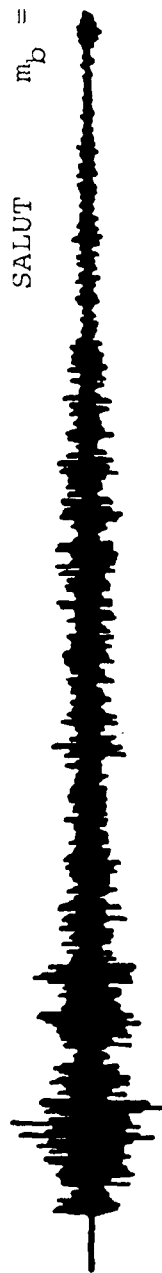
TOWANDA m_b = 5.7

ROUND VALLEY, CA m_b = 5.6
EARTHQUAKE
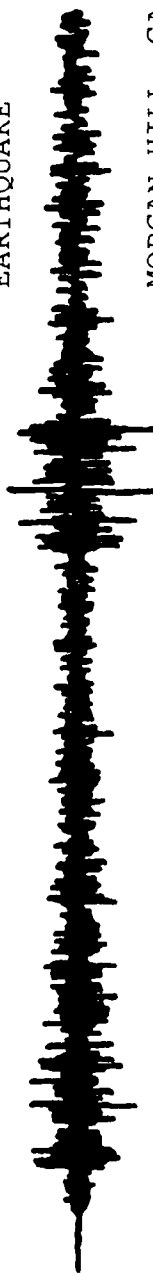
MORGAN HILL, CA m_b = 5.7
EARTHQUAKE
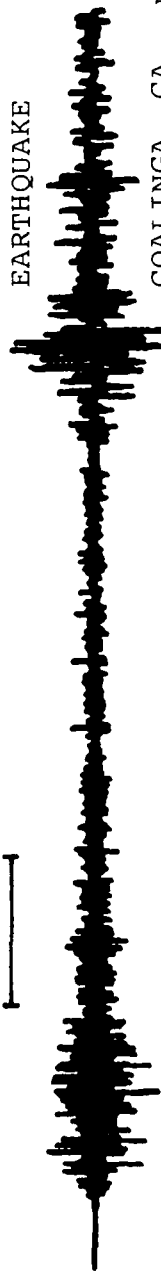
COALINGA, CA m_b = 6.2
EARTHQUAKE

50 sec
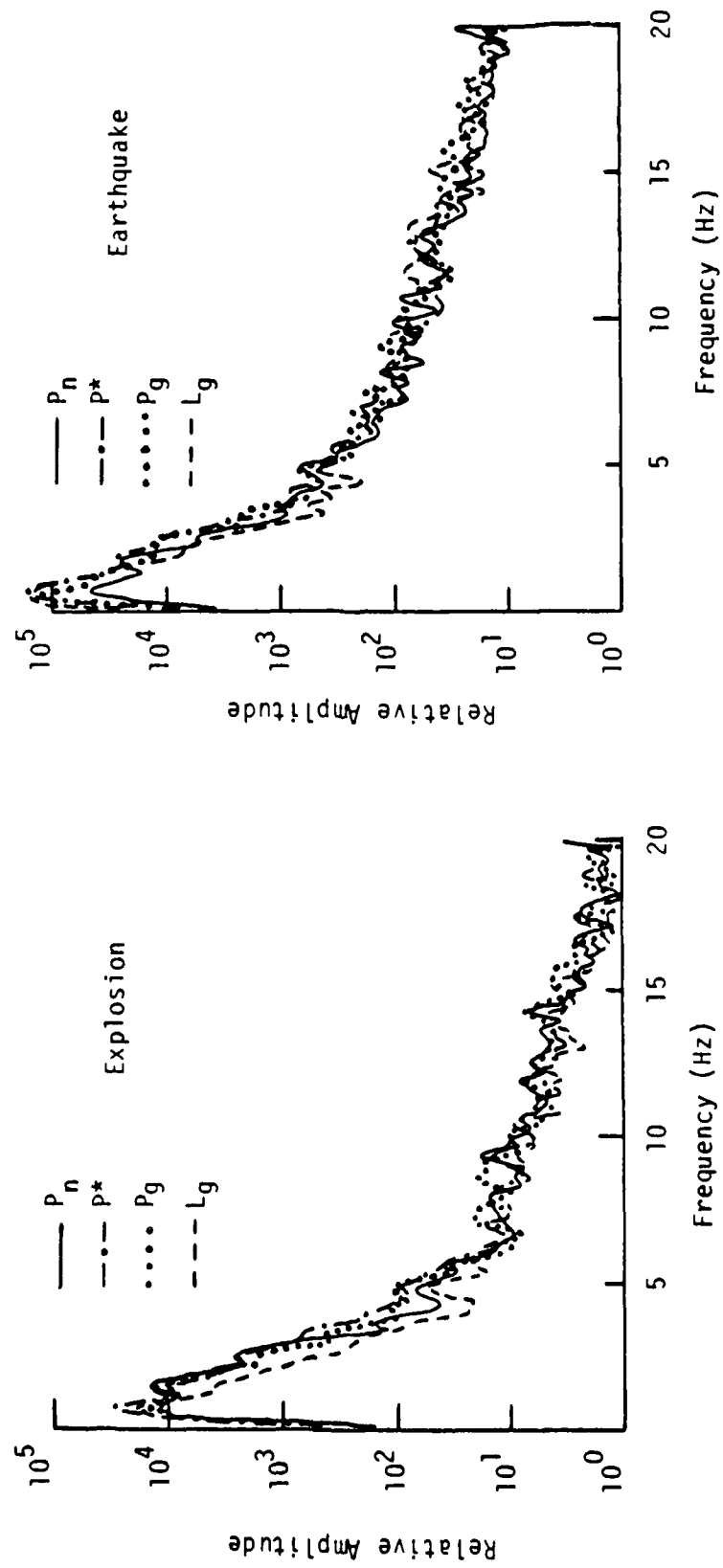
Figure 55. Comparison of regional phase spectra at RSSD for Yucca Flat explosion CAPROCK, $m_b = 5.8$, (left) and the Round Valley, California earthquake, $m_b = 5.6$, (right).

107

the explosion spectra seem to be constrained to a somewhat narrower frequency band than the earthquake spectra resulting in sharper spectral peaks. This is particularly apparent in the L_g signals for the two events. As noted above, the explosion and earthquake have somewhat different magnitudes and ranges which could affect the spectral shapes; but we would expect these two factors to compensate each other to at least some extent for these events. If the observed difference in spectra is real, it is consistent with our findings at smaller ranges that earthquake spectra are relatively richer in high frequencies than explosion spectra.

In Section III above we found from bandpass filter analysis that the L_g-to-P ratio measured at WMQ for Shagan River explosions was much smaller at high frequencies (greater than about 3 Hz) than similar ratios for the comparable earthquakes in the database. To test the applicability of such a discriminant on the NTS explosions and California earthquakes recorded at RSSD, a similar bandpass filter analysis was performed on several of the events. The results of the analyses for four representative events (two explosions and two earthquakes) are shown in Figures 56 and 57. In general, the results show that the signal-to-noise levels for events of this magnitude are greater than 1.0 for the P and L_g phases up to about the filter passband of 3 to 6 Hz, and in some cases to even higher frequencies for the P phases.

For the explosion (KINIBITO) and earthquake (Round Valley, California) in Figure 56, it can be seen that the L_g-to-P ratio at low frequencies (0 to 1.0 Hz) is somewhat less than 1.0 for the explosion and greater than 1.0 for the earthquake. The L_g-to-P ratio appears to decrease toward higher frequencies for both events, but the decrease is less rapid for the earthquake. As a result, the greatest distinction in the L_g-to-P ratio between the explosion and the earthquake seems to occur for the 1 to 3 Hz passband. It may also be noteworthy that the initial P is the predominant phase in the filter passbands between 0.5 and 4.0 Hz but not at low frequencies for the explosion in Figure 56. In contrast, the most prominent P phase for the earthquake record is not the initial P but somewhat later crustal phases for all passbands.

The events in Figure 57 (i.e., explosion SALUT and the Morgan Hill, California earthquake) show somewhat different behavior. The most prominent P phase for both the explosion and earthquake, in this case, are not the initial P
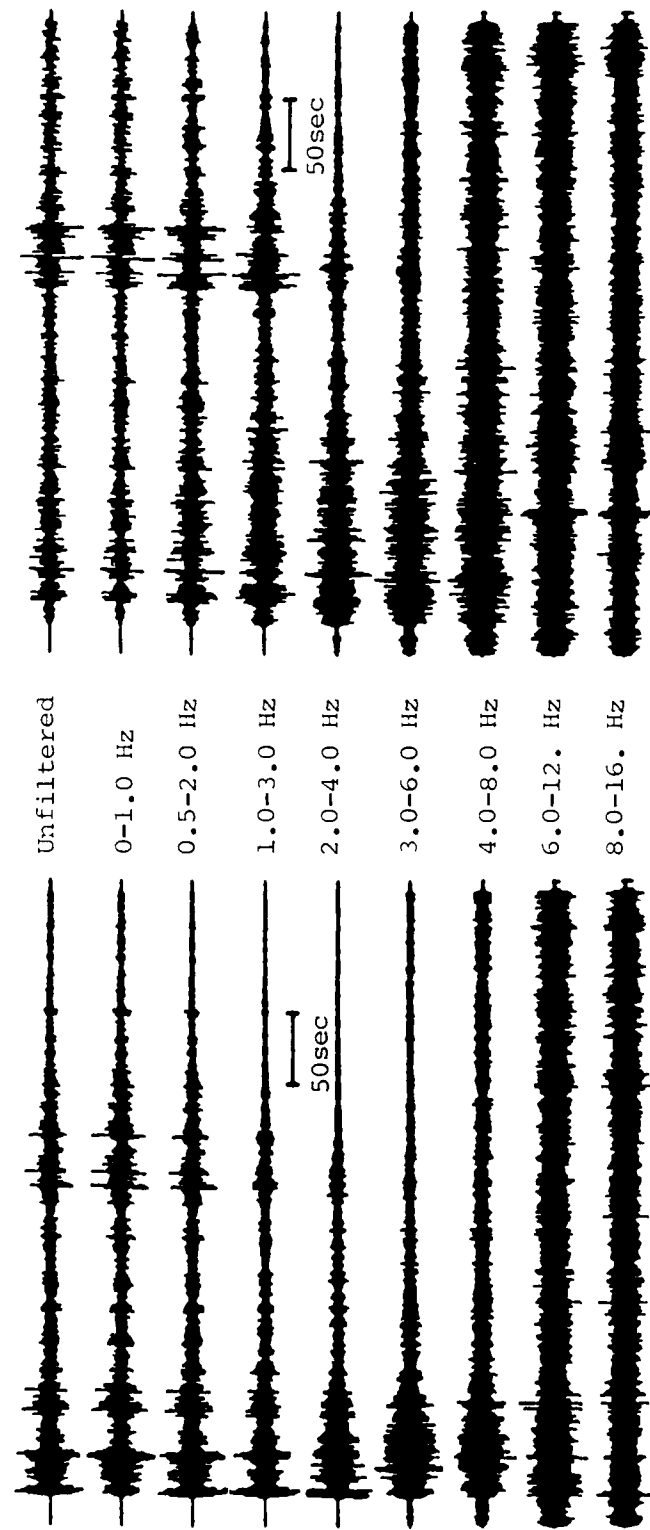
Figure 56. Bandpass filter analyses of vertical component records at station RSSD for explosion KINIBITO, $m_b = 5.7$, (left) and Round Valley, California earthquake, $m_b = 5.6$, (right).
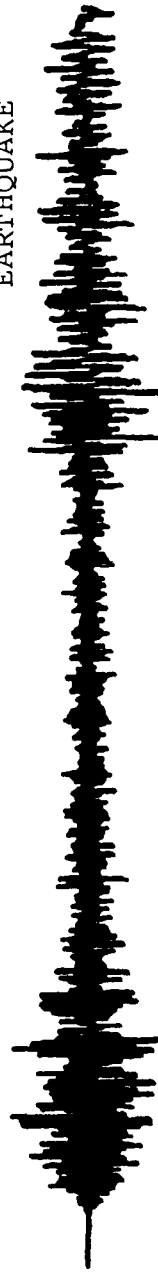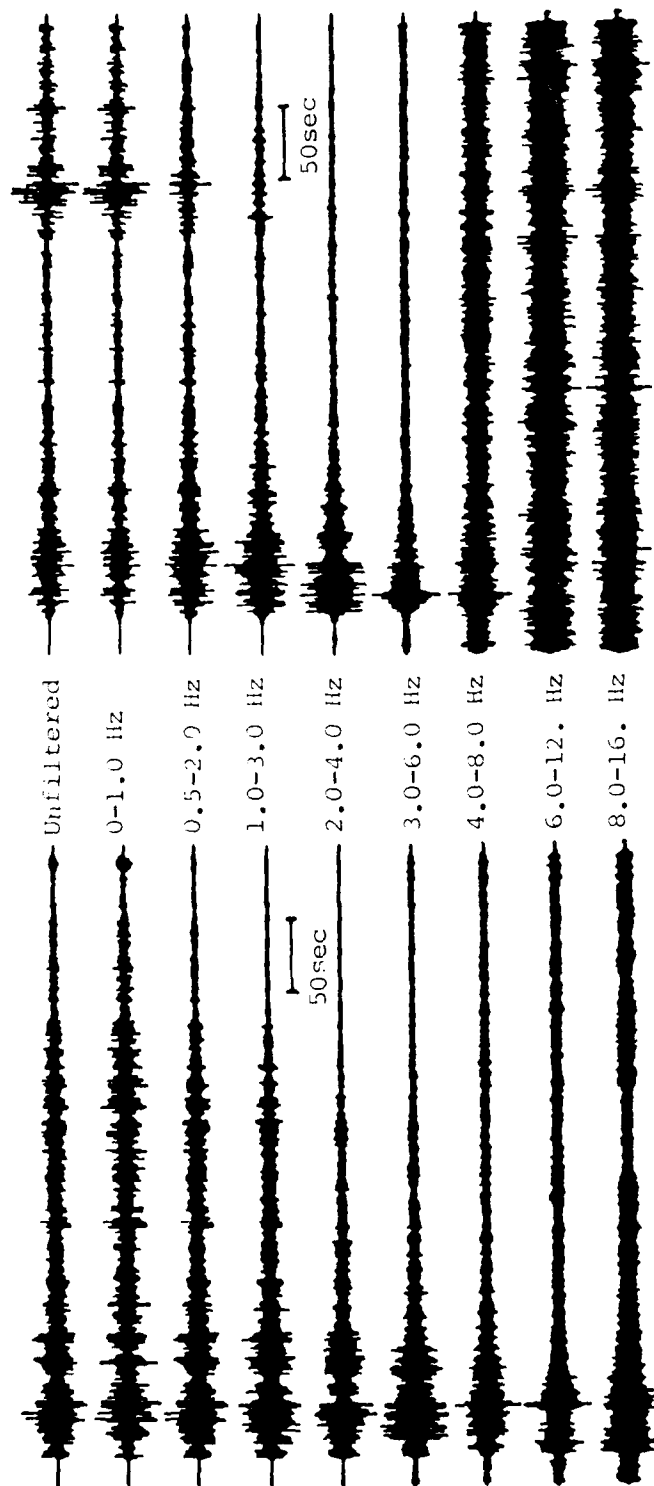
Figure 57. Bandpass filter analyses of vertical component records at station RSSD for explosion SALUT, m_b = 5.5, (left) and Morgan Hill, California earthquake, m_b = 5.7, (right).

but later crustal phases. Furthermore, the biggest distinction in the L_g-to-P ratio seems to be at lower-frequency filter passbands (viz 0 to 1.0 Hz) where the ratio is near 2.0 for the earthquake and only about 0.7 for the explosion. The L_g signals in the earthquake appear to be severely attenuated above about 2 Hz. It is not clear whether the latter is a propagation or source effect. Complex mechanisms have been attributed to both the Morgan Hill and Round Valley earthquakes (cf. Abrahamson and Darragh, 1985; Corbett, 1985) and the path for the Morgan Hill earthquake includes a segment crossing the Great Valley and Sierra Nevada Batholith which is not present for any of the other events in Figures 56 and 57. A similar analysis of the Coalinga, California earthquake record at RSSD, which also included a Great Valley/Sierra Nevada path segment, was again depleted in L_g energy at frequencies above 2 Hz.

Thus, while the RSSD observations of larger NTS explosions and comparable California earthquakes offer hope that discrimination capability may persist to some degree at larger regional distances even for some events in the western U.S., they also raise again the caveat that care must be exercised in accounting for propagation and source variations. In areas such as the Soviet Union where the empirical database to test regional discrimination is deficient, the case for regional discrimination will clearly depend on improved knowledge of propagation effects on regional phases at higher frequencies and some understanding of potential earthquake source mechanisms in areas of interest.

V. CONCLUSIONS AND RECOMMENDATIONS

The objective of this research program has been to investigate the charac-
teristics of regional seismic signals recorded by high-quality, high-frequency sta-
tions and to determine how those characteristics might be utilized to distinguish
various source types including underground nuclear explosions, earthquakes,
and commercial blasts. To accomplish this objective we collected and analyzed
the available high-quality digital data from three different tectonic environments:
(1) eastern North America, (2) southern Soviet Union, and (3) western U.S.
These data included regional signals from each of the source types of interest.
The database was drawn from a variety of sources including the RSTN and
ECTN for eastern North America, the CDSN and Soviet/NRDC network for the
southern Soviet Union, and the LLNL network and RSTN for the western U.S.
We found that data from each of these sources provide unique contributions to
different aspects of the regional discrimination problem.

For each tectonic environment we performed amplitude and spectral com-
parisons of the regional signals to delineate differences related to source type.
Those comparisons have revealed several differences in the regional phase sig-
nals which appear to be source related and which should receive further con-
sideration as potential discrimination measures. In particular, spectral com-
parisons of the relative excitation of various regional phases continues to show
differences which appear to be diagnostic of different source types. Extension
of regional signal monitoring to broader bands and higher frequencies appears
to offer an opportunity to enhance this capability. It seems likely that many
regional events could eventually be categorized by such comparisons. On the
other hand, in some cases our analyses have also indicated the sensitivity of
the regional signal behavior to propagation path characteristics in addition to
source differences. The latter observation emphasizes the need for care in
discrimination studies to isolate source differences by properly accounting for
propagation effects. This would be particularly important in applying experience
from one tectonic environment to another. This capability too should be
enhanced as we gain experience from new regional monitoring efforts in the
areas of interest. Our studies have also identified potential limitations on tech-
niques for distinguishing small, non-nuclear blasts which could be a particular

problem at lower monitoring thresholds. The results suggest that the regional signals from such events may be sensitive to shooting practice and that bandpass limitations on the signals could reduce the effectiveness of some techniques (viz cepstral analysis) used to distinguish commercial blasts.

For eastern North America we found that small regional events, including earthquakes and presumed mine blasts, generally produced strong regional P and L_g phases. At station RSCP the mine blast signals were different from the earthquake signals with respect to short-period Rayleigh wave (R_g) excitation, relative frequency content of L_g and P phases, and the L_g/P amplitude ratio. However, there was considerable variation in the observed characteristics between events. Cepstral analysis of P waves recorded by the ECTN stations revealed similar spectral modulation for both earthquakes and blasts. The most significant observed quefrencies would correspond to delays considerably longer than those used between individual shots in normal blasting practice. Alternate explanations for the spectral modulation have been identified which do not involve source multiplicity.

For the southern Soviet Union we have seen that the CDSN station WMQ records strong regional signals, including L_g and several P phases, from East Kazakh explosions and regional earthquakes. Comparisons of these signals indicated that the earthquakes produced larger L_g/P amplitude ratios than the explosions and that the differences could be enhanced by bandpass filtering at higher frequencies. However, the comparisons involved different propagation paths for the earthquakes and explosions so that attenuation differences were not completely accounted for in the analysis. The Soviet/NRDC network results revealed a large number of small seismic events in the naturally aseismic area around East Kazakh. These events frequently produced strong R_g phases and are thought to have been mainly mine blasts. The level of this man-made activity could be regarded as indicative of the many events which would need to be considered for a low-threshold monitoring effort in the region.

For the western U.S. the results of processing additional events recorded by the LLNL network were corroborative of our previous findings of spectral differences in the L_g and P_g signals for NTS nuclear explosions and nearby earthquakes of comparable magnitude. We saw some influence of the water table depth on the frequency content of the L_g and P_g signals from Yucca Flat

explosions, but these effects were small compared to the differences associated with source type. At larger regional distances from NTS, we observed strong L_g from several larger explosions and California earthquakes of similar magnitude recorded at RSTN station RSSD. Preliminary indications of differences in the L_g spectra and in the L_g/P amplitude ratio between the explosions and earthquakes recorded at RSSD cannot be considered definitive until additional knowledge is obtained on the influence of propagation path differences and more events have been analyzed.

In addition to these general conclusions several additional observations are noteworthy:

- Presumed mine blasts in the eastern U.S. frequently produce strong R_g signals with frequencies near 1 Hz which can be enhanced by bandpass filtering. R_g may not be present in some cases because of variations in shooting practice or propagation effects.

- The L_g and P_g spectra of regional blasts observed at RSCP fall off more rapidly toward higher frequencies than comparable signals from regional earthquakes.

- Although the L_g/P_{max} amplitude ratios for regional earthquakes at RSCP are on the average larger than similar blast ratios, the data show considerable intermingling.

- Cepstral analysis of P waves from a small sample of commercial blasts and earthquakes in eastern North America recorded by the ECTN stations indicates several significant quefrency peaks in the 0.2 to 1.0 second range for both types of events. These delays may correspond to crustal reverberation and not shot effects, which should be shorter, or depth phases, which should be longer.

- Cepstral analysis does not always provide an objective, model-independent analysis of seismic signals and requires careful consideration of bandwidth limitation.

- The digital seismic data recorded by the CDSN station at Urumchi (WMQ) provides an excellent source of high-quality regional signals from Soviet explosions at East Kazakh and regional earthquakes in that area.

114

The station records strong L_g signals and several regional P phases at ranges of 1000 km or more from events with magnitudes as low as 4.5 m_b.

- L_g/P_{max} amplitude ratios measured at WMQ average about 4.4 for earthquakes and 3.3 for explosions at low frequency, and the measurements overlap for the different source types. At high frequencies the L_g/P_{max} ratios are well-separated averaging about 1 for earthquakes and 0.1-0.2 for explosions.

- The L_g/P_{max} ratios measured at WMQ show no obvious dependence on magnitude but a slight tendency to decrease with epicentral distance. The latter effect does not significantly reduce the difference between event types.

- L_g spectra at WMQ corrected for instrument response appear to have lower corner frequencies for earthquakes than for explosions of comparable magnitudes.

- Interpretation of the relative difference in L_g spectral decay above 1 Hz for explosions and earthquakes at WMQ depends on assumptions regarding the attenuation differences between the paths for the individual events. These effects are not well known at this time.

- The East Kazakh region of the Soviet Union experiences a large number of commercial blasts comparable to those in the eastern U.S.

- The presumed mine blasts recorded by the Soviet/NRDC network frequently produce strong R_g which might be useful for investigating variations in geologic structure within the region.

- The NTS explosions and nearby earthquakes recorded by the LLNL network produce P_g and L_g signals which are relatively richer in high frequencies for the earthquakes than for the explosions. These differences appear to become progressively greater toward the high frequency limit of the useful frequency band.

- For explosions above and below the water table at Yucca Flat, the L_g and P_g spectra for the LLNL stations are slightly enhanced at high frequencies for the deeper events.

- RSSD records strong L_g and regional P phases from NTS explosions and California earthquakes but the useful frequency band is limited to less than about 5 Hz.

- The P phases for California earthquakes at RSSD show differences in their relative excitation and frequency content which may be related to propagation differences or source complexity.

Finally, these studies have identified several areas where additional research is needed to improve regional discrimination capabilities:

- The eastern North America data from RSTN and ECTN and the Soviet/NRDC data include numerous commercial blasts which could provide a good database for developing systematic procedures to distinguish these events. Comparison of these signals with those from similar events at NORESS could also help define general event characteristics.

- More objective criteria for evaluating the significance of cepstral analysis results are needed to evaluate the reliability of the method for identifying multiple sources. The ECTN and NORESS should provide useful databases for evaluating such methods.

- Additional efforts should be devoted to investigating the usefulness of the R_g phase for identifying commercial blasts and for determining possible geologic variations within the East Kazakh region.

- The discrimination capability of the L_g/P_{max} ratio as a function of frequency for East Kazakh explosions and regional earthquakes should be analyzed more systematically to identify the possible influences of path differences. Additional regional stations and events may be useful in defining these path effects.

- Additional investigation of the spectral characteristics of regional phases recorded by the LLNL stations may be useful in defining their dependence on explosion source conditions. Additional events, particularly smaller explosions in saturated rock, could be particularly valuable in such studies.

116

ACKNOWLEDGMENTS

117

REFERENCES

Abrahamson, N. A., and R. B. Darragh (1985). "Observation of a Double Event at Regional Distances: The Morgan Hill Earthquake of 24 April 1984," *Bull. Seism. Soc. Am., 75,* pp. 1461-1464.

Alexander, S. H., and A. H. Borkowski (1988). Personal Communication.

Baumgardt, D. R., and K. A. Ziegler (1988). "Spectral Evidence of Source Multiplicity in Explosions: Application to Regional Discrimination of Earthquakes and Explosions," *Bull. Seism. Soc. Am., 78,* pp. 1773-1795.

Bennett, T. J., and J. R. Murphy (1986). "Analysis of Seismic Discrimination Capabilities Using Regional Data from Western United States Events," *Bull. Seism. Soc. Am., 76,* pp. 1069-1086.

Bennett, T. J., J. R. Murphy, and H. K. Shah (1987a). "Theoretical Analyses of Regional Phase Behavior," S-Cubed Report, SSS-R-87-8113, Technical Report under Contract No. F08606-85-C-0034.

Bennett, T. J., J. R. Murphy, H. K. Shah, and B. W. Barker (1987b). "Theoretical and Empirical Investigations of Regional Phase Behavior," S-Cubed Report, SSS-R-87-8510, Final Report under Contract No. F08606-85-C-0034.

Bennett, T. J., J. R. Murphy, and B. W. Barker (1988a). "Observation and Synthesis of Regional Phase Signals from Quarry Blasts, Earthquakes and Underground Nuclear Explosions," Paper Presented at the 10th Annual AFGL/DARPA Seismic Research Symposium.

Bennett, T. J., B. W. Barker, and J. R. Murphy (1988b). "Regional Phases from East Kazakh Seismic Events," Abstract, Seismological Research Letters, 59, p. 101.

Berger, J., J. N. Brune, P. A. Bodin, J. S. Gomberg, D. M. Carrel, K. F. Priestley, D. E. Chavez, W. R. Walter, C. B. Archambeau, T. B. Cochran, I. L. Nersesov, M. B. Gokhberg, O. A. Stolyrov, S. K. Daragen, N. D. Tarassov, and Y. A. Sutelow (1987a). "A New U.S.-U.S.S.R. Seismological Program," *EOS, 68,* pp. 105-111.

Berger, J., H. K. Eissler, F. L. Vernon, I. L. Nersesov, M. B. Gokhberg, O. A. Stolyrov, and N. T. Tarasov (1988). "Studies of High-Frequency Seismic Noise in Eastern Kazakhstan," *Bull. Seism. Soc. Am., 78,* pp. 1744-1758.

Blandford, R. R. (1981). "Seismic Discrimination Problems at Regional Distances," in *Identification of Seismic Source - Earthquake or Underground Explosion,* D. Reidel Publishing Co.

Chun, K.-Y., G. F. West, R. J. Kokoski and C. Samson (1987). "A Novel Technique for Measuring L_g Attenuation - Results from Eastern Canada Between 1 to 10 Hz," *Bull. Seism. Soc. Am., 77,* pp. 398-419.

Chun, K.-Y., R. J. Kokoski, and G. F. West (1988). "Network Calibration for L_g Magnitude - Method and Test Results from Eastern Canada," *Bull. Seism. Soc. Am., 79,* pp. 127-140.

Corbett, E. J., D. M. Martinelli, and K. D. Smith (1985). "Aftershock Locations of the November 23, 1984 Round Valley, California Earthquakes," Abstract, *EOS, 66,* p. 952.

Dick, R. A., L. R. Fletcher, and D. V. D'Andrea (1983). "Explosives and Blasting Procedures Manual," *Information Circular 8925,* Bureau of Mines, U.S. Department of Interior.

Dowding, C. H. (1985). *Blast Vibration Monitoring and Control,* Prentice Hall, Inglewood Cliffs, N.J., 297 pages.

Flinn, E. A., T. J. Cohen, and D. W. McGowan (1973). "Detection and Analysis of Multiple Seismic Signals," *Bull. Seism. Soc. Am., 63,* pp. 1921-1936.

Frantti, G. E. (1963). "Spectral Energy Density for Quarry Explosions," *Bull. Seism. Soc. Am., 53,* pp. 989-996.

Glaser, R. W., S. R. Taylor, M. D. Denny, and E. S. Vergino (1986). "Regional Discrimination of NTS Explosions and Western U.S. Earthquakes: Multivariate Discriminants," Lawrence Livermore National Laboratory, Report No. UCID-20930 under U.S. DoE Contract No. W-7405-Eng-48.

Goncz, J. H., W. C. Dean, Z. A. Derr, A. C. Lees, K. L. Mclaughlin, T. W. McElfresh, and M. E. Marshall (1987). "Propagation and Excitation of L_g, S_n, and P-P_n Waves from Eastern United States Earthquakes by Regression Analysis of RSTN Data," Teledyne-Geotech Report TGAL-86-7, Final Report on Contract MDA903-85-C-0086.

Gupta, I. N., J. A. Burnetti, R. A. Wagner, and M. E. Marshall (1984). "Discrimination Between Quarry Blasts, Nuclear Explosions and Earthquakes," Teledyne-Geotech Report TGAL-TR-84-1, Technical Report on Contract No. F08606-84-C-0009.

Herrmann, R. B. (1969). "The Structure of the Cincinnati Arch as Determined by Short Period Rayleigh Waves," *Bull. Seism. Soc. Am., 59,* pp. 399-408.

Kafka, A. L. (1987). "R_g Waves as a Depth Discriminant for Earthquakes and Explosions in New England," Proceedings of the Annual Air Force Geophysics Laboratory Review Meeting, Nantucket, MA.

Kafka, A. L. (1988). "Investigation of R_g Waves Recorded from Earthquakes and Explosions in New England," Proceedings of the Annual Air Force Geophysics Laboratory Review Meeting, Fallbrook, CA.

Kafka, A. L., and E. C. Reiter (1987). "Dispersion of R_g Waves in Southeastern Maine: Evidence for Lateral Anisotrophy in the Shallow Crust," *Bull. Seism. Soc. Am., 77,* pp. 925-941.

Leith, W. (1987). "Geology of NRDC Seismic Station Sites in Eastern Kazakhstan," U.S.G.S. Military Geology Project Report.

Leith, W. (1988). Personal Communication.

McEvilly, T. V. (1964). "Central U.S. Crust - Upper Mantle Structure from Love and Rayleigh Wave Phase Velocity Inversion," *Bull. Seism. Soc. Am., 54,* pp. 1997-2016.

Murphy, J. R. (1981). "Near-Field Rayleigh Waves from Surface Explosions," *Bull. Seism. Soc. Am., 71,* pp. 223-248.

Murphy, J. R., and T. J. Bennett (1982). "A Discrimination Analysis of Short-Period Regional Seismic Data Recorded at Tonto Forest Observatory," *Bull. Seism. Soc. Am., 72,* pp. 1351-1366.

Murphy, J. R. and H. K. Shah (1988). "An Analysis of the Effects of Site Geology on the Characteristics of Near-Field Rayleigh Waves," *Bull. Seism. Soc. Am., 78,* pp. 64-82.

Nuttli, O. W. (1981). "On the Attenuation of L_g Waves in Western and Central Asia and Their Use as a Discriminant Between Earthquakes and Explosions," *Bull. Seism. Soc. Am., 71,* pp. 249-261.

Nuttli, O. W. (1986). "L_g Magnitudes of Selected East Kazakhstan Underground Explosions," *Bull. Seism. Soc. Am., 76,* pp. 1241-1251.

Oppenheim, A. V., and R. W. Schafer (1975). *Digital Signal Processing,* Prentice Hall, 585 pages.

Patton, H. J. (1988). "Application of Nuttli's Method to Estimate Yield of Nevada Test Site Explosions Recorded on Lawrence Livermore National Laboratory's Digital Seismic System," *Bull. Seism. Soc. Am., 78,* pp. 1759-1772.

Pomeroy, P. W. (1977). "Aspects of Seismic Wave Propagation in Eastern North America - A Preliminary Report," under Contract No. F49620-78-C-0043, Rondout Associates, Inc., Stone Ridge, New York.

Pomeroy, P. W. (1979). "Regional Seismic Wave Propagation," Semi-Annual Technical Report No. 3, under Contract No. F49620-78-C-0043, Rondout Associates, Inc., Stone Ridge, New York.

Pomeroy, P. W., W. J. Best and T. V. McEvilly (1982). "Test Ban Treaty Verification with Regional Data - A Review," *Bull. Seism. Soc. Am., 72,* pp. S89-S129.

Priestley, K. F. and W. R. Walter (1988). "Analysis of Teleseismic Data Recorded in Eastern Kazakh," Proceedings of the Annual Air Force Geophysics Laboratory Review Meeting, Fallbrook, CA.

Ringdal, F. (1988). "*Magnitudes of Large Semipalatinsk Explosions Using P Coda and L_g Measurements at NORSAR,*" Proceedings of the Annual Air Force Geophysics Laboratory Review Meeting, Fallbrook, CA.

Ruzaikin, A., I. Nersesov, U. Khalturin and P. Molnar (1977). "Propagation of L_g and Lateral Variations in the Crustal Structure of Asia," *J. Geophys. Res., 82,* pp. 307-316.

Shumway, R. H. (1988). *Applied Statistical Time Series Analysis,* Prentice Hall, 379 pages.

Smith, A. T. (1988a). "High-Frequency P-Wave Attenuation Near the East Kazakh Test Site Using a New Method with Spectral Ratio," Abstract, *Seismological Research Letters, 59,* p. 45.

Smith, A. T. (1988b). "High-Frequency Seismic Observations and Models of Chemical Explosions: Implications for the Discrimination of Ripple-Fired Mining Blasts," UCRL-99353, *Lawrence Livermore National Laboratory* preprint submitted to *Bull. Seism. Soc. Am.*

Smith, A. T. and Grose, R. D. (1987). "High-Frequency Observations of Signals and Noise Near RSON: Implications for Discrimination of Ripple-Fired Mining Blasts," Lawrence Livermore National Laboratory, Report No. UCID-20945 under U.S. DoE Contract No. W-7405-Eng-48.

Taylor, S. R., M. D. Denny, and E. S. Vergino (1986). "Regional m_b-M_s Discrimination of NTS Explosions and Western United States Earthquakes: A Progress Report," Lawrence Livermore National Laboratory, Report No. UCID-20642 under U.S. DoE Contract No. W-7405-Eng-48.

Taylor, S. R., N. W. Sherman, and M. D. Denny (1988). "Spectral Discrimination Between NTS Explosions and Western United States Earthquakes at Regional Distances," *Bull. Seism. Soc. Am., 78,* pp. 1563-1579.

Willis, D. E. (1963). "A Note on the Effect of Ripple Firing on the Spectra of Quarry Shots," *Bull. Seism. Soc. Am., 53,* pp. 79-85.

Professor Keiiti Aki
Center for Earth Sciences
University of Southern California
University Park
Los Angeles, CA 90089-0741

Professor Thomas Ahrens
Seismological Lab, 252-21
Div. of Geological and Planetary
  Sciences
California Institute of Technology
Pasadena, CA 91125

Professor Charles B. Archambeau
Cooperative Institute for Resch
  in Environmental Sciences
University of Colorado
Boulder, CO 80309

Dr. Thomas C. Bache Jr.
Science Applications Int'l Corp.
10210 Campus Point Drive
San Diego, CA 92121   (2 copies)

Dr. Muawia Barazangi
Institute for the Study of
  of the Continent
Cornell University
Ithaca, NY 14853

Dr. Douglas R. Baumgardt
Signal Analysis & Systems Div.
ENSCO, Inc.
5400 Port Royal Road
Springfield, VA 22151-2388

Dr. Jonathan Berger
Institute of Geophysics and
  Planetary Physics
Scripps Institution of Oceanography
A-025
University of California, San Diego
La Jolla, CA 92093

Dr. S. Bratt
Science Applications Int'l Corp.
10210 Campus Point Drive
San Diego, CA 92121

Dr. Lawrence J. Burdick
Woodward-Clyde Consultants
P.O. Box 93245
Pasadena, CA 91109-3245 (2 copies)

Professor Robert W. Clayton
Seismological Laboratory/Div. of
  Geological & Planetary Sciences
California Institute of Technology
Pasadena, CA 91125

Dr Karl Coyner
New England Research, Inc.
76 Olcott Drive
White River Junction, VT 05001

Dr. Vernon F. Cormier
Department of Geology & Geophysics
U-45, Room 207
The University of Conneticut
Storrs, Connecticut 06268

Dr. Steven Day
Dept. of Geological Sciences
San Diego State U.
San Diego, CA 92182

Dr. Zoltan A. Der
ENSCO, Inc.
5400 Port Royal Road
Springfield, VA 22151-2388

Professor John Ferguson
Center for Lithospheric Studies
The University of Texas at Dallas
P.O. Box 830688
Richardson, TX 75083-0688

Professor Stanley Flatte'
Applied Sciences Building
University of California,
Santa Cruz, CA 95064

Dr. Alexander Florence
SRI International
333 Ravenswood Avenue
Menlo Park, CA 94025-3493

Professor Steven Grand
University of Texas at Austin
Dept of Geological Sciences
Austin, TX 78713-7909

Dr. Henry L. Gray
Associate Dean of Dedman College
Department of Statistical Sciences
Southern Methodist University
Dallas, TX 75275

Professor Roy Greenfield
Geosciences Department
403 Deike Building
The Pennsylvania State University
University Park, PA 16802

Professor David G. Harkrider
Seismological Laboratory
Div of Geological & Planetary Sciences
California Institute of Technology
Pasadena, CA 91125

Professor Donald V. Helmberger
Seismological Laboratory
Div of Geological & Planetary Sciences
California Institute of Technology
Pasadena, CA 91125

Professor Eugene Herrin
Institute for the Study of Earth
   and Man/Geophysical Laboratory
Southern Methodist University
Dallas, TX 75275

Professor Robert B. Herrmann
Department of Earth & Atmospheric
      Sciences
Saint Louis University
Saint Louis, MO 63156

Professor Bryan Isacks
Cornell University
Dept of Geological Sciences
SNEE Hall
Ithaca, NY 14850

Professor Lane R. Johnson
Seismographic Station
University of California
Berkeley, CA 94720

Professor Thomas H. Jordan
Department of Earth, Atmospheric
 and Planetary Sciences
Mass Institute of Technology
Cambridge, MA 02139

Dr. Alan Kafka
Department of Geology &
   Geophysics
Boston College
Chestnut Hill, MA 02167

Professor Leon Knopoff
University of California
Institute of Geophysics
   & Planetary Physics
Los Angeles, CA 90024

Professor Charles A. Langston
Geosciences Department
403 Deike Building
The Pennsylvania State University
University Park, PA 16802

Professor Thorne Lay
Department of Geological Sciences
1006 C.C. Little Building
University of Michigan
Ann Arbor, MI 48109-1063

Dr. Randolph Martin III
New England Research, Inc.
76 Olcott Drive
White River Junction, VT 05001

Dr. Gary McCartor
Mission Research Corp.
735 State Street
P.O. Drawer 719
Santa Barbara, CA 93102   (2 copies)

Professor Thomas V. McEvilly
Seismographic Station
University of California
Berkeley, CA 94720

Dr. Keith L. McLaughlin
S-CUBED,
A Division of Maxwell Laboratory
P.O. Box 1620
La Jolla, CA 92038-1620

Professor William Menke
Lamont-Doherty Geological Observatory
   of Columbia University
Palisades, NY 10964

Professor Brian J. Mitchell
Department of Earth & Atmospheric
   Sciences
Saint Louis University
Saint Louis, MO 63156

Mr. Jack Murphy
S-CUBED
A Division of Maxwell Laboratory
11800 Sunrise Valley Drive
Suite 1212
Reston, VA 22091 (2 copies)

Professor J. A. Orcutt
IGPP, A-205
Scripps Institute of Oceanography
Univ. of California, San Diego
La Jolla, CA 92093

Professor Keith Priestley
University of Nevada
Mackay School of Mines
Reno, NV 89557

Professor Paul G. Richards
Lamont-Doherty Geological
Observatory of Columbia Univ.
Palisades, NY 10964

Wilmer Rivers
Teledyne Geotech
314 Montgomery Street
Alexandria, VA 22314

Dr. Alan S. Ryall, Jr.
Center of Seismic Studies
1300 North 17th Street
Suite 1450
Arlington, VA 22209-2308   (4 copies)

Professor Charles G. Sammis
Center for Earth Sciences
University of Southern California
University Park
Los Angeles, CA 90089-0741

Professor Christopher H. Scholz
Geological Sciences
Lamont-Doherty Geological Observatory
Palisades, NY 10964

Dr. Jeffrey L. Stevens
S-CUBED,
A Division of Maxwell Laboratory
P.O. Box 1620
La Jolla, CA 92038-1620

Professor Brian Stump
Institute for the Study of Earth & Man
Geophysical Laboratory
Southern Methodist University
Dallas, TX 75275

Professor Ta-liang Teng
Center for Earth Sciences
University of Southern California
University Park
Los Angeles, CA 90089-0741

Dr. Clifford Thurber
State University of New York at
  Stony Brooks
Dept of Earth and Space Sciences
Stony Brook, NY 11794-2100

Professor M. Nafi Toksoz
Earth Resources Lab
Dept of Earth, Atmospheric and
  Planetary Sciences
Massachusetts Institute of Technology
42 Carleton Street
Cambridge, MA 02142

Professor Terry C. Wallace
Department of Geosciences
Building #77
University of Arizona
Tucson, AZ 85721

Weidlinger Associates
ATTN: Dr. Gregory Wojcik
4410 El Camino Real, Suite 110
Los Altos, CA 94022

Professor Francis T. Wu
Department of Geological Sciences
State University of New York
  at Binghamton
Vestal, NY 13901

OTHERS (United States)

Dr. Monem Abdel-Gawad
Rockwell Internat'l Science Center
1049 Camino Dos Rios
Thousand Oaks, CA 91360

Professor Shelton S. Alexander
Geosciences Department
403 Deike Building
The Pennsylvania State University
University Park, PA 16802

Dr. Ralph Archuleta
Department of Geological
   Sciences
Univ. of California at
   Santa Barbara
Santa Barbara, CA

J. Barker
Department of Geological Sciences
State University of New York
 at Binghamton
Vestal, NY   13901

Mr. William J. Best
907 Westwood Drive
Vienna, VA   22180

Dr. N. Biswas
Geophysical Institute
University of Alaska
Fairbanks, AK 99701

Dr. G. A. Bollinger
Department of Geological Sciences
Virginia Polytechnical Institute
21044 Derring Hall
Blacksburg, VA   24061

Mr. Roy Burger
1221 Serry Rd.
Schenectady, NY   12309

Dr. Robert Burridge
Schlumberger-Doll Resch Ctr.
Old Quarry Road
Ridgefield, CT   06877

Dr. Terry Barker
S-CUBED, A Division of Maxwell Lab
P.O. Box 1620
La Jolla, CA   92038-1620

Dr. B.W. Barker
S-CUBED, A Division of Maxwell Lab
11800 Sunrise Valley Dr, Suite 1212
Reston, VA   22091

Science Horizons, Inc.
ATTN: Dr. Theodore Cherry
710 Encinitas Blvd., Suite 101
Encinitas, CA   92024   (2 copies)

Professor Jon F. Claerbout
Professor Amos Nur
Dept. of Geophysics
Stanford University
Stanford, CA   94305 (2 copies)

Dr. Anton W. Dainty
AFGL/LWH
Hanscom AFB, MA   01731

Professor Adam Dziewonski
Hoffman Laboratory
Harvard University
20 Oxford St.
Cambridge, MA   02138

Professor John Ebel
Dept of Geology and Geophysics
Boston College
Chestnut Hill, MA   02167

Dr. Donald Forsyth
Dept of Geological Sciences
Brown University
Providence, RI   02912

Dr. Anthony Gangi
Texas A&M University
Department of Geophysics
College Station, TX   77843

Dr. Freeman Gilbert
Institute of Geophysics &
   Planetary Physics
University of California, San Diego
P.O. Box 109
La Jolla, CA   92037

Mr. Edward Giller
Pacific Seirra Research Corp.
1401 Wilson Boulevard
Arlington, VA   22209

Dr. Jeffrey W. Given
Sierra Geophysics
11255 Kirkland Way
Kirkland, WA 98033

Rong Song Jih
Teledyne Geotech
314 Montgomery Street
Alexandria, Virginia 22314

Professor F.K. Lamb
University of Illinois at
   Urbana-Champaign
Department of Physics
1110 West Green Street
Urbana, IL 61801

Dr. Arthur Lerner-Lam
Lamont-Doherty Geological Observatory
 of Columbia University
Palisades, NY 10964

Dr. L. Timothy Long
School of Geophysical Sciences
Georgia Institute of Technology
Atlanta, GA 30332

Dr. Peter Malin
University of California at
   Santa Barbara
Institute for Central Studies
Santa Barbara, CA 93106

Dr. George R. Mellman
Sierra Geophysics
11255 Kirkland Way
Kirkland, WA 98033

Dr. Bernard Minster
IGPP, A-205
Scripps Institute of Oceanography
Univ. of California, San Diego
La Jolla, CA 92093

Professor John Nabelek
College of Oceanography
Oregon State University
Corvallis, OR 97331

Dr. Geza Nagy
U. California, San Diego
Dept of Ames, M.S. B-010
La Jolla, CA 92093

Dr. Jack Oliver
Department of Geology
Cornell University
Ithaca, NY 14850

Dr. Robert Phinney/Dr. F. A. Dahlen
Dept of Geological
Geological Science University
Princeton University
Princeton, NJ 08540

RADIX System, Inc.
Attn: Dr. Jay Pulli
2 Taft Court, Suite 203
Rockville, Maryland 20850

Dr. Norton Rimer
S-CUBED
A Division of Maxwell Laboratory
P.O. 1620
La Jolla, CA 92038-1620

Professor Larry J. Ruff
Department of Geological Sciences
1006 C.C. Little Building
University of Michigan
Ann Arbor, MI 48109-1063

Dr. Richard Sailor
TASC Inc.
55 Walkers Brook Drive
Reading, MA 01867

Thomas J. Sereno, Jr.
Service Application Int'l Corp.
10210 Campus Point Drive
San Diego, CA 92121

Dr. David G. Simpson
Lamont-Doherty Geological Observ.
 of Columbia University
Palisades, NY 10964

Dr. Bob Smith
Department of Geophysics
University of Utah
1400 East 2nd South
Salt Lake City, UT 84112

Dr. S. W. Smith
Geophysics Program
University of Washington
Seattle, WA 98195

Dr. Stewart Smith
IRIS Inc.
1616 N. Fort Myer Drive
Suite 1440
Arlington, VA 22209

Rondout Associates
ATTN: Dr. George Sutton,
Dr. Jerry Carter, Dr. Paul Pomeroy
P.O. Box 224
Stone Ridge, NY 12484 (4 copies)

Dr. L. Sykes
Lamont Doherty Geological Observ.
Columbia University
Palisades, NY 10964

Dr. Pradeep Talwani
Department of Geological Sciences
University of South Carolina
Columbia, SC 29208

Dr. R. B. Tittmann
Rockwell International Science Center
1049 Camino Dos Rios
P.O. Box 1085
Thousand Oaks, CA 91360

Professor John H. Woodhouse
Hoffman Laboratory
Harvard University
20 Oxford St.
Cambridge, MA 02138

Dr. Gregory B. Young
ENSCO, Inc.
5400 Port Royal Road
Springfield, VA 22151-2388

Dr. Peter Basham
Earth Physics Branch
Geological Survey of Canada
1 Observatory Crescent
Ottawa, Ontario
CANADA K1A OY3

Professor Ari Ben-Menahem
Dept of Applied Mathematics
Weizman Institute of Science
Rehovot
ISRAEL 951729

Dr. Eduard Berg
Institute of Geophysics
University of Hawaii
Honolulu, HI 96822

Dr. Michel Bouchon - Universite
   Scientifique et Medicale de Grenob
Lab de Geophysique - Interne et
   Tectonophysique - I.R.I.G.M-B.P.
38402 St. Martin D'Heres
Cedex FRANCE

Dr. Hilmar Bungum/NTNF/NORSAR
P.O. Box 51
Norwegian Council of Science,
Industry and Research, NORSAR
N-2007 Kjeller, NORWAY

Dr. Michel Campillo
I.R.I.G.M.-B.P. 68
38402 St. Martin D'Heres
Cedex, FRANCE

Dr. Kin-Yip Chun
Geophysics Division
Physics Department
University of Toronto
Ontario, CANADA M5S 1A7

Dr. Alan Douglas
Ministry of Defense
Blacknest, Brimpton,
 Reading RG7-4RS
UNITED KINGDOM

Dr. Manfred Henger
Fed. Inst. For Geosciences & Nat'l Res.
Postfach 510153
D-3000 Hannover 51
FEDERAL REPUBLIC OF GERMANY

Ms. Eva Johannisson
Senior Research Officer
National Defense Research Inst.
P.O. Box 27322
S-102 54 Stockholm
SWEDEN

Tormod Kvaerna
NTNF/NORSAR
P.O. Box 51
N-2007 Kjeller, NORWAY

Mr. Peter Marshall, Procurement
 Executive, Ministry of Defense
Blacknest, Brimpton,
 Reading FG7-4RS
UNITED KINGDOM (3 copies)

Dr. Robert North
Geophysics Division
Geological Survey of Canada
1 Observatory crescent
Ottawa, Ontario
CANADA, K1A OY3

Dr. Frode Ringdal
NTNF/NORSAR
P.O. Box 51
N-2007 Kjeller, NORWAY

Dr. Jorg Schlittenhardt
Federal Inst. for Geosciences & Nat'l Res.
Postfach 510153
D-3000 Hannover 51
FEDERAL REPUBLIC OF GERMANY

University of Hawaii
Institute of Geophysics
ATTN: Dr. Daniel Walker
Honolulu, HI 96822

FOREIGN CONTRACTORS

Dr. Ramon Cabre, S.J.
Observatorio San Calixto
Casilla 5939
La Paz Bolivia

Professor Peter Harjes
Institute for Geophysik
Rhur University/Bochum
P.O. Box 102148, 4630 Bochum 1
FEDERAL REPUBLIC OF GERMANY

Dr. E. Husebye
NTNF/NORSAR
P.O. Box 51
N-2007 Kjeller, NORWAY

Professor Brian L.N. Kennett
Research School of Earth Sciences
Institute of Advanced Studies
G.P.O. Box 4
Canberra 2601
AUSTRALIA

Dr. B. Massinon
Societe Radiomana
27, Rue Claude Bernard
7,005, Paris, FRANCE   (2 copies)

Dr. Pierre Mechler
Societe Radiomana
27, Rue Claude Bernard
75005, Paris, FRANCE

Dr. Svein Mykkeltveit
NTNF/NORSAR
P.O. Box 51
N-2007 Kjeller, NORWAY   (3 copies)

Dr. Ralph Alewine III
DARPA/NMRO
1400 Wilson Boulevard
Arlington, VA 22209-2308

Dr. Robert Blandford
DARPA/NMRO
1400 Wilson Boulevard
Arlington, VA 22209-2308

Sandia National Laboratory
ATTN: Dr. H. B. Durham
Albuquerque, NM 87185

Dr. Jack Evernden
USGS-Earthquake Studies
345 Middlefield Road
Menlo Park, CA 94025

U.S. Geological Survey
ATTN: Dr. T. Hanks
Nat'l Earthquake Resch Center
345 Middlefield Road
Menlo Park, CA 94025

Dr. James Hannon
Lawrence Livermore Nat'l Lab.
P.O. Box 808
Livermore, CA 94550

Paul Johnson
ESS-4, Mail Stop J979
Los Alamos National Laboratory
Los Alamos, NM 87545

Ms. Ann Kerr
DARPA/NMRO
1400 Wilson Boulevard
Arlington, VA 22209-2308

Dr. Max Koontz
US Dept of Energy/DP 5
Forrestal Building
1000 Independence Ave.
Washington, D.C. 20585

Dr. W. H. K. Lee
USGS
Office of Earthquakes, Volcanoes,
  & Engineering
Branch of Seismology
345 Middlefield Rd
Menlo Park, CA 94025

Dr. William Leith
U.S. Geological Survey
Mail Stop 928
Reston, VA 22092

Dr. Richard Lewis
Dir. Earthquake Engineering and
  Geophysics
U.S. Army Corps of Engineers
Box 631
Vicksburg, MS 39180

Dr. Robert Masse'
Box 25046, Mail Stop 967
Denver Federal Center
Denver, Colorado 80225

Richard Morrow
ACDA/VI
Room 5741
320 21st Street N.W.
Washington, D.C. 20451

Dr. Keith K. Nakanishi
Lawrence Livermore National Laboratory
P.O. Box 808, L-205
Livermore, CA 94550 (2 copies)

Dr. Carl Newton
Los Alamos National Lab.
P.O. Box 1663
Mail Stop C335, Group ESS-3
Los Alamos, NM 87545

Dr. Kenneth H. Olsen
Los Alamos Scientific Lab.
P.O. Box 1663
Mail Stop C335, Group ESS-3
Los Alamos, NM 87545

Howard J. Patton
Lawrence Livermore National
  Laboratory
P.O. Box 808, L-205
Livermore, CA 94550

Mr. Chris Paine
Office of Senator Kennedy
SR 315
United States Senate
Washington, D.C. 20510

AFOSR/NP
ATTN: Colonel Jerry J. Perrizo
Bldg 410
Bolling AFB, Wash D.C. 20332-6448

HQ AFTAC/TT
Attn: Dr. Frank F. Pilotte
Patrick AFB, Florida 32925-6001

Mr. Jack Rachlin
USGS - Geology, Rm 3 C136
Mail Stop 928 National Center
Reston, VA 22092

Robert Reinke
AFWL/NTESG
Kirtland AFB, NM 87117-6008

Dr. Byron Ristvet
HQ DNA, Nevada Operations Office
Attn: NVCG
P.O. Box 98539
Las Vegas, NV 89193

HQ AFTAC/TGR
Attn: Dr. George H. Rothe
Patrick AFB, Florida 32925-6001

Donald L. Springer
Lawrence Livermore National Laboratory
P.O. Box 808, L-205
Livermore, CA 94550

Dr. Lawrence Turnbull
OSWR/NED
Central Intelligence Agency
CIA, Room 5G48
Washington, D.C. 20505

Dr. Thomas Weaver
Los Alamos National Laboratory
P.O. Box 1663
MS C 335
Los Alamos, NM 87545

GL/SULL
Research Library
Hanscom AFB, MA 01731-5000 (2 copies)

Secretary of the Air Force (SAFRD)
Washington, DC 20330
Office of the Secretary Defense
DDR & E
Washington, DC 20330

HQ DNA
ATTN: Technical Library
Washington, DC 20305

DARPA/RMO/RETRIEVAL
1400 Wilson Blvd.
Arlington, VA 22209

DARPA/RMO/Security Office
1400 Wilson Blvd.
Arlington, VA 22209   (

GL/XO   (
Hanscom AFB, MA 01731-5000

GL/LW
Hanscom AFB, MA 01731-5000

DARPA/PM
1400 Wilson Boulevard
Arlington, VA 22209

Defense Technical
  Information Center
Cameron Station
Alexandria, VA 22314
(5 copies)

Defense Intelligence Agency
Directorate for Scientific &
  Technical Intelligence
Washington, D.C. 20301

Defense Nuclear Agency/SPSS
ATTN: Dr. Michael Shore
6801 Telegraph Road
Alexandria, VA 22310

AFTAC/CA (STINFO)   (
Patrick AFB, FL 32925-6001

                                                  '
Dr. Gregory van der Vink
Congress of the United States
Office of Technology Assessment
Washington, D.C. 20510

Mr. Alfred Lieberman
ACDA/VI-OA'State Department Building
Room 5726
320 - 21St Street, NW
Washington, D.C. 20451

TACTEC
Battelle Memorial Institute
505 King Avenue
Columbus, OH 43201 (Final report only)